Université de Montréal

Genetic Landscape of Joubert syndrome in French Canadians

par

Myriam Srour

Biologie Moléculaire, Université de Montréal

Faculté de Médecine

Thèse présentée à la Faculté de Médecine
En vue de l'obtention du grade de doctorat
en Biologie Moléculaire

juin, 2015

Résumé

Le syndrome de Joubert est une maladie récessive caractérisée par une malformation congénitale distincte du tronc cérébral et du cervelet, associée à une anomalie des mouvements oculaires (apraxie oculomotrice), une respiration irrégulière, un retard de développement, et une ataxie à la démarche. Au cours de la dernière décennie, plus de 20 gènes responsables ont été identifiés, tous ayant un rôle important dans la structure et la fonction des cils primaires. Ainsi, le syndrome de Joubert est considéré une ciliopathie. Bien que le Syndrome de Joubert ait été décrit pour la première fois dans une famille canadienne-française en 1969, le(s) gène(s) causal demeurait inconnu dans presque tous les cas de syndrome de Joubert recensés en 2010 dans la population canadienne-française, soit début de mon projet doctoral.

Nous avons identifié un total de 43 individus canadiens-français (35 familles) atteints du syndrome de Joubert. Il y avait un regroupement de familles dans la région du Bas-Saint-Laurent de la province de Québec, suggérant la présence d'un effet fondateur. L'objectif de ce projet était de caractériser la génétique du syndrome de Joubert dans la population canadienne-française. Notre hypothèse était qu'il existait un effet fondateur impliquant au moins un nouveau gène JBTS.

Ainsi, dans un premier temps, nous avons utilisé une approche de cartographie par homozygotie. Cependant, nous n'avons pas identifié de région d'homozygotie partagée parmi les individus atteints, suggérant la présence d'une hétérogénéité génétique ou allélique. Nous avons donc utilisé le séquençage exomique chez nos patients, ce qui représente une approche plus puissante pour l'étude de conditions génétiquement hétérogènes.

Nos travaux ont permis l'identification de deux nouveaux gènes responsables du syndrome de Joubert: *C5orf42* et *TMEM231*. Bien que la localisation cellulaire et la fonction de *C5orf42* soient inconnus au moment de cette découverte, nos résultats génétiques combinés avec des études ultérieures ont établi un rôle important de C5orf42 dans la structure et la fonction ciliaire, en particulier dans la zone de transition, qui est une zone de transition entre le cil et le reste de la cellule. TMEM231 avait déjà un rôle établi dans la zone de transition

ciliaire et son interaction avec d'autres protéines impliquées dans le syndrome de Joubert était connu. Nos études ont également identifié des variants rares délétères chez un patient JBTS dans le gène ciliaire *CEP104*. Nous proposons donc *CEP104* comme un gène candidat JBTS. Nous avons identifié des mutations causales dans 10 gènes, y compris des mutations dans *CC2D2A* dans 9 familles et *NPHP1* dans 3 familles. Au total, nous avons identifié les mutations causales définitives chez 32 des 35 familles étudiées (91% des cas). Nous avons documenté un effet fondateur complexe dans la population canadienne-française avec de multiples mutations récurrentes dans quatre gènes différents (*C5orf42*, *CC2D2A*, *TMEM231*, *NPHP1*).

Au début de ce projet de recherche, l'étiologie génétique était inconnue chez les 35 familles touchées du syndrome de Joubert. Maintenant, un diagnostique moléculaire définitif est identifié chez 32 familles, et probable chez les 3 autres. Nos travaux ont abouti à la caractérisation génétique du syndrome de Joubert dans la population canadienne-française grâce au séquençage exomique, et révèlent la présence d'un effet fondateur complexe avec une l'hétérogénéité allélique et intralocus importante. Ces découvertes ont éclairé la physiologie de cette maladie. Finalement, l'identification des gènes responsables ouvre de nouvelles perspectives diagnostiques ante-natales, et de conseils génétique, très précieuses pour les familles.

Mots-clés: Syndrome de Joubert, Cil, Ciliopathie, Zone de transition ciliaire, Séquençage exomique, Effet fondateur, Signe de la dent molaire, Canadiens-français, *C5orf42*, *TMEM231, CEP104*

Abstract

Joubert syndrome (JBTS) is a primarily autosomal recessive disorder characterized by a distinctive mid-hindbrain/cerebellum malformation, eye movement abnormalities (oculomotor apraxia), irregular breathing, developmental delay, and ataxia. Over the past decade, over 20 causal genes have been identified, all of which have an important role in the structure and function of the primary cilia. Thus, JBTS joins an expanding category of diseases termed "ciliopathies". Though JBTS was first described in affected siblings of a French Canadian (FC) family in 1969, the underlying genesis basis of the disorder was unknown in the overwhelming majority of FC cases at the onset of this doctoral project in 2010.

We identified a total of 43 FC individuals with JBTS from 35 families. We observed a clustering of the affected families in the Lower Saint-Lawrence region of the province of Quebec, suggesting the presence of a founder effect. The aim of this doctoral project was to characterize the genetic landscape of JBTS in the FC population, and we hypothesized the presence of a founder effect in novel JBTS gene(s). Therefore, we initially used a homozygosity mapping approach. However, we did not identify any shared regions of homozygosity amongst affected individuals, suggesting the presence of genetic and/or allelic heterogeneity. We therefore primarily used a whole exome sequencing approach in our JBTS patients, a strategy that is better suited for the study of genetically heterogeneous conditions.

Our work has resulted in the identification of two novel JBTS genes: *C5orf42* and *TMEM231*. In total, we have identified causal mutations in *C5orf42* in 14 families (including the original JBTS family described in 1969), and *TMEM231 in* 2 families. Though the function and cellular localization of C5orf42 was not known at the time of the publication of our manuscript, our genetic findings combined with subsequent animal and cellular work establish the important role of C5orf42 in ciliary structure and function, particularly at the ciliary transition zone. TMEM231 had been previously shown to localize to the ciliary transition zone and interact with several JBTS gene products. We also identified deleterious rare variants in one JBTS patient in the ciliary gene *CEP104*, implicating *CEP104* as a strong

candidate JBTS gene. We identified causal mutations in 10 JBTS genes, including *CC2D2A* in 9 families and *NPHP1* in 3 families. Definite causal mutations were identified in 32 of 35 families (91% of cases). We documented a complex founder effect in the FC population with multiple recurrent mutations in 4 different genes (*C5orf42, CC2D2A, TMEM231, NPHP1*).

Prior to the start of this research endeavor, the underlying genetic etiology of Joubert syndrome was unknown in all 35 families. Now, a definite molecular diagnosis has been identified in 32 families, and a probable molecular diagnosis in the remaining 3. Therefore, our work has resulted in the unraveling of the genetic basis of JBTS in the French-Canadian population using WES, and reveals the presence of a complex founder effect with substantial locus and allelic heterogeneity.

Keywords: Joubert syndrome, Cilia, Ciliopathy, Ciliary transition zone, Whole exome sequencing, Founder effect, Molar tooth sign, French Canadians, *C5orf42*, *TMEM231, CEP1041*

Table of Contents

List of Figures

List of Tables

List of abbreviations

ARSACS: autosomal recessive spastic ataxia of Charlevoix-Saguenay

CGNP: cerebellar granular neuronal precursors

COACH: Coloboma, Oligophrenia/developmental delay, Ataxia, Cerebellar vermis hypoplasia, Hepatic fibrosis syndrome

IFT: intraflagellar transport

JBTS: Joubert syndrome

JS: Joubert syndrome

MKS: Meckel syndrome

MRI: magnetic resonance imaging

MTS: molar tooth sign

OMA: oculomotor apraxia

OFD: orofacio-digital syndrome

PCP: planar cell polarity

SHH: Sonic Hedgehog

SNP: single nucleotide polymorphism

TZ: transition zone

WES: whole exome sequencing

Acknowledgments

When I started my clinical Neurogenetics Fellowship in 2007, I could not have anticipated that I would embark in this exciting journey in the world of genetic research, such that I would eventually pursue a PhD in molecular biology.

I wish to thank Jacques Michaud, my Phd supervisor, for introducing me to these fascinating projects. In particular, I am grateful that he taught me how to always have a critical eye, and encouraged me to continually push the project further. He is the model of the clinician-scientist, a role that I wish to follow for the remainder of my career.

I would like to thank Bernard Brais, who encouraged me to start my Masters degree at the start of my fellowship, and started the entire process. He showed me how to engage science with enthusiasm and curiosity, and how to think 'outside the box' with patients.

I would like to thank Guy Rouleau, whose Neurogenetics clinics at the Montreal General Hospital during my residency first made me interested in this field, and for pointing me towards many compelling projects.

Thank you to Fadi Hamdan for all that he has taught me, for his advice, patience, support and friendship. I am eternally grateful.

Thank you to all the students in Jacques and Bernard's Lab, who have made this journey so enjoyable and stimulating.

And of course thank you to my wonderful husband Ron who is always my pillar of support and encouragement, and to my parents, my unconditional cheerleaders.

Chapter 1: Introduction

Joubert syndrome [JBTS, MIM 213300] is one of the most frequent forms of inherited congenital cerebellar ataxias. It was first described in 1969 by Dr. Marie Joubert. Dr Joubert described 4 French-Canadian siblings with agenesis of the cerebellar vermis, episodic breathing abnormalities (hypopnea/hyperpnea), abnormal eye movements (particularly oculomotor apraxia), gait ataxia and variable severities of intellectual disability (1). Following this seminal description, similarly affected individuals were reported throughout the world, and this constellation of clinical symptoms became characterized as "Joubert syndrome".

Neuropathologic examination and advances in brain imaging have revealed that all JBTS patients have a distinctive midbrain and hindbrain malformation characterized by hypoplasia of the cerebellar vermis, thickened abnormally orientated superior cerebellar peduncles, and a deep inter-peduncular fossa. These features result in the hallmark "molar tooth sign" on axial brain magnetic resonance imaging (see Figure 1) first described by Maria

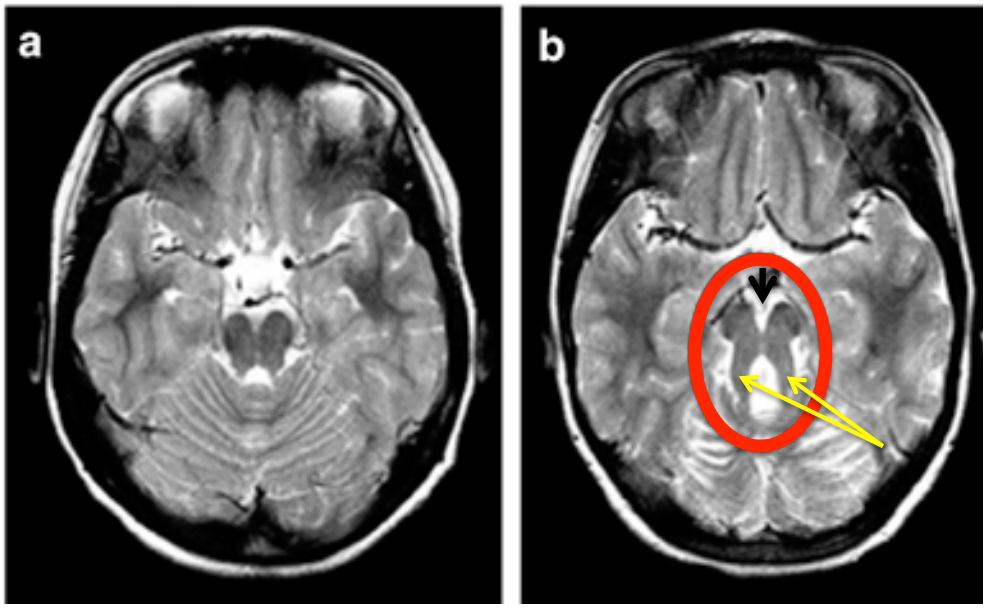

Figure 1. Molar Tooth Sign on MRI. Axial T2 brain MRI of a control individual (a) and patient with JBTS (b). Note the molar tooth sign (red circle), with deepened interpeduncular fossa (black arrow), and thickened and abnormally oriented superior cerebellar peduncles (yellow arrows).

et al. in 1997(2).

JBTS is a clinically heterogeneous condition. It combines hallmark neurologic signs with variable multi-organ involvement, mainly of the eyes, kidneys, skeleton and liver(3). The wide and variable clinical spectrum associated with JBTS is reflected by the large and confusing list of previously used syndromic designations associated with the various forms of JBTS. For example, the cerebello-oculo-renal syndrome designates individuals with ocular and renal involvement; Senior-Löken syndrome designates individuals with kidney and ocular disease; the acronym COACH refers to Coloboma, Oligophrenia/developmental delay, Ataxia, Cerebellar vermis hypoplasia, Hepatic fibrosis. These designations are no longer commonly used. The term "Joubert syndrome and related disorders" was coined to group all conditions sharing the molar tooth sign. Currently, a diagnosis of JBTS is made based on the mandatory presence of the molar tooth sign on imaging associated with the variable clinical features of hypotonia, ataxia, developmental delay, and oculomotor apraxia. Subtypes of JBTS are classified based on the extra-neural organ system involvement (see Table 1).

Table 1: Classification of JBTS based on clinical features

Clinical Subtype	**Mandatory features**	**Preferentially associated features**	**Previously used nosology**
Pure Joubert syndrome (JS)	MTS		JS
JS with ocular defects (JS-O)	MTS Retinal dystrophy		JS
JS with renal defects (JS-R)	MTS Nephronophthesis		
JS with oculorenal defacts (JS-OR)	MTS Retinal dystrophy Nephronophthesis		Cerebellooculorenal syndrome Senior-Löken syndrome
JS with hepatic defects (JS-H)	MTS Congenital hepatic fibrosis	Colobomas Nephronophthesis	COACH syndrome Gentile syndrome
JS with orofaciodigital defects (JS-OFD)	MTS Lobulated/bifid tongue (incl. hamartomas) Polydactyly	Cleft lip/palate	Orofaciodigital VI syndrome Varadi-Papp syndrome

Clinical features associated with JBTS

Neurologic features

The cardinal features of JBTS are hypotonia, evolving into ataxia and developmental delay, often associated with intellectual disability, abnormal eye movements and altered respiratory pattern in the neonatal period. Hypotonia is observed in nearly all affected patients, and is generally the first sign observed on examination. Motor and language development is usually delayed in children with JBTS. In one series, the average age of sitting was 19 months, and of walking was 4 years in those who were able to develop these skills(4). Patients have ataxia, oromotor dyspraxia, and speech dyspraxia. Some children require assistive devices or need to use sign language for communication (5). Cognitive impairment is highly variable in JBTS(6). Intellectual disability, ranging widely from mild to very severe is common, with many patients retaining the capacity to attend special schools, learn specific job skills and work in protected conditions. It is important to note however that intellectual deficit is not inevitable, and that several individuals with borderline or even normal intelligence have been reported. Seizures have been reported, although they are not common. Behavioral problems, such as impulsivity, autism, perseveration and temper tantrums commonly occur (6).

Patients with JBTS can have other central nervous system abnormalities. These include occipital meningomyelocele, heterotopias, polymicrogyria, hydrocephalus, hypothalamic hamartoma and corpus callosal abnormalities (7).

Characteristic abnormal eye movements are almost always present(4, 6). Oculomotor apraxia is present in the large majority, and manifests as an inability to visually track objects, initiate saccades (high velocity large amplitude eye movements). This results in the compensatory head-thrust movement that is the hallmark of oculomotor apraxia. Oculomotor apraxia likely reflects abnormalities of axonal decussation. These abnormalities have been documented with diffusion tensor magnetic resonance imaging. As part of the axonal decussation abnormality, mirror movements (voluntary movements in a limb are coupled with

involuntary ‘mirror’ movements of the contralateral limb) are occasionally observable. Nystagmus is also common. Both oculomotor apraxia and nystagmus improve with age.

The respiratory abnormalities consist of short alternating episodes of apnea and hyperpnea, or isolated episodic hyperpnea. These tend to start shortly after birth, intensify with emotional stress, and improve with age. They generally disappear around 6 months of age.

Neuropathological examination of the midbrain-hindbrain in patients with JBTS reveals a characteristic association of abnormalities. The cerebellar vermis is invariably hypoplastic or absent, the cerebellar nuclei are often hypoplastic or fragmented, and there is heterotopia of Purkinje-like neurons. Pontine and medullary structures, such as the basis pontis, reticular formation, inferior olivary nucleus and dorsal column, are dysplastic (8, 9). There is typically failure of the decussation of the superior cerebellar peduncles and corticospinal tracts, as seen both on histological examination and imaging of fiber tracts on MRI(10).

Ocular features

The retina is among the organs the most frequently involved in JBTS. Overall, clinically-significant retinal involvement occurs in approximately one third of subjects. Retinal involvement can range from extremely severe Leber Congenital amaurosis to pigmentary retinopathies evident on fundus exam. In some cases milder forms of retinal dystrophy can be detected only on electroretinogram. There are two main forms of retinal disease,: severe congenital blindness with a flat electroretinogram (known as congenital amaurosis), and a later-onset pigmentary retinopathy that manifests with night-blindness and has a variable course. Colobomas can be unilateral or bilateral, and mostly affect the posterior segment of the eye. Colobamas are frequent in patients with liver abnormalities, occurring in up to 30%, as part of the COACH syndrome(11).

Renal involvement

Renal involvement is present in approximately 25% of JBTS patients (12). It is usually in the form of nephronophthesis, a progressive condition characterized by tubulointerstitial nephritis and cysts concentrated at the corticomedullary junction. Most patients present around the age of 9 years, with defects in urinary concentration, and progress to end stage renal disease late in the second decade(13).

Skeletal defects

Polydactyly is reported in approximately 8 to 16% of cases(12). The most common form is post axial affecting hands and feet. Mesoaxial polydactyly is associated with orofacial digital syndrome type 6, a subtype of JBTS characterized by the presence of oral frenulae, lingual tumors or hamartomas, and craniofacial abnormalities that include wide-spaced eyes and a midline lip groove.

Pathogenesis: JBTS is a prototypical ciliopathy

Over the past decade, advances in genetic research have revealed that JBTS is not only a clinically heterogeneous, but also a genetically heterogeneous disorder. Indeed, 24 causal genes have been identified to date. The first known causal gene, *AHI1* (MIM# 608894), was identified in 2004 (14), and the second gene *NPHP1* (MIM# 6071000) identified in 2005 (15). An updated list of JBTS genes is provided in Table 2. All these genes encode proteins that localize to the cilia, and all have an important role in ciliary structure or function. JBTS is thus considered a ciliopathy, and joins an expanding groups of disorders characterized by dysfunction of the cilia. To date, more than 30 human diseases are classified as ciliopathies, Examples of other ciliopathies include Meckel syndrome (MIM# 249000), Bardet-Biedl syndrome (MIM# 209900), Nephronophthisis (MIM# 256100), Orofacial digital syndrome (MIM# 311200), Alstrom syndrome (MIM# 203800) and Jeune Asphyxiating Thoracic Dysplasia (or Short-rib thoracic dysplasia, MIM# 208500). Overall, at least 80 ciliopathy

genes have been implicated so far. Ciliopathy disorders in general share overlapping features. All typically have multi-organ involvement, because cilia are present on almost all cell types. Defects in the primary cilium can affect the kidneys, retina, liver, brain and bones. The phenotype is a varying combination of cystic kidneys, polydactyly, retinopathy, liver fibrosis, developmental delay, intellectual disability and central nervous system abnormalities. Though ciliopathies may involve any of these organs and the significant clinical overlap between them, each disorder has a classical clinical presentation, such that most patients can be diagnosed in the clinical setting. For examples, Bardet-Biedl syndrome is characterized by intellectual disability, anosmia, obesity, polydactyly, hypogonadism, and retinal degeneration; Meckel syndrome is an early lethal disorder characterized by occipital encephalocele, cystic kidney and polydactyly; Alstrom syndrome is associated with obesity and retinopathy, but unlike JBTS or Bardet-Biedl syndrome, intellectual disability, polydactyly and hypogonadism are not a feature. Although individually rare, ciliopathy disorders may collectively have a prevalence as high as 1 in 2000 (based on the prevalence of the three common disease traits: renal cysts 1 in 500, retinal degeneration 1 in 3000 and polydactyly 1 in 500)(16).

Table 2: Genes associated with JBTS. (MKS- Meckel syndrome, LCA- leber congenital amaurosis , ATD- asphyxiating thoracic dystrophy, ACLS- acrocallosal syndrome, HLS- hydrolethalus syndrome)

Gene/Protein	JBTS	Other ciliopathes	MIM numbers
INPP5E	JBTS1		*613037
TMEM216	JBTS2	MKS	*613277
AHI1/Jouberin	JBTS3		*608894
TMEM67/Mecklin	JBTS4	MKS, NPHP	*609884
NPHP1/nephrocystin 1	JBTS5	NPHP	*607100
CEP290	JBTS6	MKS, LCA	*610142
ARL13B	JBTS7		*608922
RPGRIP1L	JBTS8	MKS	*610937
CC2D2A	JBTS9	MKS	*612013
OFD1	JBTS10	OFD	*300170
TTC21B	JBTS11	NPHP, ATD	*612014
KIF7	JBTS12	ACLS, HLS	*611254
TCTN1	JBTS13		*609863
TMEM237	JBTS14		*614423
CEP41	JBTS15		*610523
TMEM138	JBTS16		*614459
C5orf42	JBTS17	OFD6	*614571
TCTN3	JBTS18	OFD4	*613847
ZNF423	JBTS19	NPHP	*604557
TMEM231	JBTS20	MKS	*614949
CSPP1	JBTS21		*611654
PDE6D	JBTS22		*602676
TCTN2	JBTS23	MKS	*613846
B9D1	Unassigned	MKS	*614144

The primary cilium – basic biology

The primary cilium is a hair-like organelle protruding from the cell membrane, and is present in almost all cell-types. Each cell contains only one non-motile cilium, which is remarkably conserved throughout evolution. In the brain, motile cilia are restricted to the ependymal cells lining the ventricle and some of the choroid plexus cells, whereas primary cilia are present on all brain cells, including neural progenitors and mature neurons, glial cells and astrocytes(17).

The axoneme is the microtubule-based core of the cilia (Figure 2). In the non-motile cilia, it is formed by nine doublet microtubules (9+0), whereas in the motile cilia, it contains nine doublet microtubules and an extra pair of tubules (9+2) that are attached to a dynein motor to generate movement. The proximal end of the axoneme is anchored to the cell by the basal body, a modified centriole. The region between the basal body and the base of the axoneme is the transition zone. The main body of the transition zone is characterized by multiple rows of Y-shaped linkers projecting from the outer doublets of the axoneme and attaching to the ciliary membrane, as well as transitional fibers attaching the basal body to the peri-ciliary membrane. The transition zone isolates the cytoplasm of the cilia from the rest of the cell by acting as a selective barrier to protein diffusion. It also functions as a loading-unloading zone for transport into and out of the cilium. Cilia lack the necessary machinery for protein synthesis. Thus both soluble and membrane-bound ciliary proteins need to be trafficked to the basal body and taken up into the cilium. Proteins that enter the cilia from its base are carried along the axoneme via a microtubule-based transport system called intraflagellar transport (IFT). Anterograde transport toward the ciliary tip is regulated by complex B, consisting of at least 14 proteins (IFT172, IFT88, IFT81, IFT80, IFT74, IFT70, IFT57, IFT54, IFT52, IFT46, IFT27, IFT25, IFT22 and IFT20), in association with kinesin motors (KIF3A, KIF3B, and KAP3). The retrograde transport (i.e. from the tip of the cilia towards the base) is provided by complex A, which is composed of six IFT proteins (IFT144, IFT140, IFT139, IFT122, IFT121, and IFT43), in association with a dynein motor (DYNC2H1 and DYNC2L1)(18).

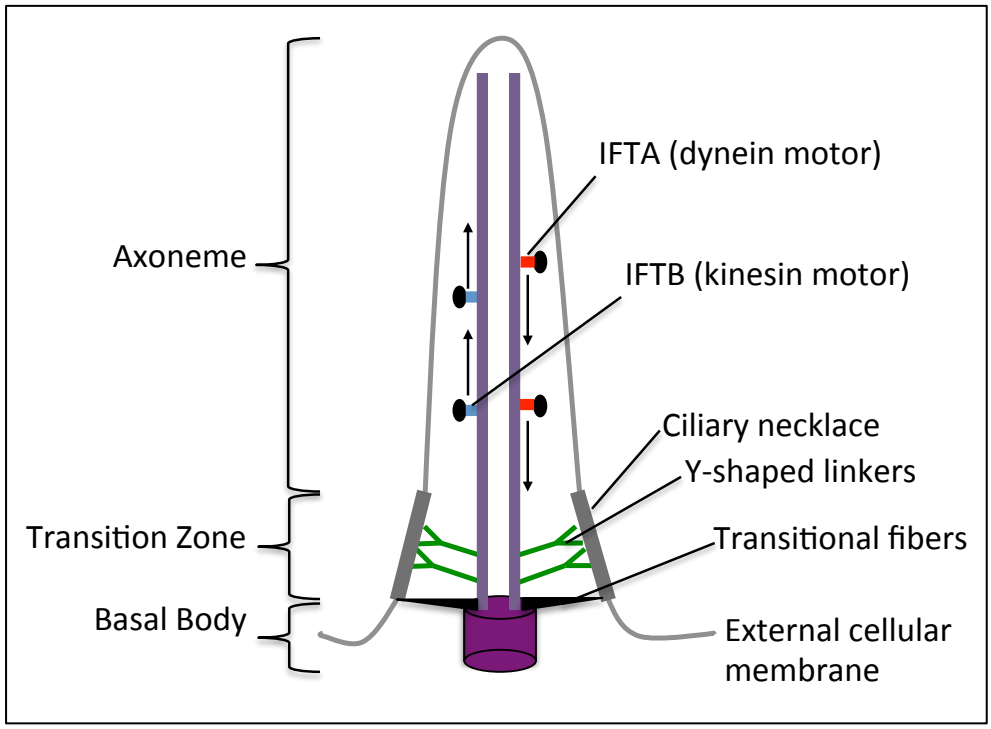

Figure 2. Schematic representation of the primary cilia. IFT: intraflagellar transport

The antennae-like shape of the cilia (typically 5-10um in length) extending into the surrounding extracellular environment makes its ideally positioned to detect changes in chemical factors, morphogens or growth factors present in the extracellular medium. Additionally, the fact that the ciliary compartment is distinct from the remainder of the cellular compartment (both at the level of the intracellular compartment and the membrane) allows the partitioning of the sensory and signaling proteins away from the main body of the cell, and fine-tuning of biological responses to various stimuli. For example, the passive bending of the cilia present on renal tubular epithelial cells by fluid flow mediate the mechanosensation of extracellular urine flow; bending of the cilia within the kidney tubules leads to calcium influx through the polycystin-1 (PC-1)/polycystin-2 (PC-2) calcium channel. Mutations in both PC-1 and PC-2 are responsible for polycystic kidney disease. Retinal photoreceptors have specialized primary cilium that connects the inner segments which contains the cellular nucleus, to the outer nucleus which contains the photo-transducing pigments such as rhodopsin (19).

Key role of the cilia in neurodevelopment

Primary cilia sense and transduce extracellular signals that influence a wide range of processes such as cell proliferation and polarity, developmental processes and neuronal growth. As exemplified with JBTS, perturbation in cilium formation or function can lead to profound defects in embryogenesis, with involvement of various organs including brain, retina, kidneys, liver, skeleton and heart. The primary cilium's role in brain and organ patterning is mediated by morphogen signaling and its central role in the regulation of the sonic hedgehog (Shh), canonical and non-canonical Wnt pathways. The primary cilium also plays a pivotal role in a number of major growth factor-regulated signaling pathways, including platelet-derived growth factor (PDGF), fibroblast growth factor (FGF), and Notch pathways, with receptors for these ligands concentrated on the ciliary membranes(17).

Cilia and Sonic HedgeHog Signaling (Shh)

Shh signaling is essential for embryonic development, acting as a morphogen that is involved in patterning of multiple tissues, notably the central nervous system and limbs(20). In the central nervous sytem, Shh and the cilia have critical roles in neural tube/spinal cord patterning, telencephalic patterning, migration and placement of interneurons in the developing cortex, hippocampal neurogenesis, and formation of adult neural stem cells.

The cilium is required for amplification of the Shh signal when the Shh ligand is present. In the absence of Shh, its transmembrane receptor Patched (Ptc) localizes to the base of the cilium. There, Ptc represses the activity of Smo, a transmembrane protein with a structure reminiscent of G-protein-coupled receptors, by preventing its localization to the cilium. Upon binding of Shh to Ptc, Ptc is translocated outside the compartment allowing Smo to enter it, in a process that depends on the anterograde IFT machinery. The ciliary accumulation of Smo in turn facilitates the activation of Smo, which ultimately results in the accumulation of the active forms of three Gli (Gli-A) transcription molecules (Gli1, Gli2 and Gli3) (21). In the absence of Shh, Gli1, Gli2 and Gli3 are proteolytically processed into

repressor forms (Gli-R) by the removal of their carboxy tails. The activation of Smo inhibits Gli protein processing and results in the accumulation of the full Gli proteins containing the transactivator domain, which can enter the nucleus and activate target genes (Figure 3). Shh-related tissue patterning stems from the regulation of the balance between Gli transcriptional activators and repressors in the developing tissues. In the absence of Shh, Gli2 and Gli3 are cleaved to repressor forms (Gli2R, Gli3R), whereas in its presence, proteolysis is inhibited and Gli2 and Gli3 function as activators (Gli2A, Gli3A). Gli2A is the primary activator of Shh target genes, Gli3R the main repressor.

Shh signaling and activation of the Gli pathway are particularly important in cerebellar development (which is highly abnormal in patients with JBTS(22)). Most cell types of the cerebellum arise from the ventricular zone progenitors that are migrating through the forming cortex during embryogenesis. The cerebellar granule cells originate from a secondary germinal zone in the rostral rhombic lip. In the mouse, progenitors called cerebellar granular neuronal precursors (CGNP) undergo a first wave of proliferation at Embyonic day13.5. Then, from E17.5 on, they migrate over the nascent cerebellum to form the external granule layer where their population massively expands. This expansion is mediated by Shh, which is secreted by the Purkinje cells and diffuses up to the outer External Granule Layer where the CGNPs are located. The CGNPs highly express Gli1, the readout of the Shh pathway(23). Among the identified mitogens in the cerebellum (e.g. FGF-2, IGF-1 and EGF), Shh is the most potent mitogenic factor, able to trigger up to a 100-fold increase of CGNP proliferation *in vitro* (24). The proliferation phase of the CGNPs peaks at P5-8 and declines thereafter to stop at around P15. From P8, CGNPs start extending processes and initiate their onwards migration. The duration and intensity of the proliferation phase generating the pool of CGNPs is critical for the final shape and function of the cerebellum. Conditional removal of ciliary genes in CGNPs gives rise to striking dysgenesis and abnormal foliation of the cerebellum, as well as decreased target genes of and proliferation of CGNPS during cerebellar development(23).

Shh signaling is also essential for spinal cord and neural tube patterning. Disruption of Shh signaling leads to dorso-ventral patterning defects of the spinal cord, and neural tube defects such as failed closure of the neural tube (occipital encephalocele or exencephaly) and midline defects (colobomas, corpus callosum defects, defects of decussation of the corticospinal tracts)(17). Shh protein is produced from the ventral pole of the neural tube and forms a ventral-to-dorsal concentration gradient. This gradient establishes the differential spatial patterns of gene expression in neural progenitor cells. High levels of Shh signaling induce the expression of the homeodomain protein Nkx2.2; consequently, Nkx2.2 is most strongly expressed ventrally. Low levels of Shh are sufficient to induce the expression of the transcription factor Olig2, which is expressed more dorsally than Nkx2.2.(25-27). Regulation of the balance between activated and repressor forms of Gli is critical in Shh-mediated patterning, and is regulated in part by the cilia. This explains why disruption of ciliary function can lead to different patterning abnormalities that reflect overactivity of either Gli-R or Gli-A.

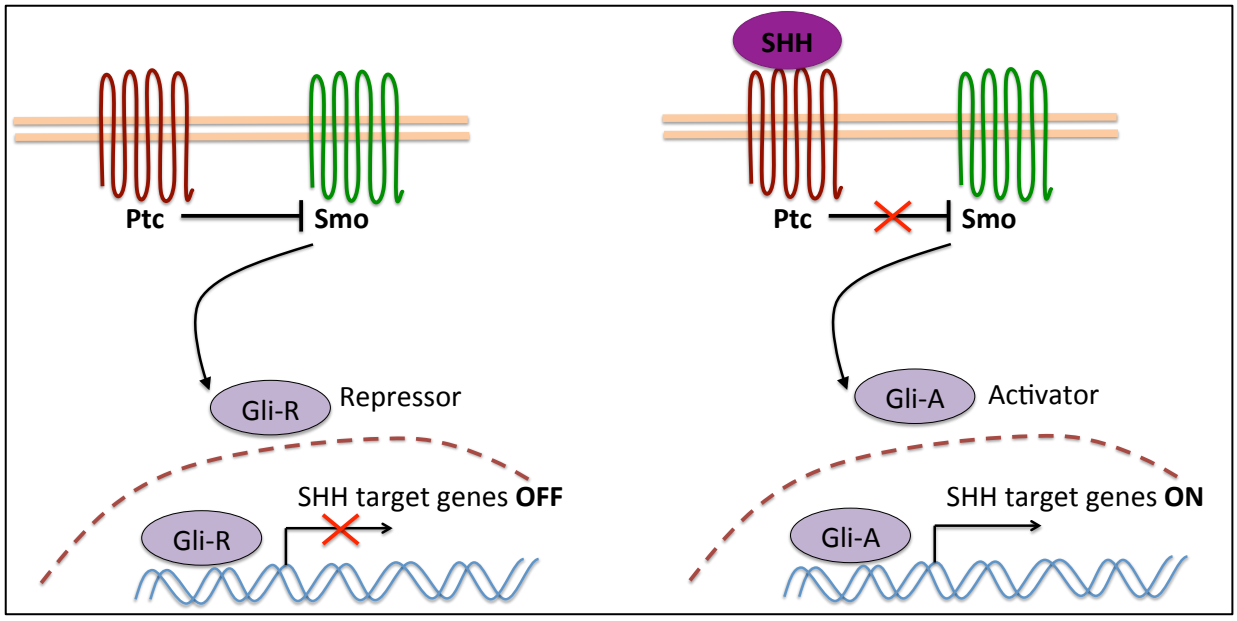

Figure 3: SHH signaling pathway schematic. In the absence of SHH, the receptor Ptc is located in the cilium and suppresses Smoothened (Smo). Full-length Gli transcription factors are truncated into their repressor forms (Gli-R). The binding of SHH to Ptc facilitates the activation of Smo, which ultimately results in the accumulation of the active forms of Gli (Gli-A) which can enter the nucleus and activate target genes. (Modified from Goetz and Anderson, *Nature Reviews Genetics*, 2010)

Disruption of Shh signaling also accounts for the limb patterning defects associated with ciliopathies, as Shh plays an important role in anteroposterior patterning of the limbs. Shh initially acts as morphogen and originates from posterior margin of the limb bud in a region called the zone of polarizing activity. Subsequently, it has mitogenic activity, which ensures the production of a sufficient number of cells to promote the normal complement of digits. Together, these two activities of Shh are responsible for specifying the identity of each digit and, as the limb bud expands, the position within the limb bud in which each digit forms. Loss-of-function mutations to Shh results in a loss of digits, whereas mutations in Gli3 cause polydactyly (28). Though the exact mechanism underlying polydactyly in ciliopathies has not been elucidated, disruption of Shh transduction signalling and abnormal Gli3 processing are key central processes (29) .

Cilia and the WNT pathway

The canonical and non-canonical (planar cell polarity, PCP) Wnt pathways are other important signaling pathways also regulated in part by the cilia. The Wnts are a family of secreted factors that bind Frizzled (Fzl) receptors to activate distinct signaling cascades, depending on the specific Wnt ligand, Wnt receptor, and the activity of Disheveled (Dvl), which acts as a molecular switch between signaling cascades (Figure 4). Canonical β-catenin-dependent Wnt signaling regulates proliferation, cell cycle progression and differentiation in the nervous system(30). The PCP Wnt signaling pathway provides cells with the positional clues required for concerted multicellular actions, such as the convergent extension cell movements that lead to neural tube closure (31). The PCP pathway is increasingly implicated in neuronal migration and axon guidance, in particular in the orderly development of large axon tracts. In absence of Wnt ligand, cytoplasmic β-catenin is constitutively phosphorylated by several kinases and targeted for proteosomal degradation(32). In canonical Wnt signaling, the binding of Wnt ligands to Fzl and LRP5 or LRP6 coreceptors transduces a signal across the plasma membrane that results in the activation of the Dvl. Activated Dvl inhibits the degradation and leads to the stabilization and accumulation of β-catenin in the cytoplasm. β-catenin then migrates into the nucleus where it

can act as a co-activator for TCF/LEF- mediated transcription of neurodevelopmental genes. Several JBTS genes, such as *AHI,* which encodes jouberin, regulate canonical Wnt signaling by facilitating β-catenin translocation to the nucleus. It has been shown that the primary cilium serves to modulate Wnt pathway responsiveness by sequestering β-catenin and jouberin within the cilium, thus limiting their nuclear entry. Similarly, other studies investigating the roles of the ciliary and basal body genes *Kif3a*, *Ift88*, and *Ofd1* have revealed an inhibitory role of the primary cilium on canonical Wnt signaling, suggesting that loss of ciliary or basal body components leads to hyper-responsiveness to external canonical Wnt stimuli (33, 34). Loss of Kif3a in mice leads to enhanced β-catenin-dependent transcriptional activation. Embryonic fibroblasts from both *Kif3a* and *Ofd1* mutant mice, as well as *Ofd1*-deficient embryonic stem cells have a hyper-responsive canonical Wnt response.

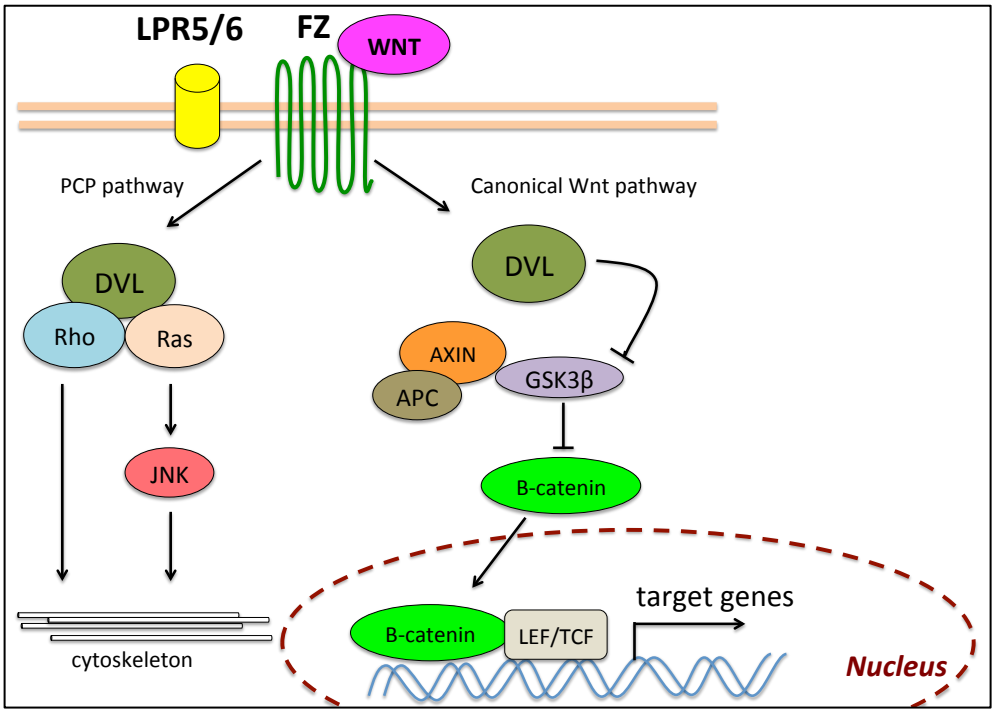

Figure 4: WNT signaling pathway schematic. The extracellular signalling molecule WNT activates the *canonical pathway* (right) and the planar cell polarity (PCP) pathway (left). In the canonical pathway, interaction of WNT with the transmembrane receptor frizzled (FZ) activates dishevelled (DVL), which induces the disassembly of a complex (axin, APC and GSK3β), and results in the accumulation of β-catenin in the cyctoplasm. β-catenin then translocates where it can activate the transcription of target genes. In the PCP pathway, FZ functions through G-proteins to activate DVL, which thereupon signals to Rho GTPases (Rho or Rac or both). Activated Ras signals through the c-Jun amino (N)-terminal kinase (JNK). Activation of Rho-GTPases induces changes in the cytoskeleton. (Modified from Moon *et al*, *Nature Reviews Genetics*, 2004)

The non-canonical PCP pathway is also activated via the binding of Wnt to Fzl and its co-receptor, however, it does not result in the downstream accumulation of β-catenin. Fzl recruits Dvl to form a complex with the Dvl-associated activator of morphogenesis 1 (DAAM) which then activates the small G-protein Rho. In turn, Rho activates Rho-associated kinase (ROCK), which is one of the major regulators of the cytoskeleton. Mutations in several ciliopathy-related genes, such as *TMEM237*, *TMEM216* or *TMEM67*, result in abnormal PCP cascade activity, and conversely, mutations in key PCP pathway proteins such as inturned (intu), fuzzy (fuz) or dvl, were found to result in abnormal ciliogenesis.

In conditions of normal ciliary signaling, the PCP pathway is favored over the canonical pathway by inhibition of Dvl and activation of B-catenin destruction complex. With disruption of normal the basal body or ciliary function, there is decreased PCP signaling and upregulation of canonical Wnt signaling. Dysregulation of the Wnt pathway plays a critical role in the formation of renal cysts associated with ciliopathies. The Wnt pathway is required for the induction of the metanephric mesenchyme to develop the proximal portions of the nephron and for regulation of cell proliferation. Both PCP defects and hyperactivity of the canonical wnt signaling in transgenic mice overexpressiving B-catenin can result in the formation of cysts. The underlying mechanism is thought to be related to the fact that normal diving cells in the renal tubules orient their mitotic spindles parallel to the lumen, resulting in tubular elongation, whereas mis-orientated mitotic spindles, as observed in animal models of cystic kidney disease, result in tubular dilation(35).

Founder effect underlies many autosomal recessive disorders in French Canadians

There are a large number of genetic disorders that have a markedly increased incidence in the French-Canadian population. These include Autosomal recessive spastic ataxia of Charlevois-Saguenay (ARSACS, MIM# 270550), Agenesis of corpus callosum and peripheral neuropathy (ACCPN, Andermann syndrome (MIM# 218000), Leigh syndrome French-Canadian type (MIM# 220111), Oculopharyngeal muscular dystrophy (OPMD, MIM# 164300), Hereditary sensory and autonomic neuropathy type II (HSAN II, MIM#

201300), Myotonic dystrophy (MIM# 160900) and many others. The increased incidence of these hereditary disorders in the FC population reflects the presence of founder effects. A founder effect refers to the reduction in genetic variation that results when a small population establishes a new colony. The gene pool of the first generation of settlers (which may not represent the gene pool of the entire population it is derived from) contributes disproportionately to the ensuing population structure. Thus, if the founding settlers carry rare gene mutations, these will be passed on to future generations. Alleles that may have been rare in the original population will occur with a higher frequency in the settlers and their descendants.

The French-Canadian population arose following successive recent immigration waves. Of Quebec's current >7 million inhabitants, 6 million are descendants from French Settlers. The French Colony of Nouvelle-France was first settled in 1608, with the foundation of the City of Quebec. From 1608 till the time it passed into British rule, approximately 8,500 permanent settlers arrived in Quebec, including only 1,600 women. The 2600 settlers who arrived before 1680 have contributed two thirds of the gene pool of the current French-Canadian population. Though settlers came from regions throughout France, the major source of immigrants to Nouvelle-France were the Atlantic seaports and the regions around Paris. French settlement in North America occurred in two main regions along the Saint Lawrence River and Acadia (now New Brunswick and Nova Scotia). In the 17th century, the population groups had limited social and geographical mobility; therefore there were limited marriages between families from different regions or social groups. By the English conquest in 1759, most of the French-Canadian population lived in farming settlements along the Saint Lawrence River and, because of language and religious barriers, intermixed minimally with the Protestant English-speaking newcomers. The French-Canadian population has had a high fertility rate, attributed to the encouragement by the clergy, and frequently referred to as "la revanche des berceaux" (the revenge of the cradles). The high fecundity rate, early marriage and overall low infant mortality rate resulted in a rapid expansion of the French-Canadian population. Thus, the founding of the French-Canadian population by a limited number of settlers, combined with the relative isolation of the population and the higher fecundity rate,

explains the presence of a number of founder effects. This has resulted in the increased incidence of these rare genetic disorders in the French-Canadian population (36, 37).

For the recessive disorders with a higher incidence in the French-Canadian population, a single common founder mutation is usually observed, present at a higher carrier frequency amongst French-Canadian individuals. This explains the increased incidence of disease despite very low rates of consanguineous marriages. For example, ARSACS affects 1 in 1519 individuals in Charlevoix and 1 in 1952 individuals in the Saguenay, where the estimated carrier frequency is 1/22. One mutation (c.6594delT) in the causal gene *SACS* represents 94% of mutated alleles. Similarly, Leigh syndrome affects 1/2916 live births in the Saguenay-Lac-Saint-Jean region. Again, in Leigh syndrome only one allele, A354V, represents 98% of mutant alleles in the causal gene *LRPPRC* (36).

Landscape of Joubert syndrome in Quebec

Despite the fact that JBTS was first described in Quebec, the overwhelming majority of French-Canadian patients with JBTS did not have causal mutations identified at the onset of my doctoral project in 2010. In fact, in 2010, only 8 JBTS genes were known. Determining the precise underlying genetic etiology of JBTS is of great importance for several reasons. For the patients and their families, it facilitates genetic counseling and prenatal testing. It also concludes the diagnostic process (providing closure for families), improves the accuracy of prognostication and allows tailored medical management. Critically, determining causal genes expands our knowledge of the pathophysiology of JBTS and allows improved understanding of mechanisms underlying normal brain development. Ultimately, the understanding of the pathophysiology of these disorders will enable the development of targeted treatments in the future.

The precise incidence of JBTS is not known, but is estimated to be between 1/80,000 and 1/100,000 live births(38). Our preliminary observation suggested that there is a high prevalence of JBTS in the French-Canadian population living in the Lower St-Lawrence

("Bas-du-Fleuve" in French) region of the province of Quebec (Figure 5). In particular, there is a striking cluster of families from the east end of the region (Matapedia region), including one family from Mont-Joli (population of 6,568), 3 families from Amqui (population 6,261) and 3 other families from Sayabec (population 1,877). This distribution strongly suggested the presence of a founder effect for JBTS.

The population of the Lower St-Lawrence region was initially established as the result of the immigration of a limited number of settlers (6,000 individuals) from Quebec City and its surroundings in the late 17th and early 18th century followed by a rapid increase of the population due to a high fertility rate(39). The establishment of settlers in the region followed a west-to-east pattern, with later settlers migrating to regions further east. A small number of Acadians also contributed to the early population of the Matapedia region(40). Thus, the demographic growth of this population appears to be characterized by a series of bottlenecks that may have resulted in regional founder effects. We hypothesized that a founder effect could underlie the clustering of individuals with JBTS in the Lower St-Lawrence region. If this were true, a single common homozygous mutation might explain a large proportion of them.

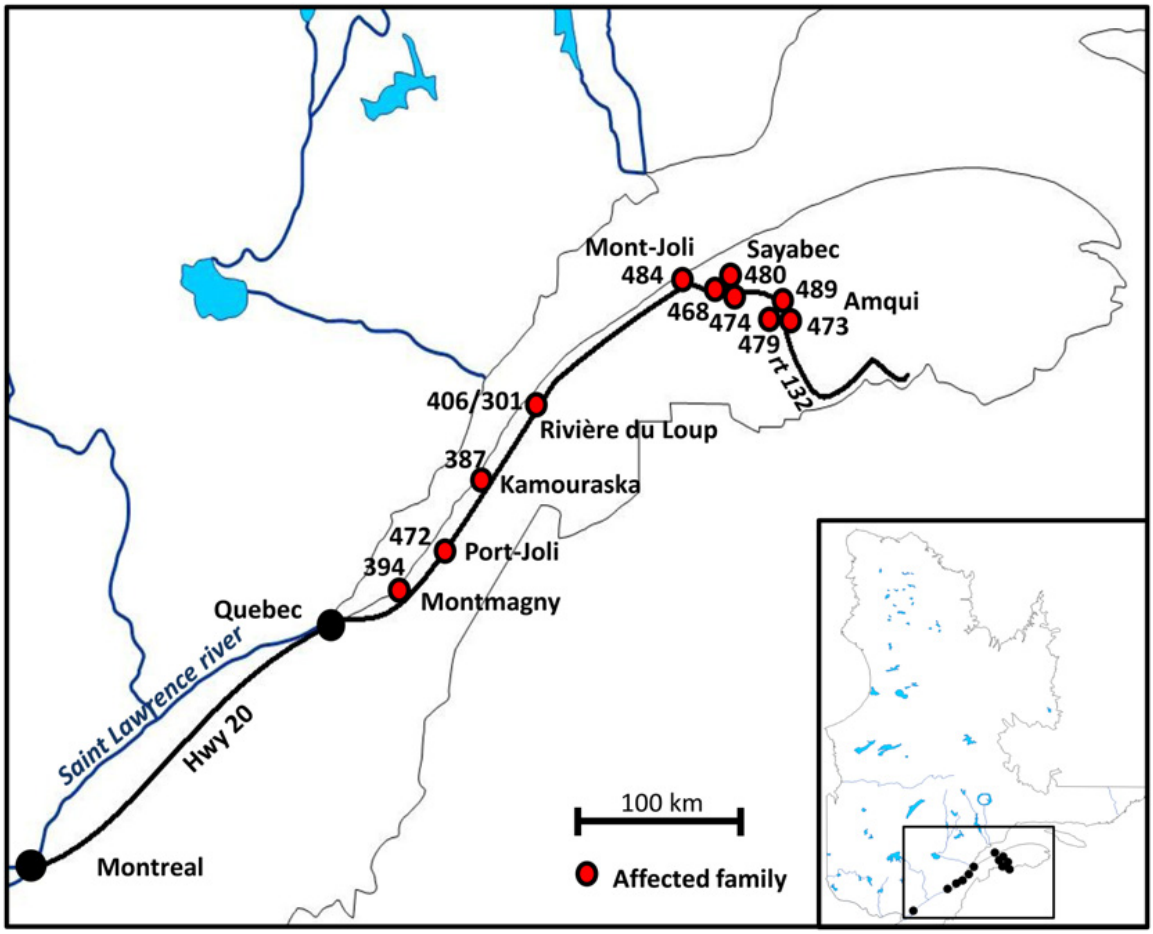

Figure 5. Distribution of individuals with Joubert syndrome in the Lower St-Lawrence region. Note the cluster of families along Route 132, which follows the Matapedia river.

Hypotheses and objectives

JBTS remains largely unexplained in French Canadians. Given the documented presence of multiple founder effects in the French-Canadian population, and our preliminary observation that multiple affected families clustered in the Lower Saint Lawrence and Matapedia regions, we hypothesized that there existed a founder effect with a recurrent mutation in one gene that explains the majority of cases. In addition, given the fact that causal mutations in known JBTS genes were rarely identified in French-Canadian JBTS families on a clinical basis, we hypothesized the presence of a recurrent founder mutation in a novel JBTS gene. Therefore, our initial objective was to study these French-Canadian families using single nucleotide polymorphism (SNP) genotyping and homozygosity mapping, a strategy that is well suited for the study of families with an autosomal recessive disorder in which a founder effect is suspected.

Because JBTS is known to be a very genetically heterogeneous condition, we also hypothesized that, though a founder mutation likely existed and explained the majority of FC JBTS families, mutations in more than one gene probably accounted for the genetic etiology in Quebec. Thus, we anticipated using WES to study all JBTS families that remained *unexplained* following our initial SNP genotyping and homozygosity approach. Indeed, WES is an extremely powerful strategy to study disorders that are clinically and genetically heterogeneous, such as JBTS.

The specific objectives of this project were:

1) To recruit a cohort of French-Canadian families with JBTS and assess their geographic distribution throughout Quebec
2) To clinically characterize the affected JBTS individuals by extensive phenotypic evaluation of all JBTS patients when possible, supplemented by review of medical records and radiographic imaging.

3) To identify the causal genes underlying JBTS in the French-Canadian population using (a) a homozygosity mapping approach and/or (b) whole exome sequencing (WES).
4) To evaluate for the presence of a genetic founder effect in the French-Canadian population.
5) To look for genotype-phenotype correlations.

Chapter 2:

Mutations in *C5ORF42* cause Joubert syndrome in the French Canadian Population

Manuscript 1:

Mutations in *C5ORF42* cause Joubert syndrome in the French Canadian Population.

Published in: Am J Hum Genet. 2012 Apr 6;90(4):693-700, PMID: 22425360

Myriam Srour[1,11], Jeremy Schwartzentruber[2,11], Fadi F. Hamdan[1], Luis H. Ospina[3], Lysanne Patry[1], Damian Labuda[4], Christine Massicotte[4], Sylvia Dobrzeniecka[1], José Capo-Chichi[1], Simon Papillon-Cavanagh[4], Mark E. Samuels[4], Kym M. Boycott[5], Michael I. Shevell[6], Rachel Laframboise[7], Valérie Désilets[4], FORGE Canada Consortium*, Bruno Maranda[8], Guy A Rouleau[9], Jacek Majewski[10], Jacques L. Michaud[1]

[1]Centre of Excellence in Neurosciences of Université de Montréal and Sainte-Justine Hospital Research Center, Montréal H3T 1C5, Canada; [2]McGill University and Genome Quebec Innovation Centre, Montréal H3A 1A4, Canada; [3]Department of Ophthalmology, Sainte-Justine Hospital Research Center, Montréal, H3T 1C5, Canada; [4]Sainte-Justine Hospital Research Center, Montréal H3T 1C5, Canada; [5]Children's Hospital of Eastern Ontario Research Institute, Ottawa, K1H 8L1 Canada; [6]Division of Pediatric Neurology, Montreal Children's Hospital-McGill University Health Center, Montreal, H3H 1P3, Canada; [7]Department of Medical Genetics, Centre Hospitalier Universitaire Laval, Québec, G1V 4G2, Canada; [8]Division of genetics, Centre Hospitalier Universitaire de Sherbrooke, Sherbrooke, J1H 5N4, Canada; [9]Centre of Excellence in Neurosciences of Université de Montréal and Department of Medicine, Montréal H2L 2W5, Canada; [10]Department of Human Genetics, McGill University, H3A 1A4, Montréal, Canada.

[11] Equal contribution

*FORGE Steering Committee listed in Acknowledgements

ABSTRACT

Joubert syndrome (JBTS) is an autosomal recessive disorder characterized by a distinctive mid-hindbrain malformation, developmental delay with hypotonia, ocular-motor apraxia and breathing abnormalities. Although JBTS was first described more than 40 years ago in French Canadian siblings, the causal mutations have not yet been identified in this family, nor in most French Canadian individuals subsequently described. We ascertained a cluster of 15 individuals with JBTS from 11 families living in the Lower St-Lawrence region. SNP genotyping excluded the presence of a common homozygous mutation that would explain the clustering of these individuals. Exome sequencing performed in all the 15 subjects showed that 9 affected individuals from 7 families (including the original JBTS family) carried rare compound heterozygous mutations in *C5ORF42*. Two missense variants (c.4006C>T [p.Arg1336Trp], c.4690G>A [p.Ala1564Thr]) and a splicing mutation (c.7400+1G>A), which causes exon skipping, were found in multiple subjects, not known to be related, whereas three other mutations, all truncating (c.6407delC [p.Pro2136Hisfs*31], c.4804C>T [p.Arg1602X], c.7477C>T [p.Arg2493X]), were identified in single individuals. None of the unaffected first-degree relatives were compound heterozygotes for these mutations. Moreover, none of the 6 putative mutations was detected among 477 French Canadian controls. Our data suggests that mutations in *C5ORF42* explain a large fraction of French Canadian individuals with JBTS.

Joubert syndrome (JBTS; MIM 213300) is an autosomal recessive disorder characterized by the presence of hypotonia, apnea or hyperpnea in infancy, oculomotor apraxia, and variable developmental delay or intellectual impairment (reviewed in[1]). The diagnostic hallmark of JBTS is the presence of a complex malformation of the midbrain-hindbrain junction that comprises cerebellar vermis hypoplasia or aplasia, deepened interpeduncular fossa, and elongated superior cerebellar peduncles. This malformation takes the appearance of a molar tooth on axial brain MRI. In a subset of individuals, JBTS also involves other organs, resulting in cystic kidneys, retinopathy, or polydactyly. JBTS is a genetically heterogeneous condition with 15 genes described to date(41-58). All of these genes appear to play a role in the development and/or function of non-motile cilia. Although JBTS was first described in French Canadian siblings more than 40 years ago by Marie Joubert and colleagues, until now the causal mutations have not yet been identified in the original family nor in most French Canadians subjects(1).

There is a high prevalence of JBTS in the French Canadian population living in the Lower St-Lawrence ("Bas-du-Fleuve" in French) region of the province of Quebec (Fig. 6). In total, we identified 16 living affected individuals (from 11 unrelated families) with at least one grandparent originating from that region. Informed consent was obtained from all individuals or their legal guardians. This project was approved by our institutional ethics committee. We were initially able to collect blood-derived DNA from 15 of these individuals, including an affected individual (II-1 in family 394; individual BD in(1)) from the original JBTS family described by Marie Joubert and colleagues in 1969. There was a striking cluster of 7 families from the east end of the region (Matapedia region), including one family from Mont-Joli (population of 6,568), 3 families from Amqui (population 6,261) and 3 other families from Sayabec (population 1,877). Individual II-1 from family 394 did not undergo brain imaging studies but an MRI scan performed in her brother (II-2) showed the molar tooth sign (MTS)(59, 60). All the other affected individuals showed the MTS and variable expression of the classical JBTS features. The cohort included three families with two affected siblings, and in no case were parents affected, consistent with a recessive mode of transmission.

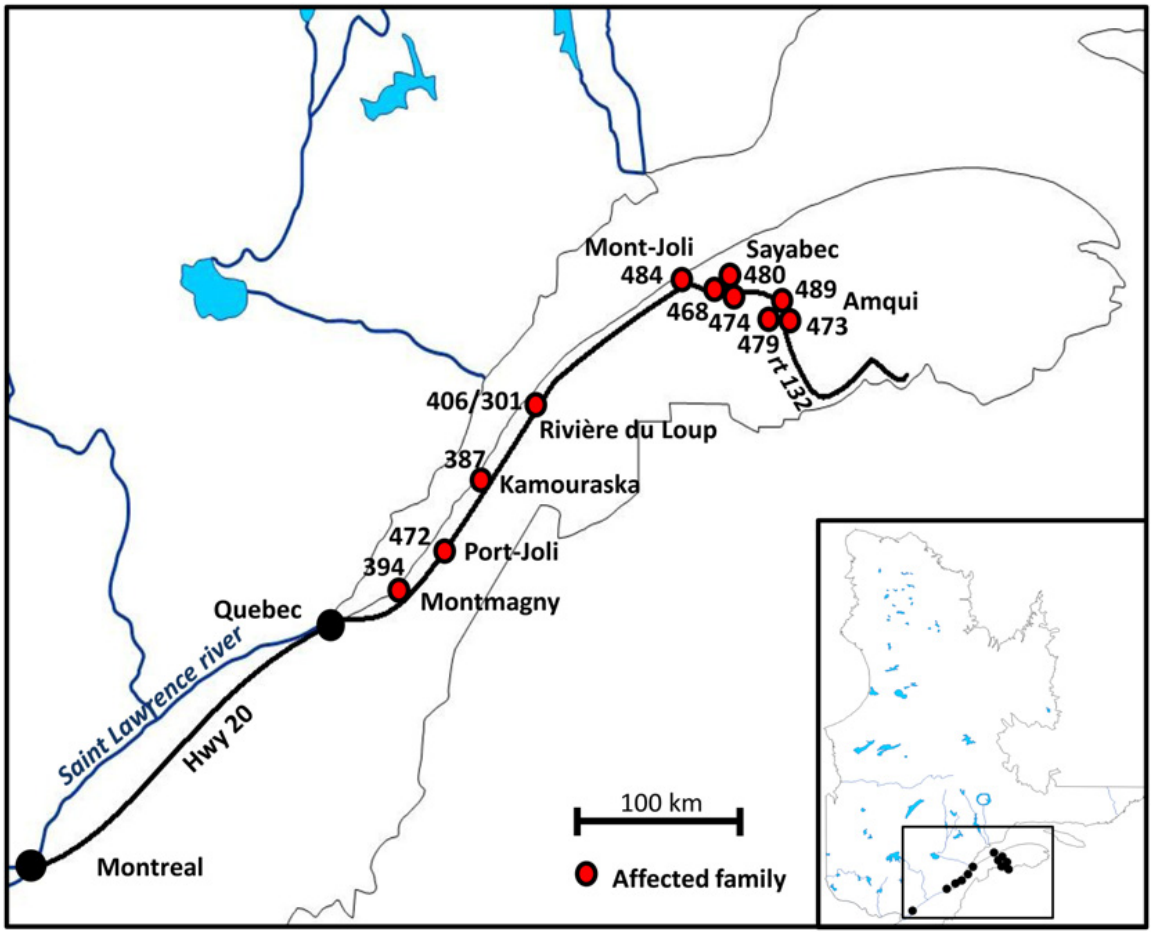

Figure 6. Distribution of individuals with Joubert syndrome in the Lower St-Lawrence region. Numbers refer to families (pedigrees in Figure 7). Note the cluster of families along Route 132, which follows the Matapedia river.

The population of the Lower St-Lawrence region was initially established as the result of the immigration of a limited number of settlers (6,000 individuals) from Quebec City and its surroundings in the late 17th century and beginning of the 18th century followed by a rapid increase due to a high fertility rate(39). The establishment of settlers in the region followed a west-to-east pattern, with later settlers migrating to regions further east. A small number of Acadians also contributed to the early population of the Matapedia region(40). The demographic growth of this population thus appears to be characterized by a series of bottlenecks that may have resulted in regional founder effects. We hypothesized that a founder effect could underlie the clustering of individuals with JBTS in the Lower St-

Lawrence region, raising the possibility that a common homozygous mutation explains a large fraction of them. We performed whole-genome SNP genotyping in all 15 individuals with JBTS using the Illumina Human 610 Genotyping BeadChip panel, which interrogates 620,901 SNPs, and searched for regions of homozygosity containing >30 consecutive SNPs and extending over >1Mb with PLINK(61). We identified several overlapping regions of shared homozygosity, but these regions were not found in more than 5 families, were small (1 megabase or less), and contained genes that are unlikely to play a role in cilia development and/or function (supplementary data; Table S1, p. 35). Altogether, the genotyping data suggest the presence of allelic and/or genetic heterogeneity within our cohort.

Given the lack of hints from genotype-based mapping, we decided to sequence the protein-coding exomes of all our subjects with JBTS in the hope of identifying a unique candidate gene harboring private pathogenic variants in a large fraction of the samples. Genomic DNA from each sample was captured with the Agilent SureSelect 50 Mb oligonucleotide library, and the captured DNA was sequenced with paired-end 100 bp reads on Illumina HiSeq2000 resulting in an average of 14.7 gigabases (Gb) of raw sequence for each sample. Data were analyzed as previously described(62). After removing putative PCR-generated duplicate reads using Picard (v. 1.48), we aligned reads to human genome assembly hg19 using a Burroughs-Wheeler algorithm (BWA v. 0.5.9). Median read depth of bases in consensus coding sequence (CCDS) exons was 115 (determined with Broad Institute Genome Analysis Toolkit v. 1.0.4418)(63). On average 88% (±2.9%) of bases in CCDS exons were covered by at least 20 reads. We called sequence variants using Samtools (v. 0.1.17), Pileup, and varFilter using custom scripts, requiring at least 3 variant reads as well as >20% variant reads for each called position, with Phred-like quality scores of at least 20 for single nucleotide variants (SNVs) and at least 50 for small insertions or deletions (indels). Annovar was used to annotate variants according to the type of mutation, occurrence in dbSNP, SIFT score, and 1000 Genomes allele frequency(64). To identify potentially pathogenic variants we filtered out: 1) synonymous variants or intronic variants other than those affecting the consensus splice sites; 2) variants seen in more than one of 261 exomes from individuals with rare, monogenic diseases unrelated to JBTS that were sequenced at the McGill University and

Genome Quebec Innovation Centre; and 3) variants with a frequency greater than 0.5% in the 1000 genomes dataset (Table 3).

We first examined the exome datasets to look for rare variants in the 15 genes already associated with JBTS (*INPP5E* [MIM 613037]*, TMEM216* [MIM 613277], *AHI1* [MIM 608894], *NPHP1* [MIM 607100], *CEP290* [MIM 610142], *TMEM67* [MIM 609884], *RPGRIP1L* [MIM 610937], *ARL13B* [MIM 608922], *CC2D2A* [MIM 612013], *CXORF5* [MIM 300170], *KIF7* [MIM 611254], *TCTN1* [MIM 609863], *TCTN2* [MIM 613885], *TMEM237* [MIM 614424], *CEP41*)(41-58), as well as in the JBTS candidate gene *TTC21B* (MIM 612014)(65)[28]. Two individuals (II-1 from family 484 and II-2 from family 473, Figure S2. p. 37), not known to be related, were each found to be carrying two heterozygous missense variants (c.4667A>T [p.Asp1556Val] and c.3376G>A [p.Glu1126Lys]) in *CC2D2A* (RefSeq NM_001080522.2)(51, 52). These amino acids are highly conserved and both mutations are predicted to be deleterious according to SIFT (scores <0.05)(66) and Polyphen-2 (scores >0.90)(67) (supplementary data; Fig. S1, p 42). The c.4667A>T (p.Asp1556Val) mutation has already been reported in individuals with JBTS(68). Segregation studies indicated that the affected individuals, but none of their unaffected first-degree relatives, were

Filters Applied (Sequentially)	Number of Variants Retained
Nonsynonymous, splicing, and coding indel variants	34,157[a]
After excluding variants present in >1 in-house exome	7,075
After excluding variants reported in 1,000 Genomes Browser (frequency > 0.5%)	6,911

[a]Total number of variants identified in the combined 13 exomes; redundant variants were counted only once.

Table 3. Variant prioritization steps in the analysis of combined sequences from 13 individuals with JBTS

compound heterozygotes for these mutations (supplementary data; Fig. S2, p. 42). We conclude that these mutations are likely pathogenic. Both individuals have a mild phenotype. They have oculomotor apraxia and only mild motor delay (they walked at 18 and 19 months and do not have gait ataxia). The individual who is school-aged performs well in a regular classroom. Four additional individuals were singly heterozygous for rare variants in the other known JBTS genes (c.265C>T [p.Leu89Phe] in *TMEM216 [NM_001173991.2]*, c.3257A>G [p.Glu1086Gly] in *AHI1 [NM_001134831]*, c.1600G>A [p.Glu534Lys] in *CEP290* [NM_025114.3], c.3032T>C [p.Met1011Thr] in *TTC21B [NM_024753.4*]). As each of these genes has previously been associated with recessive JBTS, these heterozygous variants are unlikely to fully explain the disorder for these persons.

We next looked at the whole exome data for other protein-coding genes containing homozygous or multiple heterozygous variants in the 13 affected individuals not explained by *CC2D2A* (Table 4). Strikingly, five subjects, including a member of the initial JBTS family, carried two different heterozygous variants in an unstudied anonymous gene, *C5ORF42* (Refseq # NM_023073.3). Mutations in 6 other genes were found in affected individuals among sets of three families (Table 4). Because these latter genes (*MUC5B, PLEC, FAT3, FLG, TTN, LAMA5*) are known to accumulate mutations at a high rate, they are unlikely to be linked to the disease

Number of Families with Mutations in the Same Gene	Number of Genes	Gene Identity
1 family	528	*C5ORF42*, …
2 families	16	*C5ORF42, ACAN, ADAMTS18, C10orf68, FSIP2, LRP1B, MUC12, MUC16, MUC4, MYO16, PKD1L2, PKHD1L1, RGPD4, SHROOM4, TMEM231, ZNF717*
3 families	7	*C5ORF42, MUC5B, PLEC, FAT3, FLG, TTN, LAMA5*
4 families	1	*C5ORF42*
5 families	1	*C5ORF42*
>5 families	0	-

Table 4. Genes with rare homozygous or multiple heterozygous variants from the combined exome sequences from 13 individuals with JBTS

(supplementary Table S2, p. 40). All 5 affected individuals with changes in *C5ORF42* carried the same missense mutation (c.4006C>T [p.Arg1336Trp]; NM_023073.3) as well as one of three different mutations: one mutation that affects a consensus donor splice site (c.7400+1G>A; NM_023073.3) and two truncating mutations (c.6407delC [p.Pro2136Hisfs*31] and c.4804C>T [p.Arg1602X]; NM_023073.3) (Fig. 7-8; Table 5). Sanger sequencing in the five affected individuals confirmed the presence of these variants. Segregation studies indicated that the affected individuals, but not their unaffected first-degree relatives, were compound heterozygotes for these variants (Fig. 7; Table 5). Subsequently, we were able to collect DNA from individual II-2 (individual M.D. in refs (1, 60)), the affected brother of II-1 in the initial JBTS family (family 394), and found that he was a compound heterozygote for the same *C5ORF42* mutations as those identified in his affected sister (Fig 7B; Table 5). None of these 4 variants was detected in 261 in-house control exomes, which were derived from other projects including some French Canadian subjects, and in the 1000 genomes dataset. RT-PCR done on RNA extracted from the blood of individuals II-2/family 394 and III-4/family 406-301 carrying the c.7400+1G>A splicing mutation, showed that this mutation causes skipping of exon 35 in *C5ORF42* (NM_023073.3), resulting in the creation of a premature stop codon (supplementary data; Fig. S2. p. 41). The p.Arg1336Trp amino acid substitution is predicted to be damaging (SIFT = 0.00; Polyphen-2 = 0.99), affecting a residue that is conserved across vertebrate species (Fig. 8B).

Based on the exome sequencing data, four additional individuals with JBTS from three families (301, 468, 489) were each carrying a single heterozygous mutation in *C5ORF42*, including the already described mutations c.4006C>T (p.Arg1336Trp) and c.7400+1G>A as well the truncating mutation c.7477C>T (p.Arg2493X) (NM_023073.3) (Fig. 7, Table 5). The c.7477C>T (p.Arg2493X) mutation was absent from our 261 control exomes and the 1000 genomes dataset. Our SNP genotyping data suggested that these four individuals, but not the other individuals with JBTS in our cohort, are heterozygous for a unique 5 Mb haplotype that encompasses *C5ORF42* (supplementary data; Fig. S3, p. 42). It seemed unlikely that this haplotype would be carrying three different rare mutations, hence this observation suggested

that the four individuals might carry a second mutation linked to this haplotype. Upon fur ther inspection of the exome data, we discovered that all four individuals are also heterozygous for

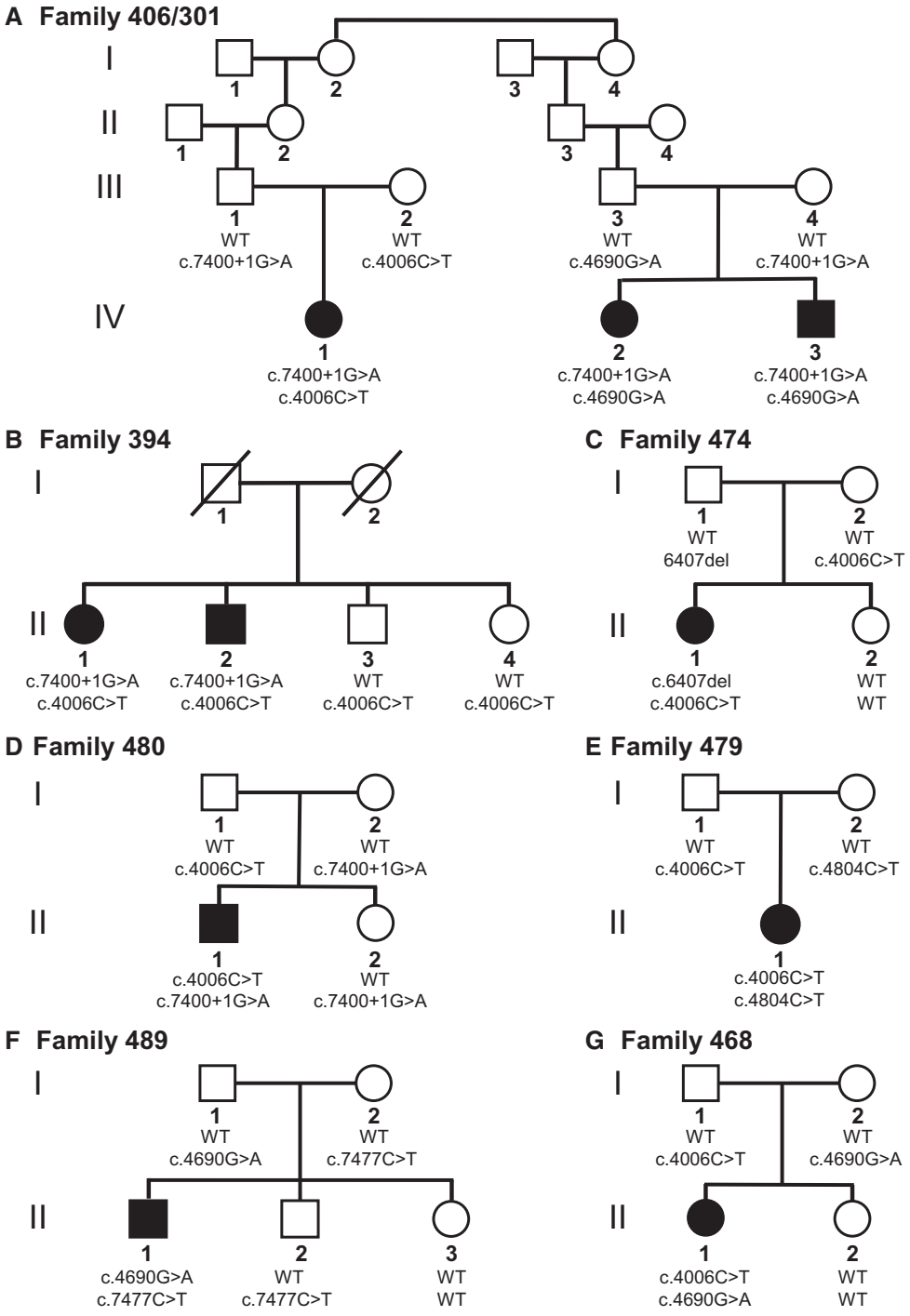

Figure 7. Segregation of *C5orf42* mutations in families affected with JBTS

another missense variant, c.4690G>A (p.Ala1564Thr) (based on the ENST00000388739 transcript annotated by the Ensemble Genome Browser). This allele was not included in our original filtered dataset because it is located in an internal coding exon (chr5:37157522-37157415) not annotated by RefSeq for the longest isoform of the gene (NM_023073.3). Sanger sequencing confirmed the presence of the various mutations in the four affected individuals. Segregation studies showed that the four affected individuals, but none of their unaffected first-degree relatives, were compound heterozygous for the mutation c.4690G>A (p.Ala1564Thr) and for one of the 3 other mutations (c.4006C>T [p.Arg1336Trp], c.7400+1G>A, c.7477C>T [p.Arg2493X]) (Fig. 7). The additional, alternative exon with the c.4690G>A (p.Ala1564Thr) mutation, which we designate exon 40a, occurs between RefSeq (NM_023073.3) annotated exons 40 and 41, is present in brain EST clones with accession numbers AK096581 and BC144070, and retains the large open reading frame of the gene. Using RNA-sequencing data made publicly available by Illumina's Body Map 2.0 (see URL below), we were able to confirm the expression of the exon. The assembly of raw data from 16 different tissues identified a large number of reads mapping to that exon in both brain and testes samples with significantly fewer reads in other tissues (supplementary data; Fig. S4, p. 43). Reads covering both ends of the exon, splicing correctly to neighboring exons, were found in either brain or testes samples. c.4690G>A (p.Ala1564Thr) was also absent from our 261 control exomes, and in the 1000 genomes dataset. It was not possible to get accurate SIFT or Polyphen-2 predictions on this mutation due to the lack of annotation of the corresponding exon across species.

We further addressed the frequency of the six putative *C5ORF42* mutations identified in our JBTS individuals, in the French Canadian population. Genotyping 477 French Canadian controls, including 96 Acadians subjects and 96 subjects from the Gaspésie region located immediately east of Matapedia, did not identify any of the six *C5ORF42* mutations. However, some of these mutations are reported in the heterozygous state at very low frequencies in the NHLBI Go Exome Sequencing Project (ESP) dataset, including c.4006C>T (p.Arg1336Trp) (2/10754; MAF = 0.0186%), c.7477C>T (p.Arg2493X) (1/10755; MAF = 0.009%; rs139675596), and c.7957+288G>A (p.Ala1564Thr) (12/4574; MAF = 0.262%;

rs111294855). It should be noted that c.4006C>T and c.7477C>T correspond to CpG sites, which are associated with a higher mutation rate, possibly explaining the recurrence of these nonetheless rare mutations in different populations.

The presence of 5 potentially deleterious mutations in *C5ORF42,* segregating with the disease in 7 presumably unrelated (though all French-Canadian) families, strongly suggests that disruption of this gene causes JBTS in our subjects. It remains uncertain whether the mutation c.4690G>A (p.Ala1564Thr) is pathogenic, considering that it is not clearly deleterious, and that it is found at a higher frequency (0.26%) in the ESP dataset than the other mutations. It is possible that this variant is linked to another mutation on the same haplotype that was not identified by our exome sequencing approach.

	Family 406/301			Family 394		Family 474	Family 480	Family 489	Family 479	Family 468
Genotype	**IV-1**	**IV-2**	**IV-3**	**II-1**	**II-2**	**II-1**	**II-1**	**II-1**	**II-1**	**II-1**
c.4006C>T (p.Arg1336Trp)	+	–	–	+	+	+	+	–	+	+
c.7400+1G>A	+	+	+	+	+	–	+	–	–	–
c.6407del (p.Pro2136Hisfs*31)	–	–	–	–	–	+	–	–	–	–
c.7477C>T (p.Arg2493*)	–	–	–	–	–	–	–	+	–	–
c.4804C>T (p.Arg1602*)	–	–	–	–	–	–	–	–	+	–
c.7957+288G>A (c.4690G>A [p.Ala1564Thr])	–	+	+	–	–	–	–	+	–	+
Age (years)	8	1.5	3	52	45	4	10	7	13	31
Sex	F	M	F	F	M	F	M	M	F	F
Developmental delay	+	+	+	+	+	+	+	+	+	+
Oculomotor apraxia	–	+	+	+	+	+	+	+	+	+
Breathing abnormality	+	+	+	+	+	+	+	+	–	–
Limb abnormality[a]	–	+	–	–	–	+	–	–	–	–
Brain MRI	MTS	MTS	MTS	ND	MTS	MTS	MTS	MTS	MTS	MTS
Retinal involvement[b]	– (f)	– (e)	– (e)	– (h)	– (h)	– (f)	– (e)	– (e)	– (f)	– (h)
Renal involvement[c]	– (us)	– (us)	– (us)	– (h)	– (h)	– (us)	– (us)	– (us)	– (us)	– (h)

The nucleotide and amino acid positions are based on reference sequence NM_023073.3 except for c.4690G>A (p.Ala1564Thr), which is based on Ensembl transcript ENST00000509849. The following abbreviations are used: F, female; M, male; MRI, magnetic resonance imaging; MTS, molar tooth sign; ND, not done; f, fundoscopy; e, electroretinogram; h, history; and us, ultrasound.
[a]Individual IV-2 from family 406/301 has a 3/4 syndactyly in the left hand and individual II.1 from family 474 has preaxial and postaxial polydactyly of the four limbs. Individual II-1 from family 394 did not undergo an MRI, but the MRI of her brother (individual II-2 from family 394) documented a MTS.
[b]Lack of retinal involvement was determined by electroretinogram, fundoscopy, or history.
[c]Lack of renal involvement was determined by renal ultrasound or history.

Table 5: Clinical description of JBTS individuals with *C5orf42* mutations

Very little is known about *C5ORF42* function. The RefSeq version of the full-length transcript (NM_023073.3; Ensemble ENST00000425232) apparently derives from virtual assembly of overlapping mRNA and EST clones. The predicted major mRNA isoform comprises 11,199 bp and contains 52 exons; the putative encoded protein is similarly large, comprising 3198 amino acids. With the exception of c.4690G>A (p.Ala1564Thr), all mutations reported herein are common to all annotated protein coding transcripts (Fig 8A). The predicted protein sequence is well conserved across much of the gene length in other vertebrates. It does not appear to contain any specific known functional domains, although Gene Ontology suggests it may be a transmembrane protein and ProtoNet predicts a coiled-coil structure within the protein. Proteomic studies reported interactions between C5ORF42 and the p21-activating kinase 1 (PAK1) and the small ubiquitin-like modifier 1 (SUMO1)(69, 70). Although the significance of these interactions remains to be validated and further investigated, it is noteworthy that these latter genes play a role in neural development(71, 72). EST-expression (Unigene data), microarray profiling (Allen Brain Atlas) and BioGPS, indicate that *C5ORF42* is widely expressed in a variety of tissues, including the brain.

In terms of genotype-phenotype correlation, all JBTS individuals with mutations in *C5ORF42* showed global developmental delay with onset of independent walking between 30 months and 8 years of age (Table 5). Cognitive impairment was present in all individuals but was variable, ranging from borderline intelligence to mild intellectual disability. The majority of individuals also showed oculo-motor apraxia and breathing abnormalities mainly characterized by episodes of hyperventilation. Two individuals showed limb abnormalities: pre- and post-axial polydactyly in one person and syndactyly of the third and fourth finger of a hand in another. There was no evidence of retinal or kidney involvement. There was no clear correlation between the type of *C5ORF42* mutation and the associated phenotype.

Surprisingly, we found that three mutations (c.4006C>T [p.Arg1336Trp], c.7400+1G>A, and c.4690G>A [p.Ala1564Thr]) in *C5ORF42* were present in multiple

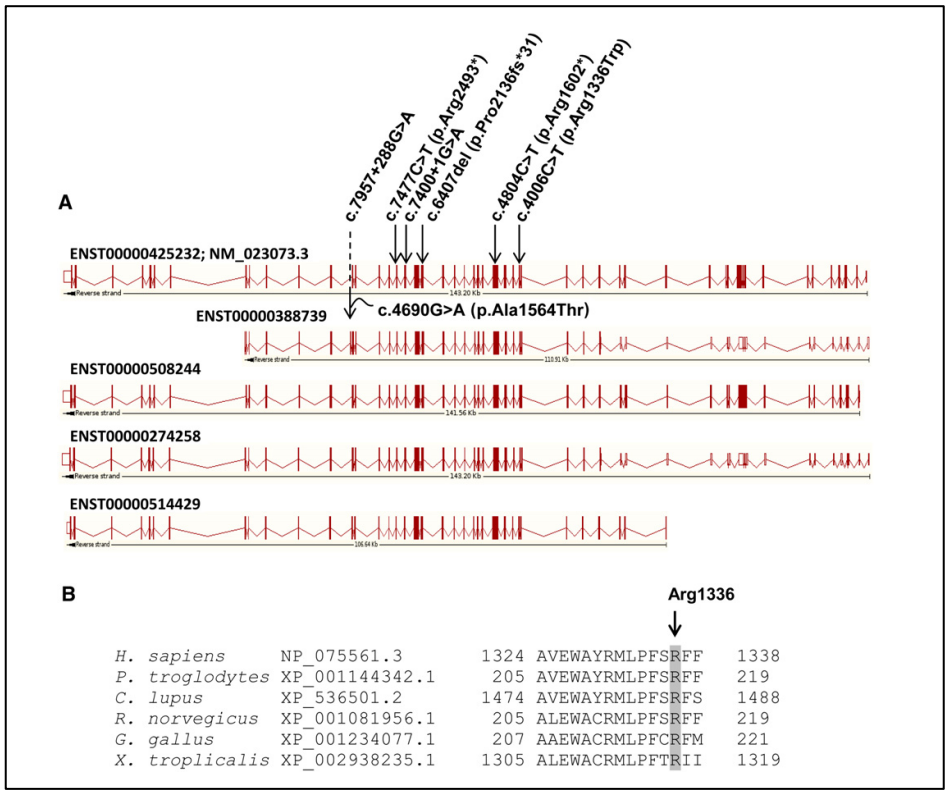

Figure 8. *C5orf42* mutations identified in individuals with Joubert Syndrome. A) Scheme showing the positions of the mutations with respect to the different *C5orf42* ENSEMBLE-annotated trancripts that are predicted to produce proteins. Numbering on top is based on the cDNA positons of ENST00000425232 (identical to NCBI Refseq # NM_023073.3). c.7957+288G>A is annotated as part of a coding exon in ENST00000388739, causing a missense change (p.Ala1564Thr). B) Homologene-generated (NCBI) amino acid alignment of human *C5orf42* with its predicted orthologues showing the conservation of the p.Arg1336 residue.

individuals in our cohort. Haplotyping studies indicate that each of these mutations is linked to a distinct haplotype in these families, despite the lack of documented genealogical relationships among them (supplementary data; Fig. S3, p.43). The higher frequency of these mutations in the population of the Lower St-Lawrence region could be explained by a founder effect with the coincidental occurrence of the three mutations in the same group of settlers or by multiple regional founder effects corresponding to sequential pioneer fronts. Although founder effects are typically associated with an increase in the frequency of a specific

allele(70), often accompanied by other alleles that remain at their usual background frequency, they can also involve multiple common mutations(73, 74).

In summary, after the initial description of JBTS in a French Canadian family 40 years ago, we have shown that mutations in *C5ORF42* explain this neurodevelopmental disorder in many affected individuals from the French Canadian population. We have also found that *C5ORF42* is associated with a complex founder effect in this population. Although the function of *C5ORF42* remains unknown, future studies will likely elucidate its role in cilia development and/or function.

Supplemental data

Supplemental data include 2 tables and 5 figures

ACKNOWLEDGEMENTS

Foremost we thank the families who generously contributed their time and materials to this research study. This work was selected for study by the FORGE Canada Steering Committee, consisting of K. Boycott (U. Ottawa), J. Friedman (U. British Columbia), J. Michaud (U. Montreal), F. Bernier (U. Calgary), M. Brudno (U. Toronto), B. Fernandez (Memorial U.), B. Knoppers (McGill U.), M. Samuels (U. de Montreal), and S. Scherer (U. Toronto). We would like to thank Janet Marcadier (Clinical Coordinator) and Chandree Beaulieu (Project Manager) for their contribution to the infrastructure of the FORGE Canada Consortium. The authors wish to acknowledge the contribution of the high throughput sequencing platform of the McGill University and Génome Québec Innovation Centre, Montréal, Canada.This work was funded by the Government of Canada through Genome Canada, the Canadian Institutes of Health Research (CIHR) and the Ontario Genomics Institute (OGI-049). Additional funding was provided by Genome Quebec and Genome British Columbia. K. Boycott is supported by a Clinical Investigatorship Award from the CIHR Institute of Genetics. J.L. Michaud is a National Scholar from the Fonds de la Recherche en Santé du Québec (FRSQ). M. Srour holds a training award from the FRSQ.

Web Resources
1000 Genomes Project, http://browser.1000genomes.org/index.html
Allen Brain Atlas, http://www.brain-map.org/
BioGPS, http://biogps.org
dbSNP, http://www.ncbi.nlm.nih.gov/projects/SNP/
Ensemble Genome Browser: http://www.ensembl.org
ESP exome variant server: http://evs.gs.washington.edu/EVS/
Gene Ontology, http://www.geneontology.org/
Illumina's Body Map 2.0 transcriptome:
http://www.ebi.ac.uk/arrayexpress/browse.html?keywords=E-MTAB-513
NCBI homologene, http://www.ncbi.nlm.nih.gov/homologene
NCBI Nucleotide database, http://www.ncbi.nlm.nih.gov/nuccore
Online Mendelian Inheritance in Man (OMIM), http://www.omim.org
Polyphen-2: http://genetics.bwh.harvard.edu/pph2/
SIFT: http://sift.jcvi.org/
Unigene, http://www.ncbi.nlm.nih.gov/unigene

Contributorship statements: MS: study design, data analysis and interpretation, writing and revision, patient recruitment, examination and counseling. FFH, JM and JLM: study design, data analysis and interpretation and writing and revision. JS: data analysis and manuscript writing and revision. GM, EL, LP, JMCC, SPC and SD: laboratory follow-up of candidate variants and segregation studies. MS, JLM, LHO, MIS, VD, DA, EA, BM, KMB, RL: patient recruitment, examination and counseling. DL, GAR: contribution of control samples. CM: coordination of samples and patient consents.

Supplemental Data and Figures

Chromosome	Size (Mb)	Start position	End position	# of patients	Genes in interval
12	1.01	38,120,168	39,128,892	5	*ALG10B, CPNE8*
8	1.15	48,439,013	49,589,706	4	*KIAA0145, CEBPD, PRKDC, MCM4, UBE2V2*
4	0.96	151,184,163	152,147,262	4	*LRBA, MAB21L2, RPS3A, SNOD73A, SH3D19*
7	0.57	119,321,200	119,887,000	4	*KCND2*
7	0.37	118,773,000	119,239,292	4	none
2	1.07	135,745,129	136,740,556	3	*YSK4, RAB3GAP1, ZRANB3, R3HDM1, MIR128-1, UBXN4, LCT, LOC100507600, MCM6, DARS*
2	0.58	186,303,487	186,895,680	3	*FSIP2*
12	0.28	39,288,892	39,566,178	3	*CPNE8*
4	0.25	150,854,889	151,103,870	3	*DCLK2*

Table S1. Regions of identical homozygosity shared by 3 or more patients with Joubert syndrome. In each patient, Plink was used to identify regions of homozygosity >30 consecutive SNPs and >1Mb in size. Thereafter, Excel was used to identify overlapping regions of identical homozygosity shared by 3 or more individuals. RefSeq genes from the intervals (hg19) are noted in the table.

Gene	Rank (out of 20870) by mutation frequency	Number of rare mutations
TTN	2	191
MUC5B	4	130
FLG	9	88
PLEC	10	82
LAMA5	12	73
FAT3	74	37
C5ORF42	2248*	9

* *C5ORF42* is tied with 519 other genes.

Table S2- Frequency of rare mutations in the candidate genes. We have observed that certain genes frequently have private mutations in our previous samples. To quantify this, we determined the number of "rare" mutations in each of 20870 genes annotated in Ensembl, where we defined a rare mutation as one with a 1000 genomes minor allele frequency < 0.005 and which was seen in two or fewer of our control exomes. The table shows the number of such rare mutations in our 261 control exomes for the frequently mutated genes in which multiple mutations were found in 3 JBTS families each.

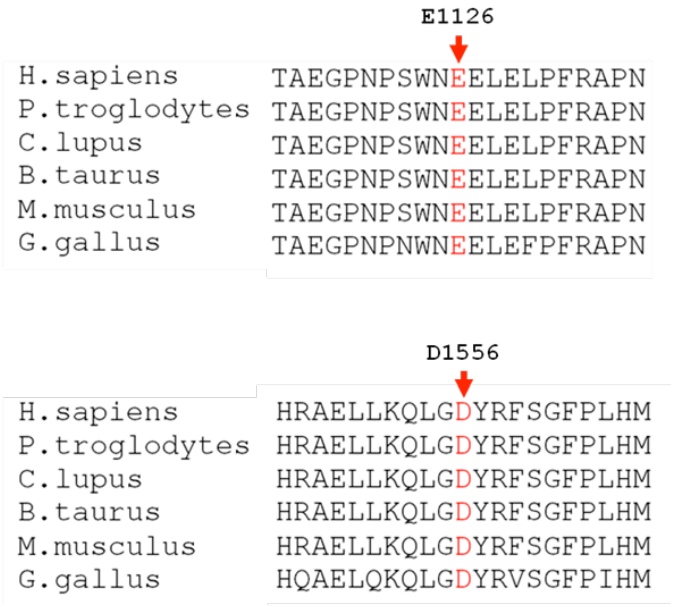

Figure S1: Amino acid conservation of the residues affected by the p.D1556V and p.E1126K mutations in *CC2D2A*. Amino acid alignments were generated using homologene (NCBI).

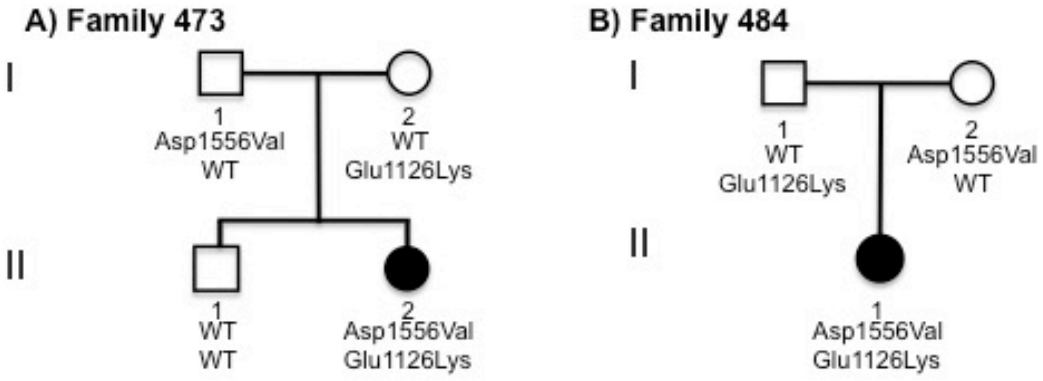

Figure S2: Segregation of p.D1556V and p.E1126K *CC2D2A* mutations. We identified compound heterozygous mutations in *CC2D2A* (c.G3376A/p.D1556V and c.A4667T/p.E1126K, numbering according to Refseq NM_001080522.2) in two unrelated individuals with JBTS. These mutations are predicted to be damaging according to SIFT and

Polyphen-2. Both patients had a mild phenotype with oculomotor apraxia and mild developmental delay.

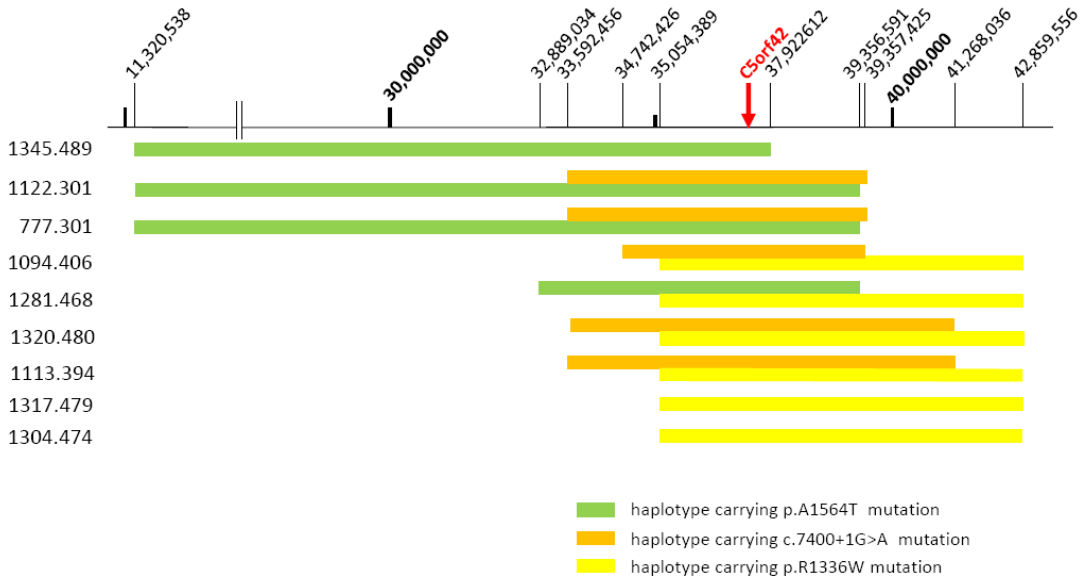

Figure S3. Schematic diagram showing shared haplotypes in region surrounding *C5ORF42* in the JBTS patients. Patient numbers are noted in the left-hand column. Chromosome 5 coordinates are noted on the horizontal axis (hg19). Position of *C5ORF42* is identified by the red arrow. The Homozygosity Haplotype (HH) method [1, 2] was used to assess whether patients with identical *C5ORF42* mutations shared a common haplotype around *C5ORF42*. Briefly, instead of formally phasing haplotypes, the HH method uses a reduced haplotype described only by the homozygous SNPs (the heterozygous SNPs are removed) from the high density SNP genotyping data. Patients who inherited the same mutation from a common ancestor share a chromosomal segment identical by descent around the mutation, and do not have discordant homozygous calls in that region. Analysis shows that patients with identical mutations share a common haplotype around *C5ORF42* spanning 5.03Mb (chr5:32,889,034-37,922,612) for the p.A1564T mutation, 4.61Mb (chr5:34,742,426-39,357,425) for the c.7400+1G>A mutation and 7.8Mb (chr5:35,054,389-42,823,549) for the p.R1336W mutation.

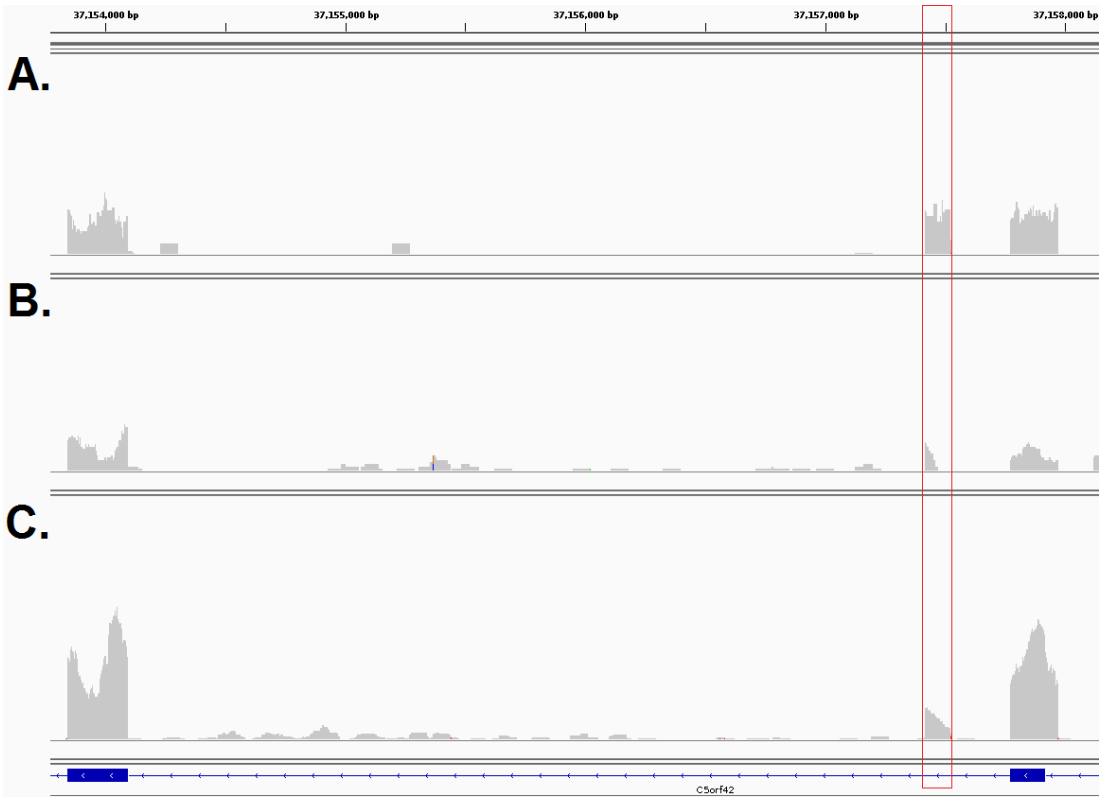

Figure S4. Coverage histograms of RefSeq unannotated *C5ORF42* exon 40a (in red box) in different tissues. The vertical grey bars indicate the number of reads from (a) testis, (b) brain and (c) a mixture of adipose, adrenal, breast, colon, heart, kidney, liver, lung, lymph, ovary, prostate, skeletal muscle, thyroid, and white blood cell tissues. The proportions of reads containing the target exon versus the ones that do not are respectively (a) 21/23, (b) 13/18 and (c) 44/130. Reads were controlled for quality using FastX tools, assembled with TopHat, indexed with SAMtools and displayed with IGV. The tissue mixture (c) was obtained by merging the reads from the various tissues using SAMtools.

References

1. Miyazawa, H., Kato, M., Awata, T., Kohda, M., Iwasa, H., Koyama, N., Tanaka, T., Huqun, Kyo, S., Okazaki, Y. et al (2007). Homozygosity haplotype allows a genomewide search for the autosomal segments shared among patients. Am J Hum Genet *80*, 1090-1102.

2. Jiang, H., Orr, A., Guernsey, D.L., Robitaille, J., Asselin, G., Samuels, M.E., Dube, M.P. (2009). Application of homozygosity haplotype analysis to genetic mapping with high-density SNP genotype data. PLoS. One. *4*, e5280.

Chapter 3:

Mutations in *TMEM231* cause Joubert syndrome in French Canadians

Following the publication of the previous manuscript, we identified 8 additional French-Canadian JBTS families from other regions of Quebec. We performed WES in these affected individuals, and analyzed the data by combining the WES datasets of all our unexplained JBTS individuals.

Manuscript 2:
Mutations in *TMEM231* cause Joubert syndrome in French Canadians

Published in: J Med Genet. 2012 Oct;49(10):636-41; PMID: 23012439

Myriam Srour[1], Fadi F. Hamdan[1], Jeremy Schwartzentruber[2], Lysanne Patry[1], Luis H. Ospina[3], Michael I. Shevell[4], Valérie Désilets[5], Sylvia Dobrzeniecka[1], Géraldine Mathonnet[5], Emmanuelle Lemyre[5], Christine Massicotte[1], Damian Labuda[5], Dina Amrom[1], Eva Andermann[6], Guillaume Sébire[7], Bruno Maranda[8], Guy A. Rouleau[9], Jacek Majewski[2,6], Jacques L. Michaud[1]

[1]Centre of Excellence in Neurosciences of Université de Montréal and Sainte-Justine Hospital Research Center, Montréal H3T 1C5, Canada; [2]McGill University and Genome Quebec Innovation Centre, Montréal H3A 1A4, Canada; [3]Department of Ophthalmology, Sainte-Justine Hospital Research Center, Montréal, H3T 1C5, Canada; [4]Division of Pediatric Neurology, Montreal Children's Hospital-McGill University Health Center, Montreal, H3H 1P3, Canada; [5]Sainte-Justine Hospital Research Center, Montréal H3T 1C5, Canada; [6]Department of Human Genetics, McGill University, H3A 1A4, Montréal, Canada; [7]Division of Pediatric Neurology, Centre Hospitalier Universitaire de Sherbrooke, Sherbrooke, J1H 5N4, Canada; [8]Division of genetics, Centre Hospitalier Universitaire de Sherbrooke, Sherbrooke, J1H 5N4, Canada ; [9]Centre of Excellence in Neurosciences of Université de Montréal and Department of Medicine, Montréal H2L 2W5, Canada;

ABSTRACT

Background: Joubert syndrome (JBTS) is a predominantly autosomal recessive disorder characterized by a distinctive mid-hindbrain malformation, ocular-motor apraxia, breathing abnormalities and developmental delay. JBTS is genetically heterogeneous, involving genes required for formation and function of non-motile cilia. Here we investigate the genetic basis of JBTS in 12 French Canadian individuals. **Methods and Results:** Exome sequencing in all subjects showed that six carried rare compound heterozygous mutations in *CC2D2A* or *C5ORF42*, known JBTS genes. In addition, three individuals (2 families) were compound heterozygous for the same rare mutations in *TMEM231*(c.12T>A[p.Tyr4*]; c.625G>A[p.Asp209Asn]). All three subjects showed a severe neurological phenotype and variable presence of polydactyly, retinopathy and renal cysts. These mutations were not detected among 385 French Canadian controls. TMEM231 has been previously shown to localize to the ciliary transition zone and interact with several JBTS gene products in a complex involved in the formation of the diffusion barrier between the cilia and plasma membrane. siRNA knockdown of TMEM231 was previously shown to affect barrier integrity, resulting in a reduction of cilia formation and ciliary localization of signaling receptors. **Conclusion:** Our data suggest that mutations in *TMEM231* cause JBTS, reinforcing the relationship between this condition and the disruption of the barrier at the ciliary transition zone.

Joubert syndrome (JBTS [MIM213300]) is a predominantly autosomal recessive disorder characterized by ocumolotor apraxia, abnormal breathing, ataxia, and variable developmental delay or intellectual impairment (reviewed in Sattar et al)(75). A cardinal sign of JBTS is the presence of a complex mid-hindbrain malformation consisting of hypoplasia of the cerebellar vermis, abnormally deepened interpeduncular fossa at the level of the upper pons and elongated and thickened superior cerebellar peduncles. This malformation takes the appearance of a molar tooth on MRI. Extra-neurological manifestations, including retinopathy, renal cysts and polydactyly, are present in a subset of affected individuals. JBTS is genetically heterogeneous, with 17 genes described to date (41-44, 47, 50, 53-57, 76, 77), all of which appear to play a role in the development and/or function of nonmotile cilia.

There is a high prevalence of JBTS in the French Canadian (FC) population of the Lower Saint-Lawrence region of Quebec. We recently performed exome sequencing in 15 individuals (11 families) with JBTS from that region and found that mutations in *C5ORF42* explain JBTS in 9 individuals (seven families)(77). In addition, we identified pathogenic compound heterozygous mutations in *CC2D2A*, a previously known JBTS gene, in 2 affected individuals from 2 different families. The genetic basis of JBTS remained unexplained in 4 individuals (2 families) from this initial study. Here, we follow up on our previous investigation by performing exome sequencing in 8 additional individuals with JBTS (6 unrelated families) originating from other regions of Quebec.

The 6 probands had a molar tooth sign (MTS) on imaging, and variable expression of the classical JBTS features. The two additional individuals are the uncle (II-4) and aunt (II-6) of subject IV-1 in family 385/447. These individuals were considered to have a variable expression of JBTS as they both had oculomotor apraxia, and II-4 additionally had gait ataxia and a history of developmental delay. Brain MRI was normal in II-6 but was not done in II-4. Informed consent was obtained from each individual or legal guardian. This study was approved by our institutional ethics committee. Genomic DNA from each sample was captured with the Agilent SureSelect 50 Mb exome capture oligonucleotide library, and the captured DNA was sequenced with paired-end 100 bp reads on Illumina HiSeq 2000 resulting

in an average of 12.7 gigabases (Gb) of raw sequence for each sample. Data were analyzed as previously described(63). After removing putative PCR-generated duplicate reads using Picard (v. 1.48), we aligned reads to human genome assembly hg19 using a Burroughs-Wheeler algorithm (BWA v. 0.5.9). Median read depth of bases in consensus coding sequence (CCDS) exons was 99 (determined with Broad Institute Genome Analysis Toolkit v. 1.0.4418)(64). On average 87% (±2.0%) of bases in CCDS exons were covered by at least 20 reads. We called sequence variants using Samtools (v. 0.1.17) mpileup and varFilter, and required at least 3 variant reads as well as >=20% variant reads for each called position, with Phred-like quality scores of at least 20 for single nucleotide variants (SNVs) and at least 50 for small insertions or deletions (indels). We used Annovar and custom scripts to annotate variants according to the type of mutation, occurrence in dbSNP, SIFT score, 1000 Genomes allele frequency, and NHLBI exomes allele frequency(66). To identify potentially pathogenic variants we filtered out: 1) synonymous variants or intronic variants other than those affecting the consensus splice sites; 2) variants seen in more than two of 416 exomes from patients with rare, monogenic diseases unrelated to JBTS that were sequenced at the McGill University and Genome Quebec Innovation Centre; and 3) variants with a frequency greater than 0.5% in either the 1000 genomes or NHLBI exome datasets.

We first examined the 8 exome datasets to look for rare variants in the 17 known JBTS genes (*INPP5E*[MIM613037], *TMEM216*[MIM613277], *AHI1*[MIM608894], *NPHP1*[MIM607100], *CEP290*[MIM610142], *TMEM67*[MIM609884], *RPGRIP1L*[MIM610937], *ARL13B*[MIM608922], *CC2D2A*[MIM612013], *CXORF5*[MIM300170], *KIF7*[MIM611254], *TCTN1* [MIM609863], *TCTN2*[MIM613885], *TMEM237*[MIM614424], *CEP41*[MIM610523], *TMEM138*[MIM614459], *C5ORF42*[MIM614571](41, 43, 45, 49, 50, 52, 54, 58, 75, 78) as well as in the JBTS candidate gene *TTC21B*(MIM612014)[17]. Five individuals from 3 families (II-1 from family 379, II-4, II-6 and IV-1 from family 385/447, and II-1 from family 492- Figure S1, p. 58) were each found to carry two rare heterozygous variants in *CC2D2A*(NM_001080522.2). One in-frame amino acid deletion (c.3450_3452del[p.Val1151del]) and 4 different missense variants (c.3376G>A[p.Glu1126Lys], c.4559A>G[p.Asn1520Ser],

c.4667A>T[p.Asp1556Val], c.4702T>C[p.Tyr1568His]) were identified, two of which, c.3376G>A(p.Glu1126Lys) and c.4667A>T(p.Asp1556Val), were identified previously in FC individuals with JBTS(77). The novel mutations c.4559A>G(p.Asn1520Ser) and c.4702T>C(p.Tyr1568His) are predicted to be damaging (by SIFT, Polyphen-2 and Mutation Taster) and neither variant has been reported in the Exome Variant Server (EVS; NHLBI GO Exome Sequencing Project), dbSNP135 or 1000 Genome datasets. These five *CC2D2A* mutations cluster in either the C2 domain [amino acids 1062-1174] or the C-terminal part of the protein, as do most missenses that cause JBTS[18]. Segregation analysis revealed that all the affected individuals but none of their unaffected relatives were compound heterozygous for the mutations (Figure S1, p. 58). We conclude that these mutations are pathogenic and responsible for JBTS in these 5 individuals.

We also identified a frameshift mutation (c.8257_8258insA[p.Lys2753fs]) and a splice-site mutation (c.7400+1G>A) in *C5ORF42*(NM_023073.3) in individual II-2 from family 551. Sanger sequencing showed that the proband is compound heterozygous for these mutations. The splice site (c.7400+1G>A) mutation has been previously identified in patients with JBTS and shown to result in skipping of exon 35 and the creation of a premature stop codon while c.8257_8258insA(p.Lys2753fs), which is novel, is predicted to truncate *C5ORF42* in the middle of its sequence, close to where other truncating mutations have been previously identified in JBTS patients(77). Both *C5ORF42* mutations are thus considered pathogenic in this individual. Table 6 summarizes the genotypes and phenotypes of these patients with mutations in *CC2D2A* and *C5ORF42* as well as those of FC patients previously described with mutations in these genes. Individuals in our cohort with mutations in *CC2D2A* do not have any extra-neural manifestations, and appear to have a milder phenotype, with all affected individuals walking independently before the age of 4 years, and intelligence ranging from normal to mild intellectual impairment. Individuals with mutations in *C5ORF42* have a more variable phenotype. They have borderline to moderate cognitive impairment and age at walking ranging between 30 months and 8 years. Some patients also showed limb abnormalities, including one individual with combined pre- and post-axial polydactyly, an unusual finding in JBTS, which is typically associated with post-axial polydactyly.

We then combined the exome data of the 2 remaining individuals with unexplained JBTS and the exome data of 4 individuals with unexplained JBTS from our previous study[12], making a total of 6 individuals from 4 different families. We analyzed the data by looking for protein-coding genes that contained homozygous or multiple heterozygous variants in each affected individual. For multiplex families, we only considered genes with the same variants in the affected siblings (Supplemental Tables 1 and 2, pages 60-61). Only one gene, *TMEM231*, harbored multiple rare mutations in more than one family. Three JBTS individuals from 2 families (II-1 and II-2 from family 387, and II-1 from family 483) harbored the same two variants in *TMEM231*(NM_001077418.1): c.12T>A(p.Tyr4*) and c.625G>A(p.Asp209Asn). Sanger sequencing showed that all affected individuals were compound heterozygous for these variants (Figure 9A). The c.12T>A(p.Tyr4*) mutation targets exon 1 of the canonical isoform of *TMEM231*(NM_001077418.1; ENST00000258173), as well as the 2 other predicted protein-coding isoforms reported in the Ensemble Genome Browser. In ENST00000565067 it leads to the same nonsense change

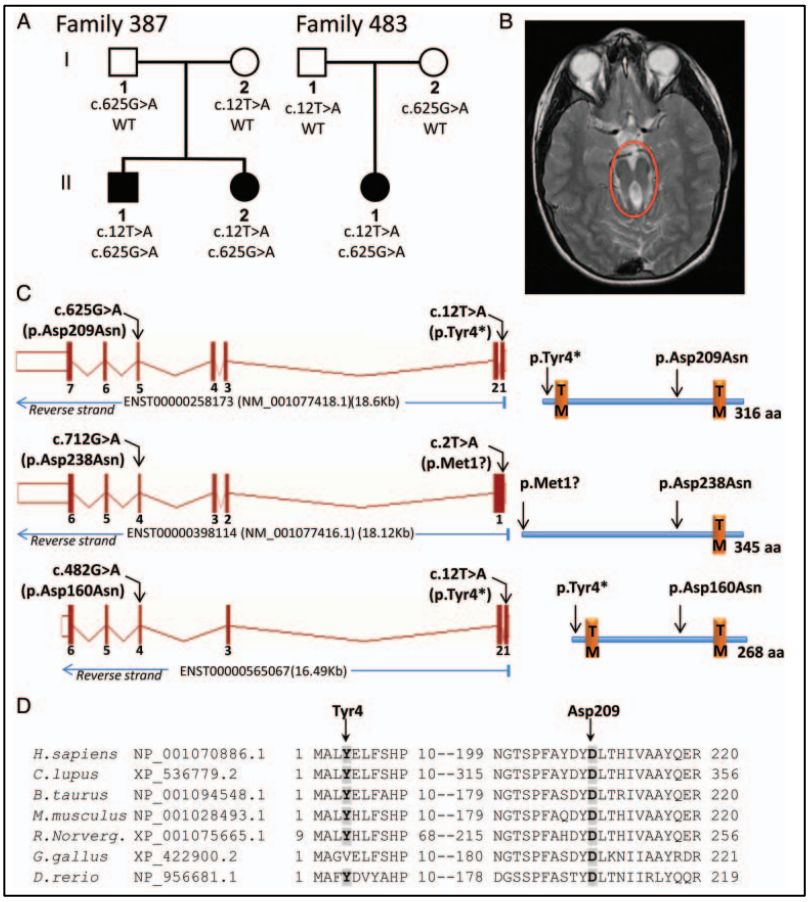

Figure 9. *TMEM231* mutations identified in JBTS individuals. (A) Segregation of mutations in *TMEM231* in JBTS families. (B) Brain MRI from individual II-1 from family 387 showing the "molar tooth sign"; (C) *Left panel*, scheme showing the presence of the mutations with respect to the different *TMEM231* Ensemble-annotated transcripts predicted to produce proteins; *right panel*, the corresponding TMEM231 proteins are depicted in the right panel. TM, denotes the presence of a transmembrane domain, as predicted by *SMART* algorithm. (D) Amino acid conservation of the residues affected by the p.Tyr4* and p.Asp209Asn mutations in TMEM231. Amino acid alignments were generated using homologene (NCBI).

(p.Tyr4*), while in the longer isoform ENST00000398114 it abolishes the translation initiation methionine (c.2T>A[p. Met1?]), which would likely prevent translation of this isoform due to the absence of any other in-frame methionine in exons 1 and 2. The c.625G>A(p.Asp209Asn) causes the same amino acid change in the different *TMEM231* predicted isoforms (Fig.9C). It affects a highly conserved amino acid (Fig.9D), and is predicted to be damaging by Polyphen-2 and Mutation Taster but not by SIFT. Both p.Tyr4* and p.Asp209N are extremely rare. Amongst the 416 in-house exomes, the c.12T>A(p.Tyr4*) was not found, and the c.625G>A(p.Asp209Asn) variant was seen in the heterozygous state in one FC individual. No additional *TMEM231* coding/splicing variants were present in this individual's exome. To determine the carrier rate of c.625G>A and c.12T>A, we genotyped 385 healthy FC controls by Sanger sequencing but did not find any carriers of either of these mutations, indicating that they are very rare. Only p.Asp209Asn is reported in the 1000 genomes and EVS, but at a very low frequency (0.01%), while p.Tyr4* is not reported in any of these public SNP databases. Furthermore, no truncating mutations in *TMEM231* were seen in 416 control exomes of patients with other rare diseases, and only one other truncating variant (stopgain SNV) is reported in EVS, at a frequency of 0.04%. For the three individuals with compound heterozygous *TMEM231* mutations, we examined all SNV genotypes in regions surrounding the two mutations. This revealed a region of shared genotypes (two shared haplotypes) extending over at least 1.7 Mb, suggesting the existence of founder effects (Supplemental Table S1, p.60).

The three individuals with mutations in *TMEM231* are amongst the most severely affected in our French-Canadian JBTS cohort. They are dependent in all activities of daily living, are non-verbal, and can take steps only if assisted with a walker. Both siblings from family 387 had significant aggressive and self-mutilating behavior consisting of head banging and biting, requiring treatment with antipsychotic agents, mouth guard and protective helmet. Individuals II-2 from family 387 and II-1 from family 483 show extra-neural manifestations consisting of retinopathy, bilateral macroscopic renal cysts (but normal renal function), and post-axial polysyndactyly of one foot (Table 6).

	Srour *et al*[12]												This study								
	406/301			394		474	480	489	479	468	473	484	385/447			379	492	551	387		483
Genotypes	**IV-1**	**IV-2**	**IV-3**	**II-1**	**II-2**	**II-1**	**II-1**	**II-1**	**II-1**	**II-1**	**II-2**	**II-1**	**II-4**	**II-6**	**IV-1**	**II-1**	**II-1**	**II-2**	**II-1**	**II-2**	**II-1**
C5ORF42																					
c.4006C>T(p.Arg1336Trp)	+	–	–	+	+	+	+	–	+	+	–	–	–	–	–	–	–	–	–	–	–
c.7400+1G>A	+	+	+	+	+		+	–	–	–	–	–	–	–	–	–	–	+	–	–	–
c.6407del(p.Pro2136Hisfs*31)	–	–	–	–	–	+	–	–	–	–	–	–	–	–	–	–	–	–	–	–	–
c.7477C>T(p.Arg2493*)	–	–	–	–	–	–	–	+	–	–	–	–	–	–	–	–	–	–	–	–	–
c.4804C>T(p.Arg1602*)	–	–	–	–	–	–	–	–	+	–	–	–	–	–	–	–	–	–	–	–	–
c.7957+288G>A; c.4690G>A(p.Ala1564Thr)	–	+	+	–	–	–	–	+	–	+	–	–	–	–	–	–	–	–	–	–	–
c.8257_8258insA(p.K2753fs)	–	–	–	–	–	–	–	–	–	–	–	–	–	–	–	–	–	+	–	–	–
CC2D2A																					
c.4667A>T(p.Asp1556Val)	–	–	–	–	–	–	–	–	–	–	+	+	–	–	+	–	+	–	–	–	–
c.3376G>A(p.Glu1126Lys)	–	–	–	–	–	–	–	–	–	–	+	+	+	+	+	+	–	–	–	–	-–
c.4559A>G(p.Asn1520Ser)	–	–	–	–	–	–	–	–	–	–	–	–	+	+	–	–	–	–	–	–	–
c.4702T>C(p.Tyr1568His)	–	–	–	–	–	–	–	–	–	–	–	–	–	–	–	+	–	–	–	–	–
c.3450_3452del(p.Val1151del)	–	–	–	–	–	–	–	–	–	–	–	–	–	–	-	-	+	-	-	-	-
TMEM231																					
c.12T>A(p.Tyr4*)	–	–	–	–	–	–	–	–	–	–	–	–	–	–	–	–	–	–	+	+	+
c.625G>A(p.Asp209Asn)	–	–	–	–	–	–	–	–	–	–	–	–	–	–	–	–	–	–	+	+	+
Age (years)	8	1.5	3	52	45	4	10	7	13	31	3	12	62	53	5	10	5	16	14	9	4
Developmental delay	+	+	+	+	+	+	+	+	+	+	Mild	Mild	+	–	+	+	+	+	+	+	+
Age at walking	Walks with aid	Not amb	NA	NA walks	3	Not amb	8	3.5	7	2.5	1.5	1.5	4	1	2	4	2.5	7	Not amb	Not amb	Not amb
Oculomotor apraxia	–	+	+	+	+	+	+	+	+	+	+	+	+	+	+	+	+	–	+	+	+
Breathing abnormality	+	+	+	+	+	+	+	+	–	–	–	–	–	–	–	+	–	+	+	+	+
Limb abnormality†	–	+	–	–	–	+	–	–	–	–	–	–	–	–	–	–	–	–	–	+	+
Brain MRI	MTS	MTS	MTS	ND	MTS	MTS	MTS	MTS	MTS	MTS	MTS	MTS	NA	N	MTS	MTS	MTS	MTS	MTS	MTS	MTS
Retinal involvement‡	–(f)	–(e)	–(e)	–(h)	–(h)	–(f)	–(e)	–(e)	–(f)	–(h)	–(e)	–(e)	–(f)	–(e)	–(e)	–(e)	–(e)	–(f)	–(f)	+(f)	+(e)
Renal involvement§	–(us)	–(us)	–(us)	–(h)	–(h)	–(us)	– (us)	–(us)	–(us)	–(h)	–(us)	–(h)	–(h)	–(h)	–(us)	–(us)	–(h)	–(us)	–(us)	+(us)	+(us)

The nucleotide and amino acid positions for *CC2D2A* are based on reference sequence #NM_001080522.2, for *TMEM231*on reference sequence #NM_001077418.1, and for *C5ORF42* on reference sequence #NM_023073.3 except for c.G4690A/p.A1564T that is based on ENSEMBLE transcript ID #ENST00000509849.

†IV-2 from family 406/301 has a 3–4 syndactyly in the left hand, II-1 from family 474 has pre- and postaxial polydactyly of the four limbs, and II-2 from family 387 and II-1 from family 483 have postaxial polydactyly and 4-5-6 syndactyly of the right foot.

‡Retinal involvement was determined by electroretinogram (erg), fundoscopy (f) or history (h).

§Renal involvement was determined by renal ultrasound (us) or history (h). Individuals II-2 from family 387 and II-1 from family 483 have renal cysts with normal renal function.

MTS, Molar tooth sign; N, normal; NA, not available; Not amb, Not ambulatory.

Table 6: Genotypes and phenotypes of French Canadian individuals with JBTS

The presence of rare and potentially deleterious mutations in *TMEM231*, which segregate with the disease in two unrelated FC families, strongly suggests that disruption of this gene causes JBTS in our subjects. The fact that the three individuals with mutations in TMEM231 show a similar form of JBTS also supports the involvement of this gene.

Furthermore, several observations indicated that *TMEM231* plays a role in the cilia and physically interacts with known JBTS genes. *TMEM231* encodes a transmembrane protein that localizes at the base of the ciliary axoneme at the transition zone(79). Recently, TMEM231 was shown to be part of the B9 complex, which is required for a diffusion barrier between the cilia and plasma membranes that maintains the integrity of the cilia as a privileged membrane domain[19]. The B9 complex includes at least 13 proteins (BD91, BD92, TCTN1, TCTN2, TCTN3, CC2D2A, TMEM216, TMEM67, TMEM237, TMEM231, MKS1, AHI1, TMEM17), all of which, with two exceptions (TCTN3, TMEM17), are involved in JBTS and/or Meckel-Gruber syndrome (MKS), a related ciliopathy(18, 79). Proteomic studies using the MKS proteins BD91 or BD92 as baits have shown that TMEM231 is in a complex with TCTN1, TCTN2, MKS1, AHI1 and CC2D2A(79). siRNA knockdown of TMEM231 disrupts the integrity of the ciliary barrier and the localization of components of the B9 complex at the transition zone, resulting in a reduction of cilia formation and ciliary localization of signaling receptors[19]. TMEM231 knock-out mice die at E15.5 with severe vascular defects and display typical features of ciliopathy, namely microphthalmia, polydactyly and abnormalities in patterning of ventral spinal cord(79). All together, these observations indicate that autosomal recessive mutations in *TMEM231* are a cause of JBTS.

JBTS in French Canadians show both locus and allelic heterogeneity. We identified three JBTS genes in this population with a total of 14 different alleles. Three mutations in *C5ORF42*, two mutations in *CC2D2A* and two mutations in *TMEM231* were found in at least two unrelated affected individuals (Table 6). Our analysis indicates that each of these mutations is located within a distinct haplotype in these individuals, suggesting the existence of multiple founder effects(77). Founder effects are typically associated with an increase in the

frequency of a specific autosomal recessive allele, which is often accompanied by other alleles that remain at their usual background frequency. Interestingly, for each of these three JBTS genes, we found at least two founding mutations. It is likely that more of these complex founder effects will be unraveled with the use of genomic sequencing.

In summary, combining this study and our previous one, we were able to explain the underlying genetic cause of JBTS in 21/24 FC individuals using exome sequencing. In the course of this work, we identified *TMEM231* as a novel JBTS gene. This discovery gives further support to the concept that JBTS results from disruption of the barrier at the ciliary transition zone.

Acknowledgements: Foremost we thank the families who generously contributed their time and materials to this research study. This work was selected for study by the FORGE Canada Steering Committee, consisting of K. Boycott (U. Ottawa), J. Friedman (U. British Columbia), J. Michaud (U. Montreal), F. Bernier (U. Calgary), M. Brudno (U. Toronto), B. Fernandez (Memorial U.), B. Knoppers (McGill U.), M. Samuels (U. de Montreal), and S. Scherer (U. Toronto). We would like to thank Janet Marcadier (Clinical Coordinator) and Chandree Beaulieu (Project Manager) for their contribution to the infrastructure of the FORGE Canada Consortium. The authors wish to acknowledge the contribution of the high-throughput sequencing platform of the McGill University and Génome Québec Innovation Centre, Montréal, Canada. J.L. Michaud is a National Scholar from the Fonds de la Recherche en Santé du Québec (FRSQ). M. Srour holds a CIHR clinician-scientist training award.

Competing Interests: All authors declare no competing interests pertaining to this paper.

Funding: This work was funded by the Government of Canada through Genome Canada, the Canadian Institutes of Health Research (CIHR) and the Ontario Genomics Institute (OGI-049).

Contributorship statements: MS, FFH, JM and JLM: study design, data analysis and interpretation and writing and revision. JS: data analysis and manuscript writing and revision. GM, EL, LP and SD: laboratory follow-up of candidate variants and segregation studies. MS,

JLM, LHO, MIS, VD, DA, EA, GS, BM: patient recruitment, examination and counseling. DL, GAR: contribution of control samples. CM: coordination of samples and patient consents.

WEB RESOURCES

1000 Genomes Project, http://browser.1000genomes.org/index.html
dbSNP, http://www.ncbi.nlm.nih.gov/projects/SNP/
Ensemble Genome Browser: http://www.ensembl.org
ESP Exome Variant Serve (EVS)r: http://evs.gs.washington.edu/EVS/
Gene Ontology, http://www.geneontology.org/
Mutation Taster: http://www.mutationtaster.org/
NCBI homologene, http://www.ncbi.nlm.nih.gov/homologene
NCBI Nucleotide database, http://www.ncbi.nlm.nih.gov/nuccore
Online Mendelian Inheritance in Man (OMIM), http://www.omim.org
Polyphen-2: http://genetics.bwh.harvard.edu/pph2/
SIFT: http://sift.jcvi.org/
SMART sequence analysis: http://smart.embl-heidelberg.de/

Supplemental Figures and Tables

Supplemental Figure 1: Segregation studies of mutations in *CC2D2A* (NM_001080522.2) in families 385/447, 379 and 492, and of mutations in *C5ORF42* (NM_023073.3) in family 551.

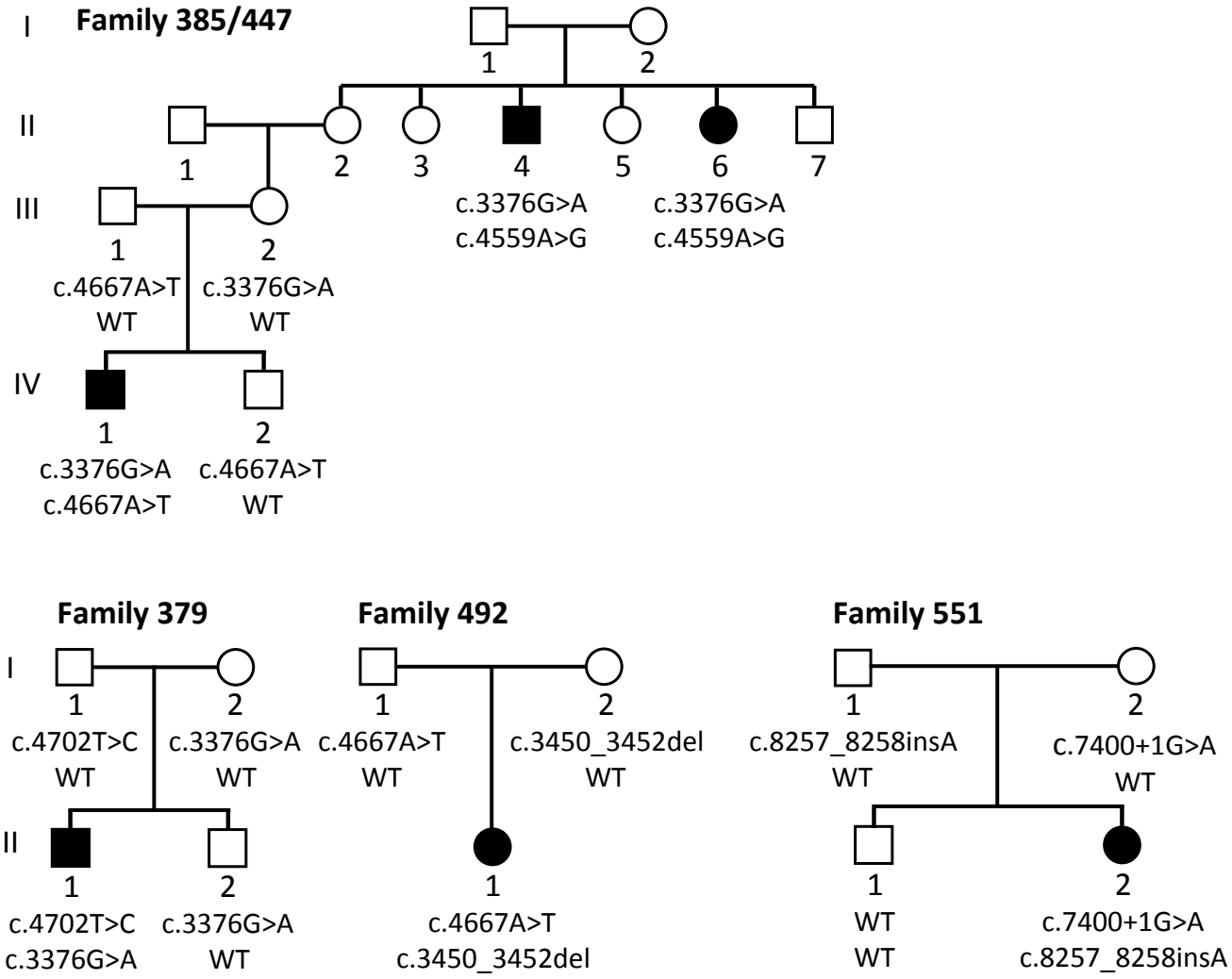

Supplemental Figure 2: Sagittal T1(A) and axial T2 (B) brain MRI of individual II:6 from family 385/447 who has compound heterozygous mutations in *CC2D2A*, and ocumolotor apraxia as the sole manifestation. Right (C) and left (D) renal ultrasounds from individual II:2 from family 387 with compound heterozygous mutations in *TMEM231* showing macroscopic cysts (arrows). Post-axial polysyndactyly in individual II:1 from family 483 (Ei and ii) and II:2 from family 387 (F i and ii).

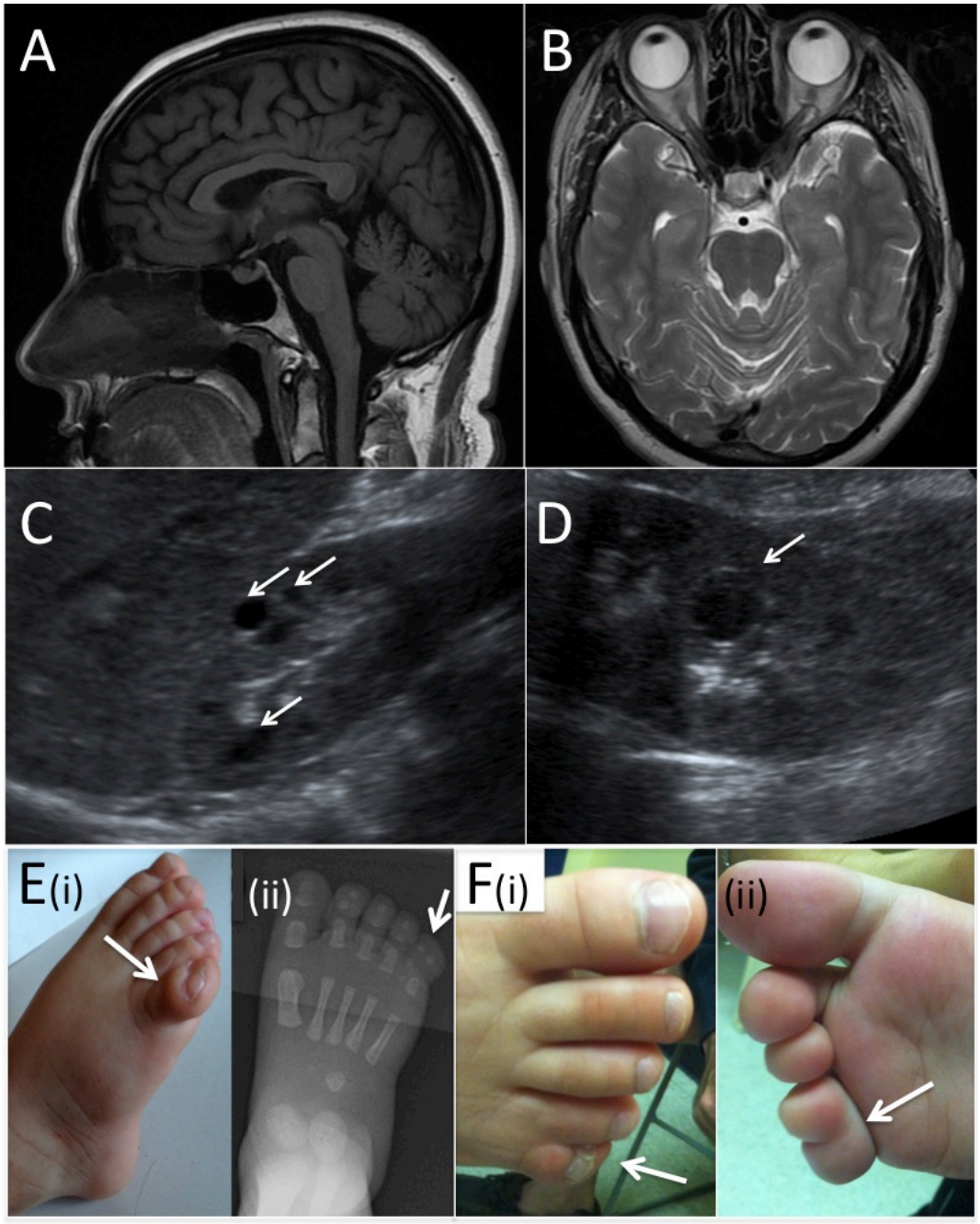

Supplemental Table 1. Analysis of combined exome sequences from the 6 individuals (from 4 families) with unexplained JBTS

Variant prioritization steps in the combined exomes dataset	
Filters applied (sequentially)	***Number of variants retained***
Non-synonymous/splicing/coding indel variants	19884
After excluding variants present in > 2 in-house exomes	1035
After excluding variants reported in 1000 genomes and EVS datasets (frequency > 0.5%)	987

*Total number of variants identified in the combined 6 exomes; redundant variants were counted only once.

Supplemental Table 2. Genes with rare homozygous or multiple heterozygous variants in the 6 individuals (from 4 families) with unexplained JBTS

Number of families with mutations in the same gene	Number of genes	Genes
1 family	19	*C14orf135,C9orf174,CLCN1, ENTPD3,FBXL22,FCGR3B,FLG,LRRK2,MUC12,PDE8A,PPL,PUS10, RASIP1,RCC2,SHROOM4,TACC3,* ***TMEM231****, TRAF5,TTN*
2 families	1	***TMEM231***
> 2 families	0	-

Chapter 4:

Genetics of Joubert syndrome in the French Canadian population

We have collected 22 additional FC JBTS patients since the publication of the previous 2 manuscripts. In total, we have identified 43 affected individuals from 35 families. We use a stepwise approach, combining screening of recurrent FC mutations and exome sequencing to study the genetic basis of JBTS in the newly identified individuals. This third manuscript represents a summary of the genetic landscape of JBTS in French Canadians.

Manuscript 3:

Genetics of Joubert syndrome in the French Canadian population

Myriam Srour[1], Fadi F. Hamdan[1], Jeremy Schwartzentruber[2], Lysanne Patry[1], Christina Nassif[1], Luis H. Ospina[3], Emmanuelle Lemyre[1], Christine Massicotte[1], Dina Amrom[4], Eva Andermann[4,5], Rachel Laframboise[6], Bruno Maranda[7], Damian Labuda[1], Jean-Claude Décarie[7], Françoise Rypens[8], Catherine Fallet-Bianco[9], Jean-François Soucy[1], FORGE Canada Consortium*, Kym Boycott[10], Bernard Brais[5], Renée-Myriam Boucher[11], Guy A. Rouleau[5], Jacek Majewski[2,4], Jacques L. Michaud[1]

[1]CHU Sainte-Justine Research Center, Montréal, H3T 1C5, Canada;
[2]McGill University and Genome Quebec Innovation Centre, Montréal, H3A 1A4, Canada;
[3]Department of Ophthalmology, Sainte-Justine Hospital, Montréal, H3T 1C5, Canada;
[4]Neurogenetics Unit, Department of Neurology & Neurosurgery, Montreal Neurological Hospital, McGill University, Montreal H3A 2B4, Canada;
[5]Department of Neurology and Neurosurgery, McGill University, Montreal, H3A 1A4, Canada; [6]Division of medical genetics, Centre Hospitalier Universitaire de Québec, Québec, G1V 4G2, Canada;
[7]Division of medical genetics, Centre Hospitalier Universitaire de Sherbrooke, Sherbrooke, J1H 5N4, Canada ;
[8]Department of medical imaging, CHU Sainte-Justine, Montréal, H3T 1C5, Canada;
[9]Department of Pathology, Sainte-Justine Hospital, Montréal, H3T 1C5, Canada;
[10]Department of Genetics, Children's Hospital of Eastern Ontario, Ottawa, K1H 8L1, Canada,
[11]Division of neurology, Centre Hospitalier Universitaire de Québec, Québec, G1V 4G2, Canada
*FORGE Steering Committee listed in Acknowledgements

ABSTRACT

Joubert syndrome (JBTS) is a primarily autosomal recessive disorder characterized by a distinctive mid-hindbrain/cerebellum malformation, oculomotor apraxia, irregular breathing, developmental delay, and ataxia. JBTS is a genetically heterogeneous ciliopathy with 23 known genes. We sought to characterize the genetic landscape associated with JBTS in the French Canadian (FC) population. We characterized 43 FC JBTS patients from 35 families using a stepwise approach, combining screening of recurrent FC mutations and exome sequencing. We identified causal mutations in 32 families (91% of cases). Fourteen families had mutations in *C5orf42*, 9 in *CC2D2A*, 3 in *NPHP1* and 2 in *TMEM231* whereas single families had mutations in *TCTN1*, *TMEM67* or *B9D1*. In addition, we report the first JBTS individual with mutations in *C2CD3*, previously associated with the related oral-facial-digital syndrome. Interestingly, we documented a complex founder effect with multiple recurrent mutations in 4 genes (*C5orf42, CC2D2A, TMEM231, NPHP1*). In the remaining families, we identified potentially pathogenic mutations in known JBTS genes (*CEP290, OFD1)* and in the cilia gene *CEP104*, which is therefore a strong candidate for JBTS. In conclusion, although JBTS shows substantial locus and allelic heterogeneity in the FC population, the great majority of cases are explained by mutations in known disease genes.

INTRODUCTION

Joubert syndrome (JBTS, MIM #213300) is a predominantly autosomal recessive disorder characterized by oculomotor apraxia, hypotonia, neonatal breathing abnormalities, ataxia and variable developmental delay. The hallmark of JBTS is a malformation of the brainstem and cerebellum consisting of cerebellar vermis hypoplasia or aplasia, horizontal elongated cerebellar peduncles and a deep interpeduncular fossa that take on the pathognomonic appearance of a "molar tooth". A subset of patients with JBTS have also extraneural manifestations such as polydactyly, retinopathy, cystic kidneys and liver fibrosis (reviewed by Romani et al, 2013(80)).

JBTS is a ciliopathy, as the majority of the 23 known JBTS genes have been shown to play a role in the development and/or function of the non-motile cilia. The cilium is a compartmentalized extension of the extracellular membrane that functions as an antenna, sensing extracellular signals and transducing them intracellularly. The cilium is composed of a microtubule-based cytoskeleton called the axoneme, which nucleates from the basal body, a modified centriololar structure. At the base of the cilium, Y-shaped structures connect the basal body to the cell membrane, forming the transition zone, which constitutes a diffusion barrier between the cilium and the remainder of the plasma membrane (for review see (19)). The majority of JBTS genes encode proteins that localize to the basal body or ciliary transition zone. Many of these proteins physically interact with one another to form large complexes. The most important complex in the pathogenesis of JBTS is the B9 complex (also known as tectonic complex), in which 9 of its known 15 members are associated with JBTS, Meckel syndrome (a related ciliopathy with overlapping features with JBTS including cystic kidneys, occipital encephalocele, polydactyly and/or biliary dysgenesis and congenital hepatic fibrosis), or both(18, 79, 81).

Although JBTS was first described in a French Canadian (FC) family in 1969(1), little is known about its molecular etiology in this population. We thus sought to characterize the genetic landscape associated with JBTS in the FC population. We report here on a cohort of 43 FC JBTS subjects, including 21 cases previously described(77, 82) and 22 new cases. Using a stepwise approach of Sanger and exome sequencing, we were able to explain most cases and identify a strong candidate gene.

METHODS

Patients

All individuals included in the study are of FC ancestry and originated from various regions throughout Quebec. These subjects had a diagnosis of JBTS based on the presence of: 1) at least one JBTS classical neurological manifestation (oculomotor apraxia, ataxia, history of breathing abnormalities); and 2) the molar tooth sign (MTS) on brain imaging in at least one affected family member (Supplemental figure S1). In addition, four fetuses were included in the study. All of these fetal cases showed cerebellar vermis hypoplasia or aplasia on prenatal imaging. One fetus had a sibling with JBTS whereas the three other cases showed elongated cerebellar peduncles, suggestive of JBTS.

Screening of recurrent FC mutations in *C5orf42, CC2D2A* and *TMEM231*

We screened, by Sanger sequencing, all unexplained JBTS families in our cohort for the seven known recurrent FC mutations in *CC2D2A* (MIM 6120313, NM_001080522.2, c.3376G>A [p.Glu1126Lys] and c.4667A>T [p.Asp1556Val]), *C5orf42* (MIM 614571, NM_023073.3, c.4006C>T [p.Arg1336Trp], c.7400+1G>A and ENSEMBLE transcript ID# ENST00000509849, c.4690G>A [p.Ala1564Thr]) and *TMEM231* (MIM 614949, NM_001077418.1, c.12T>A [p.Tyr4*]; c.625G>A [p.Asp209Asn])(77, 82).

Whole exome sequencing (WES) and initial variant filtering

WES was performed in all individuals in whom Sanger sequencing or clinical testing did not identify causal mutations. Genomic DNA from each sample was captured with the Agilent SureSelect 50 Mb exome capture oligonucleotide library, and the captured DNA was sequenced with paired-end 100 bp reads on Illumina HiSeq 2000 resulting in an average of 12.8 gigabases (Gb) of raw sequence for each sample. Exome capture and sequencing was performed at the McGill University and Genome Quebec Innovation Center (MUGQIC). Data were analyzed as previously described(62). We aligned reads to human genome assembly hg19 using a Burrows-Wheeler algorithm (BWA v. 0.5.9), then removed putative PCR-generated duplicate reads using Picard (v. 1.48). Median read depth of bases in consensus coding sequence (CCDS) exons was 102 (determined with Broad Institute Genome Analysis Toolkit v. 1.6.7)(63). On average 91% (±3%) of bases in CCDS exons were covered by at

least 20 reads. We called sequence variants using Samtools (v. 0.1.17) mpileup and bcftools, and required at least 3 variant reads as well as >=20% variant reads for each called position, with Phred-like quality scores of at least 20 for single nucleotide variants (SNVs) and at least 50 for small insertions or deletions (indels). We used Annovar(64) and custom scripts to annotate variants according to the type of mutation, occurrence in dbSNP, SIFT score, 1000 Genomes minor allele frequencies, and NHLBI Exome Sequencing Project (ESP) exomes minor allele frequencies, available from the Exome Variant Server (EVS). To identify potentially pathogenic variants we filtered out: 1) synonymous variants or intronic variants other than those affecting the consensus splice sites; 2) variants seen in more than 5 of 1128 exomes from patients with rare, monogenic diseases unrelated to JBTS that were sequenced at the MUGQIC; and 3) variants with a minor allele frequency greater than 0.5% in either the 1000 genomes or NHLBI ESP exome datasets.

RESULTS

We identified 43 FC cases with JBTS (from 35 families) who met our inclusion criteria. We previously explained JBTS in 21 of these cases who showed pathogenic mutations either in *C5orf42*, *TMEM231* or *CC2D2A(77, 82)* ((see supplemental Table S1). Since publication of these cases one family with mutations in *C5orf42* had an affected fetus (family 474 in Srour *et al*, 2012(77)). Causal mutations were identified on a clinical basis in 7 additional individuals. Two patients (HSJ-JBTS-3 and HSJ-JBTS-4) had a homozygous c.4006C>T [p.Arg1336Trp] mutations in *C5orf42*. Two patients had mutations in *NPHP1*: individual 1712.604 had a 0.152 Mb homozygous deletion on chromosomal microarray on chromosome 2q13 (110,826,262-110,978,224, GRCh37/hg19 genome assembly) encompassing *NPHP1*, and individual 1915.669 had a homozygous frameshift c.555delA [p.Lys185Asnfs*7] in *NPHP1*. Parents were confirmed carriers of the mutations. Individual HSJ-JBTS-1 had a homozygous mutation in *TMEM67* (NM_153704.5, c.2132A>C [p.Asp711Ala]). This mutation has been previously identified in a French patient with JBTS(47). Individual 1123.415 harbored compound heterozygous mutations in *CC2D2A* (NM_001080522.2, c. 4667A>T [Asp1556Val] and c.3544T>C [Trp1182Arg]). The c. 4667A>T missense is a recurrent FC mutation, and the c.3544T>C has been previously

reported as pathogenic in a patient with nephronophthisis(83). In total, 14 JBTS cases from 12 families remained unexplained.

Screening of recurrent FC mutations by Sanger sequencing

Our previous JBTS WES studies established the presence of a complex founder effect in FC JBTS cases with a total of 7 recurrent mutations in *C5orf42*, *CC2D2A* and *TMEM231*(77, 82). We screened all our unexplained JBTS families (n=12) for these known recurrent mutations. Two individuals had homozygous or compound heterozygous mutations in *C5orf42* (1673.590 and 1951.677) and 2 individuals from the same family had compound heterozygous mutations in *CC2D2A* (1342.488 and 1343.488) (Table 7). Screening identified a single heterozygous mutation in *CC2D2A* in one individual (1610.572), and a single heterozygous mutation in *C5orf42* in a second individual (2049.708). Sequencing the remaining exons of *C5orf42* in individual 2049.708 revealed a heterozygous truncating mutation (NM_023073.3, c.6354dupT [p.Ile2119Tyrfs*2]) whereas sequencing the remaining exons of *CC2D2A* in individual 1610.572 identified a heterozygous canonical splice-site mutation (c.2181+G>A) (Table 2). Both cases were compound heterozygotes for their respective mutations.

Identification of mutations in known JBTS genes by exome sequencing

Identification of mutations in known JBTS genes by exome sequencing

WES was performed in 8 individuals from the remaining 7 families in whom we did not identify recurrent FC mutations in *C5orf42*, *CC2D2A* and *TMEM231*. We first looked at the exome datasets for rare variants in the 23 genes already associated with JBTS (*INPP5E* [MIM 613037]*, TMEM216* [MIM 613277], *AHI1* [MIM 608894], *NPHP1* [MIM 607100], *CEP290* [MIM 610142], *TMEM67* [MIM 609884], *RPGRIP1L* [MIM 610937], *ARL13B* [MIM 608922], *CC2D2A* [MIM 612013], *CXORF5 (OFD1)* [MIM 300170], *KIF7* [MIM 611254], *TCTN1* [MIM 609863], *TCTN2* [MIM 613885], *TMEM237* [MIM 614424], *CEP41* [MIM 610523]*, TMEM138* [MIM 614459]*, C5orf42* [MIM 614571] , *TMEM231* [MIM 614949], *TCTN3* [MIM 613847], *ZNF423* [MIM 604557], *CSPP1* [MIM 611654], *B9D1* [MIM 614209](41-53, 55-58, 76, 77, 82, 84-88) as well as the JBTS candidate gene *TTC21B* [MIM 612014](65).

In one individual (1310.476), we identified a homozygous frameshift c.555delA [p.Lys185Asnfs*7] in *NPHP1* (NM_207181.2), the same one that was identified in individual 1915.669. However, array genomic hybridization showed that the patient is also heterozygous for a 116 kb deletion on chromosome 2q13 (110,862,369-110,978,000, GRCh37/hg19 genome assembly) encompassing *NPHP1*. This deletion is similar to that found in patient 1712.604. The mother was heterozygous for the frameshift mutation, but paternal DNA was unavailable. It is thus appears that the proband in this family is a compound heterozygous for mutations in *NPHP1*.

In one fetus (HSJ-JBTS-2), we identified compound heterozygous mutations in *TCTN1* (NM_001082538.2; c.342-2A>C and c.898C>T [p.Arg300*]). The splicing mutation c.342-2A>C had previously been reported to be causative for JBTS(54). This fetus came to medical attention because of the presence of a small vermis, large cerebellomedullary cistern, elongated cerebellar peduncles, and post-axial polydactyly of the hands on the ultrasound and MRI (supplemental figure S2, p. 53). It should be noted that neuropathological examination showed severe hypoplasia of the posterior vermis and dysmorphism of the dentate and olivary nuclei without elongation of the cerebellar peduncles.

In one individual (1639.581), we identified a nonsense (c.493C>T[p.Gln165*], NM_001243473.1) and a

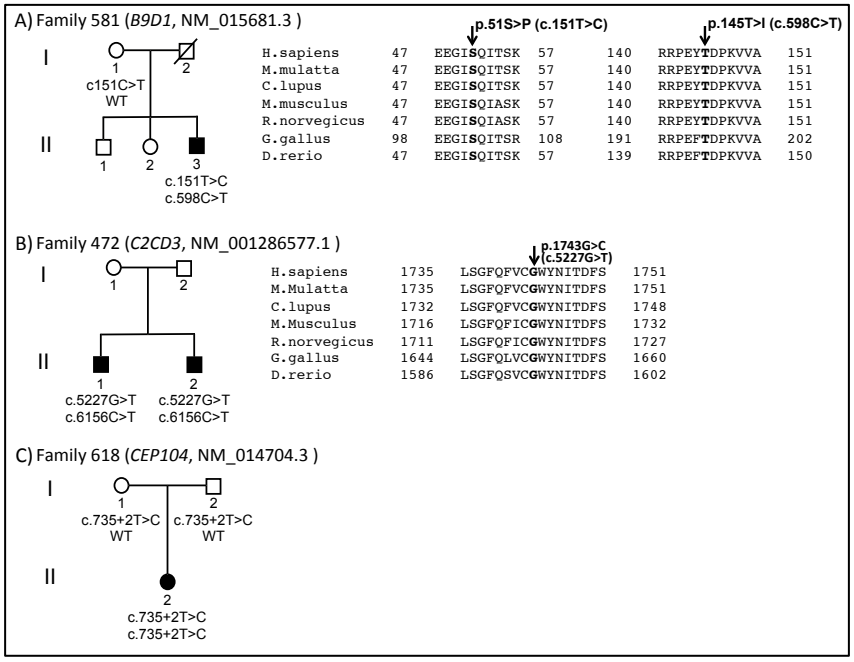

Figure 10: Segregation of mutations in candidate JBTS genes. (A, B, C) Segregation of mutations within families in *B9D1* (A), *C2CD3* (B) and *CEP104* (C). The panels on the right show conservation of the affected amino acids in B9D1 and C2CD3. Amino acid alignments were generated using homologene (NCBI).

missense (c.151T>C [p.Ser51Pro], NM_015681.3) variant in *B9D1* (Table 7). These variants are both extremely rare as they are absent in EVS. The c.151T>C [p.Ser51Pro] missense mutation is predicted to be damaging on Polyphen-2 and SIFT (score=0.989 and =0.0 respectively). Sanger sequencing showed that the proband is compound heterozygous for these mutations (Figure 10A). Similarly to the previously-described JBTS individuals with mutations in *B9D1*, our patient has a mild phenotype. He had congenital clubfeet and mild developmental delay. He walked at 18 months and benefited from speech therapy for a language delay. He has normal intelligence and attended college. He has mild gait ataxia, dysarthria and oculomotor apraxia, but no retinal, renal or liver involvement. Brain imaging showed the presence of the MTS.

Case 1767.621 is a fetus in whom prenatal ultrasound showed findings consistent with the MTS. In addition, the fetus showed occipital encephalocele, olfactory bulb agenesis, polydactyly and renal cysts. This case thus has some features of both JBTS and Meckel syndromes. We identified 2 rare compound heterozygous variants in *CEP290*: a missense c.6401T>C [p.Ile2134Thr] and a canonical splice-site mutation, c.4195-1G>A (NM_025114.3). This acceptor splice-site mutation has been previously reported in a patient with a JBTS-related ciliopathy, Senior-Lorken syndrome (nephrophthiasis and congenital leber amaurosis)(89). The c.6401T>C missense is predicted damaging by Polyphen-2 (score=0.99) and Mutation Taster but tolerated by SIFT (score=0.51). It affects an aminoacid that is perfectly conserved down to the lower vertebrates. However, it is found at a minor allele frequency of 0.55% in EVS (64/11600), and at a relatively high frequency of 2.2% in in-house FC samples, suggesting that it is unlikely to be pathogenic. Sanger sequencing did not show any other rare variant in *CEP290* or in the other known JBTS genes. Moreover, search for a deletion or duplication in *CEP290* using multiplex ligation-dependent probe amplification was negative. Subsequently, the mother became pregnant of a second fetus, which showed the same phenotype and genotype as the proband. It is unclear whether the c.6401T>C missense is pathogenic, whether these fetuses carry another yet unidentified mutation in *CEP290*, or whether JBTS in this family is explained by mutations in another gene.

In a fourth case (1686.595), we identified a hemizygous c.920T>A [p.Val307Asp] missense in *OFD1* (NM_003611.2), on chromosome X. This missense, which is located in a coiled-coil domain, is predicted damaging on Polyphen-2 (score=0.995) but tolerated on SIFT (score= 0.60) and Mutation Taster. It is absent in EVS. Segregation studies were not performed as parental DNA was unavailable. It remains unclear whether this mutation is pathogenic.

Mutations in *C2CD3* in a case with JBTS

We then focused our attention on the 3 remaining cases without mutations in known JTBS genes. We searched the exome dataset for rare variants in the genes associated with other ciliopathies with overlapping features with JBTS. We first sought to determine whether any patient harbored rare variants in the MKS genes not yet associated with JBTS (*MKS1*, *NPHP3* and *B9D2)* but none were found. The oral-facial-digital syndromes (OFD, MIM 311200) are also displaying features of JBTS, including the MTS, as well as distinctive patterns of malformations of the face, oral cavity and digits (PMID:17963220). Several genes, namely *OFD1*, *TMEM216*, *C5orf42* and *TCTN3*, are responsible for both OFD and JBTS phenotypes (87, 90-92). We searched for rare variants in the OFD genes not previously associated with JBTS: *C2CD3*(87) and *TBC1D32* (93) and *DDX59* (94). In the two affected siblings of family 472, we identified compound heterozygous mutations in *C2CD3*: a nonsense mutation (c.5929C>T[.p.Arg1977*], NM_001286577.1) and a missense mutation (c.5227G>T [p.Gly1743Cys]) (Table 7). The c.5227G>T [p.Gly1743Cys] missense is predicted to be highly damaging by SIFT (score=0.0), Polyphen-2 (score=1.00) and Mutation Taster. It affects a conserved aminoacid (including in zebrafish), located in the 5th C2 domain (Figure 10B). The two siblings with *C2CD3* mutations have severe global developmental delay, though one is more severely affected than the other. Individual 1299.472 walked at 3 years and 2 months. At the age of 6 years, he could write his name, but could not recognize letters nor numbers. He had an ataxic gait, but did not have oculomotor apraxia, retinopathy, breathing irregularities nor extraneural manifestations. Individual 1294.472 is more severely affected. At the age of 2.5 years, he was unable to sit, could grab and transfer objects and say 3 words. He had significant respiratory difficulties with central sleep apneas. He also had significant swallowing difficulties and gastroesophageal reflux necessitating a gastrostomy

Pt number	Gene	Mutations	gender	age	MTS	OMA	Retinal involvement	Renal involvement	Limb anomalies	Developmental delay	Cognition	Respiratory abnormalities	Hypotonia	Ataxia	Other
Fetus 474	*C5ORF42*	c.4006C>T [p.Arg1336Trp] c.6407del [p.Pro2136Hisfs*31][a]	F	22 wks	+	NA	-	-	-	NA	NA	NA	NA	NA	
HSJ-JBTS-3	*C5ORF42*	c.4006C>T [p.Arg1336Trp] c.4006C>T [p.Arg1336Trp]	F	28	+	+	-(f)	-(h)	-	-	Borderline	-	+	+	Strabismus
HSJ-JBTS-4	*C5ORF42*	c.4006C>T [p.Arg1336Trp] c.4006C>T [p.Arg1336Trp]	F	3	+	+	+(f)	-(u)	+	+	NA	-	NA	NA	Bifid epiglottis, strabismus, right had central polydactyly, bilateral preaxial poldaytyly in feet
1712.604	*NPHP1*	*NPHP1* Del *NPHP1* Del	F	2	+	+	-(e)	- (u)	-	-	NA	-	-	+	
1915.669	*NPHP1*	c.555delA [p.Lys185Asnfs*7] c.555delA [p.Lys185Asnfs*7]	F	3	+	+	-(f)	- (u)	-	+	NA	-	+	NA	
HSJ-JBTS-1	*TMEM67*	c.2132A>C [p.Asp711Ala] c.2132A>C [p.Asp711Ala]	F	3.5	+	+	- (f)	- (u)	-	+	Mild ID	-	+	+	
1123.415	*CC2D2A*	c.3544T>C [Trp1182Arg] c. 4667A>T [Asp1556Val]	F	4	+	+	-(f)	- (u)	-	+	NA	-	+	+	
1673.590	*C5ORF42*	c.4006C>T [p.Arg1336Trp] c.4006C>T [p.Arg1336Trp]	F	12	+	+	- (f)	- (u)	-	+	Mild ID	-	+	+	ADHD, motor apraxia
1951.677	*C5ORF42*	c.4006C>T [p.Arg1336Trp] c.7400+1G>A	F	1	+	+	+ (e)	- (u)	-	+	NA	+	+	NA	Swallowing difficulties
1342.488	*CC2D2A*	c.4667A>T [p.Asp1556Val] c.3376G>A [p.Glu1126Lys]	M	28	+	+	- (f)	- (h)	-	+	Moderate ID	-	+	+	Autism, ADHD
1343.488	*CC2D2A*	c.4667A>T [p.Asp1556Val] c.3376G>A [p.Glu1126Lys]	M	31	+	+	- (f)	- (h)	-	+	Normal (university)	-	+	+	
2049.708	*C5ORF42*	c.4690G>A [p.Ala1564Thr] p.Ile2119Tyrfs*2	F	1.5	+	-	- (f)	- (u)	+	+	NA	+	+	+	Oromotor apraxia, swallowing difficulties, tongue and hypothalamic hamartomas, neonatal seizures
1610.572	*CC2D2A*	c.4667A>T [p.Asp1556Val] c.2181 +G>A	F	2	+	+	- (e)	- (u)	-	+	NA	-	+	+	
1310.476	*NPHP1*	c.555delA [p.Lys185Asnfs*7] *NPHP1* Del	M	18	+	+	-(f)	+ (u)	-	+	Mild ID	+	+	+	Severe dysphasia
HSJ-JBTS-2	*TCTN1*	c.342-2A>C c.898C>T [p.Arg300*]		27w ks	+	NA	NA	- (us)	+	NA	NA	NA	NA	NA	Abnormal gyration of the frontal lobes
1639.581	*B9D1*	c.493C>T[p.Gln165*], c.151T>C [p.Ser51Pro],	M	22	+	+	- (f)	- (h)	-	-	normal	-	+	+	Congenital club feet, dysphasia
1767.621	*CEP290*	c.6401T>C [p.Ile2134Thr] c.4195-1G>A	F	21 wks	+	NA	NA	+ (u)	+	NA	NA	NA	NA	NA	Occipital encephalocele, olfactory bulb agenesis, bifid uterus
Fetus2 621	*CEP290*	c.6401T>C [p.Ile2134Thr] c.4195-1G>A	F	20 wks	+	NA	NA	+ (u)	-	NA	NA	NA	NA	NA	
1686.595	*OFD1*	c.920T>A [p.Val307Asp]	M	15	+	+	+ (f)[b]	+ (u)	-	+	Severe ID	+	+	+	Autism, end-stage renal failure, swallowing difficulties, abdominal situs inversus
1299.472	*C2CD3*	c.5929C>T [.p.Arg1977*] c.5227G>T [p.Gly1743Cys]	M	7	+	-	- (f)	- (u)	-	+	NA	-	+	+	
1294.472	*C2CD3*	c.5929C>T [.p.Arg1977*] c.5227G>T [p.Gly1743Cys]	M	4	+	+	-(e)	- (u)	-	+	NA	+	+	+	Swallowing difficulties, oromotor apraxia, gastrostomoy, fundoplication
1763.618	*CEP104*	c.735+2T>C c.735+2T>C	F	2	+	+	+ (e)	- (u)	-	+	NA	+	+	+	

The following abbreviations are used: ADHD, attention deficit and hyperactivity disorder; F, female; e, electroretinogram; f, fundoscopy; h, history ID, intellectual disability; M, male; MTS, molar tooth sign; NA, not available/not applicable and us, ultrasound.[a] Genotype of fetus not tested but assumed based on genotype of similarly affected sibling 1304.474 (supplemental table 1), [b]hypertensive retinopathy

and a NIssen fundoplication He had oculomotor apraxia and growth retardation but no retinopathy, polydactyly, renal or liver dysfunction. Both brothers showed the MTS.

***CEP104*, a novel candidate JBTS gene**

We were now left with only one individual (1763.618) without any candidate variants. We examined the patient's exome dataset for genes that contained homozygous or multiple rare heterozygous variants. Thereafter, for each of these genes, we searched Pubmed (http://www.ncbi.nlm.nih.gov/pubmed/) to see whether the gene product localized to or had a role in cilia function (by using the search-term "cilia" and the name of the gene of interest). Individual 1763.618 had 18 genes that contained homozygous or multiple rare variants. Only one of these, *CEP104,* is known to be implicated in cilia function(95-97). *CEP104* has 22 exons and encodes a centrosomal protein containing 2 coiled-coil domains. C*EP104* harbored a homozygous splice-site mutation (c.735+2T>C, NM_014704.3) affecting the canonical donor splice site following exon 8, likely causing its skipping. Exon 8 encodes part of the coiled-coil domain. Sanger sequencing confirmed that this mutation was homozygous in the patient and heterozygous in the unaffected parents (Figure 10C). At the current age of 2.5 years, this individual is not yet sitting independently, nor is she saying any words (Table 7). She has oculomotor apraxia, significant hypotonia and ataxia. She does not have breathing irregularities, polydactyly, neither retinal, renal nor kidney involvement. Brain imaging showed the MTS.

DISCUSSION

In this study, we surveyed the genetic landscape associated with JBTS in the FC population. We found that JBTS is characterized by great genetic heterogeneity within this population, with possibly as many as 11 genes involved. Of a total of 35 families, 14 had causal mutations in *C5orf42*, 9 in *CC2D2A*, 3 in *NPHP1* and 2 in *TMEM231*, with individual families explained by mutations in *TCTN1*, *TMEM67*, *B9D1* or *C2CD3* (Fig. 11). We identified possible pathogenic mutations in *CEP290* in one family and *OFD1* in another. In addition, we identified *CEP104* as a strong candidate JBTS gene. There is also significant

allelic heterogeneity with a total of 8 different mutations identified in *C5orf42* and 7 in *CC2D2A* (Fig. 11).

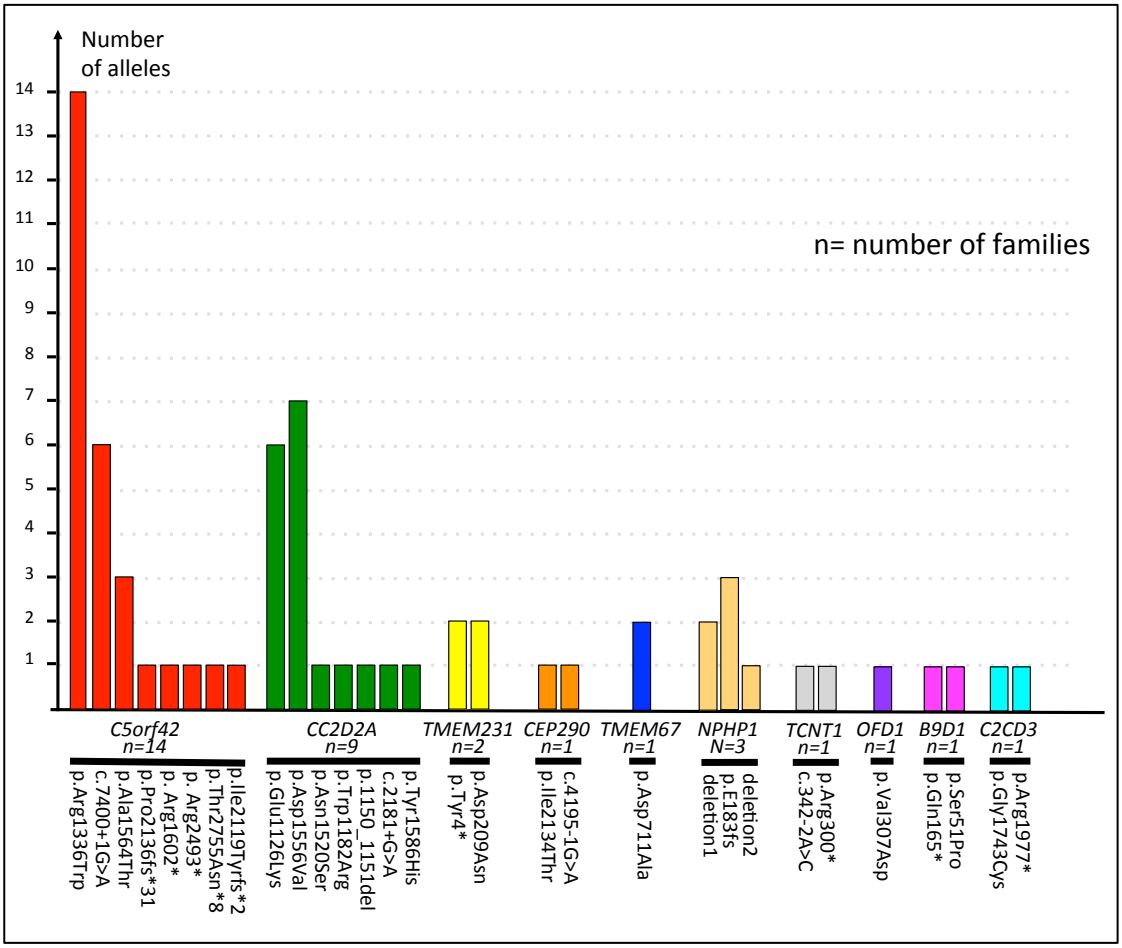

Figure 11: Locus and allelic heterogeneity of JBTS in French Canadians. Graph showing the number of the different alleles associated with JBTS in FC cases. The total number of JBTS families for each of the genes is shown beneath the gene name. Deletion1 refers to chr2: 110,826,262-110,978,224 and deletion 2 refers to chr2: 110,862,369-110,978,000 (GRCh37/hg19 genome assembly).

Overall, we were able to identify the definite causal gene in 32 of 35 families (91.4%), possible causal genes in 2 families and a strong candidate gene in the remaining family. Thus, the genetics of JBTS in the FC population appears to be relatively well elucidated. This is in contrast to the estimation that mutations in known JBTS genes account for only half of

patients(80). The high yield in our study is partially related to the use of WES in this extremely genetically heterogeneous condition.

JBTS in French Canadians: a complex founder effect

We identified 3 recurrent mutations in *C5orf42*, 2 recurrent mutations in *CC2D2A*, and 2 recurrent mutations in *TMEM231*, each of which were previously shown to be present on a common haplotype indicating the presence of a complex founder effect(77). In addition, we documented the presence of the same nonsense mutation in *NPHP1* in two unrelated cases. For *C5orf42* and *CC2D2A*, all known FC cases carried at least one of the recurrent mutations. There is a clear cluster of families with mutations in *C5orf42* in the lower Saint Lawrence region of Quebec, especially in the Matapedia Valley (population: 20,000) where the 3 recurrent mutations can be found (Fig. 12). The distribution of patients with mutations in *CC2D2A* is more widespread, with a crowding of affected families around the Montreal region but with also the presence of two recurrent mutations in the Matapedia Valley (Fig. 12). There is no obvious geographical clustering of cases with mutations in *TMEM231* and *NPHP1*.

Founder effects are typically characterized by the introduction of a major "driver" mutation that explains the disease in the majority of the patients. For recessive conditions, distinct low frequency variants can be found in the compound heterozygotes and with the increasing number of patients analyzed. As illustrative examples, a single founder mutation is responsible for 95% of FC mutant alleles in tyrosinemia type 1 (MIM 276700), and another single mutation represents 98% of FC mutant alleles in Leigh syndrome (MIM 220111)(36). Yet, accumulation of more than one frequent variant, underlying a clinically recognized founder effect, is increasingly observed challenging the "one (major) mutation, one disease" model. For instance, in autosomal recessive spastic ataxia of Charlevoix-Saguenay (ARSACS, MIM 270550), one founder mutation is responsible for 94% of mutant FC alleles, though there are also 5 other recurrent mutations identified, albeit at a low frequency(36, 98). In hereditary sensory autonomic neuropathy type 2 (HSAN2, MIM 201300)(74), two mutations are responsible for 60% and 40% of mutant alleles in FC patients, and in autosomal recessive

cerebellar ataxia (ARCA1, MIM 610743), 3 mutations each account for 50, 13 and 10% of mutant FC alleles(99).

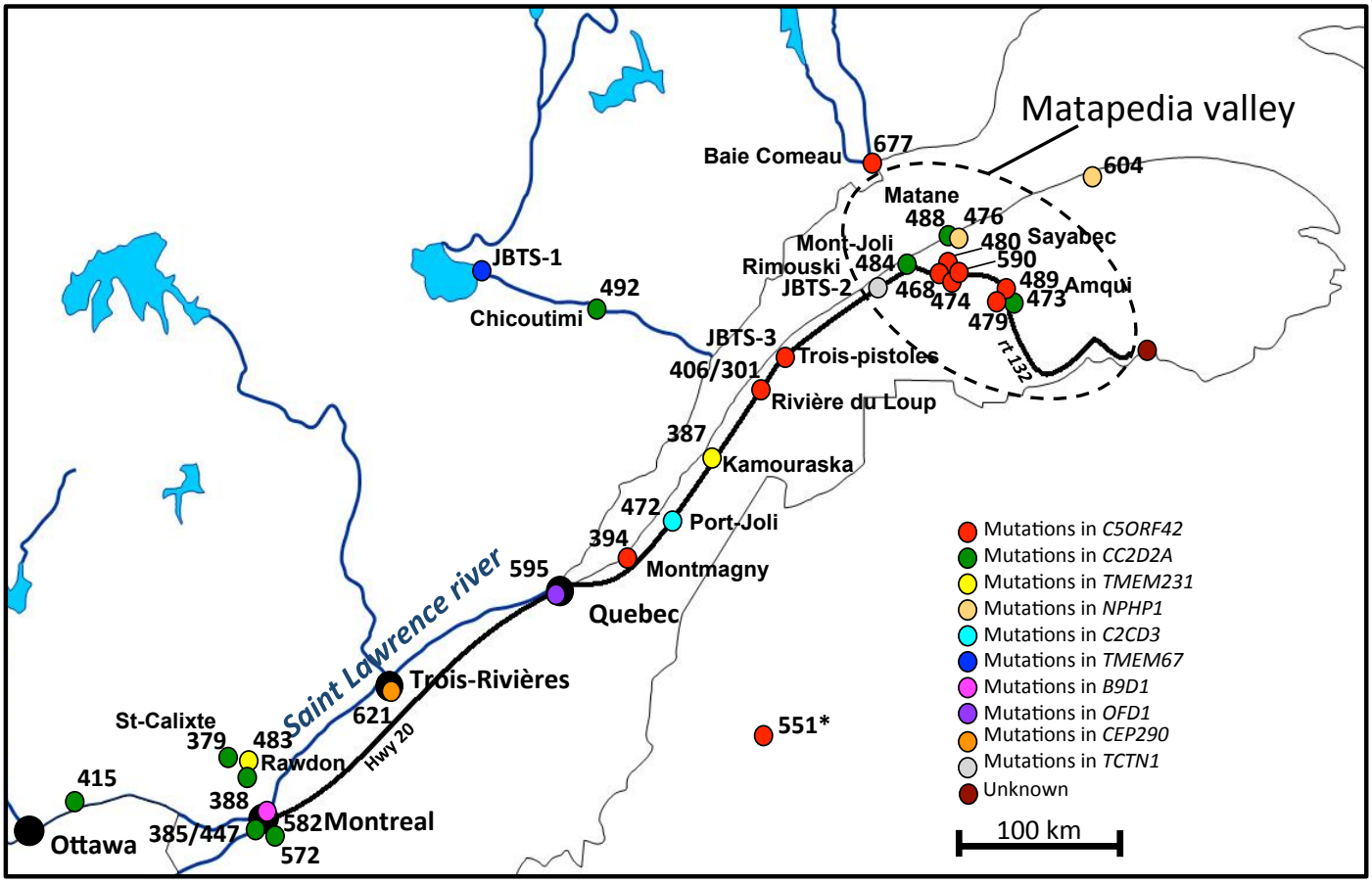

Figure 12. Map of Quebec showing the geographic distribution and the genetic heterogeneity of FC families with JBTS. *Note that this individual is of FC ancestry, but born and living in the Unites States of America.

The complexity of the founder effect in Quebec is partly explained by (1) an initial settlement of a small number French pioneers in the 17th century (approximately 8,500 including 1,600 women) mainly originating from North-Western France who gave rise to the FC population, (2) relative isolation of the population with little intermarriage with the British who had a differing language and religion, and (3) later waves of pioneering fronts in the mid-19th century along the eastern area of the Lower Saint-Lawrence region, creating a series of genetic bottle necks and a regionalization of the gene pool(36, 100).

_C2CD3_ is a novel JBTS gene

We identified compound heterozygous nonsense and missense mutations in *C2CD3* in two JBTS siblings. This is the first report of mutations in *C2CD3* resulting in JBTS. Thavin-Robinet *et al* recently reported two families with an unclassified form of OFD with recessive mutations in *C2CD3*. In one family with a homozygous truncating mutation (NM_015531.5, c.184C>T, p.Arg62*), two siblings had orofacial dysmorphism, severe microcephaly, bilateral hand post-axial polydactyly and broad hallux, micropenis, severe intellectual disability, MTS, subarachnoid cyst and corpus callosum hypoplasia. The affected fetus from the second reported family had compound heterozygous mutations in *C2CD3* (c.3085TG, p.Cys1029Gly and c.3911_3914delCAAG, p.Ala1304Valfs*3). The fetus also had severe microcephaly, micropenis, bilateral hand post-axial polydactyly, broad hallux, MTS, subarachnoid cysts and abnormalities of the corpus callosum. The patients we describe in our study have a pure form of JBTS without any extraneural manifestations, highlighting the broad and overlapping clinical spectrum associated with mutations in cilia genes. The reason for the milder phenotype in our patients is unclear, but may be related to the fact that the nonsense mutation results in a more distally truncated protein in our family (c.5929C>T[.p.Arg1977*] than the previously reported OFD patients.

CEP104, Novel JBTS candidate gene

We have identified a homozygous canonical splice-site mutation affecting the donor splice site following exon 8 in *CEP104*, which is predicted to result in skipping of that exon. *CEP104, which* contains 21 exons, encodes a 925 amino-acid centrosomal protein that

localizes to the centriole(95) and the distal end of the growing cilium (96, 97). It has been shown to be critical for ciliogenesis as Retinal Pigment Epithelial cells treated with siRNA against *CEP104* had severe defects in ciliogenesis: cells were either unable to form cilia under starvation, or if they did, the cilia were short and abnormal(96). CEP104 is known to interact with CEP97 and CP110, two proteins that are required for centrosome and primary cilia function (101). Both CEP97 and CP110 suppress ciliogenesis as depletion of either protein promotes primary cilia formation. Interestingly, CP110 mediates ciliary formation by suppressing the ability of CEP290, a JBTS gene product, to cooperate with Rab8a to enable cilia assembly(102, 103). The identification of other JBTS patients with mutations in *CEP104* will be needed to confirm that it is a *bona fide* JBTS gene.

Genotype-phenotype correlations

A summary of the clinical features of all 43 FC JBTS individuals is presented in table 8. We have reviewed the clinical information on our 17 FC cases with mutations in *C5orf42*, as well as all additional cases reported by other groups (91, 104-106). None of these cases showed renal or liver involvement. Retinal involvement, though rare, can be associated with mutations in *C5orf42* as one of our cases (1951.677) and a previously reported affected individual had abnormal electroretinograms(104). Features absent in our patients, but reported in others include left ventricular outflow tract obstruction (coarctation of the aorta or left hypoplastic ventricle in 3 cases) and occipital meningocele (in 3 cases)(91, 104, 105). Recently, *C5orf42* has been shown to be the major gene responsible for OFD type VI (MIM 277170), explaining 9 of 11 OFD-VI families (91). Criteria for OFD-VI include the presence of a MTS and at least one of the following: (1) tongue hamartoma and/or additional frenula and/or upper lip notch, (2) mesoaxial polydactyly, (3) hypothalamic hamartoma(90). Another group however noted that *C5orf42* mutations only explained 11.7% (2 of 17) of their OFDVI patient cohort. Comparison of the phenotypes of the two groups revealed that *C5orf42* was mainly associated with preaxial and/or mesoaxial polydactyly, and hypothalamic hamartomas. OFDVI patients without mutations in *C5orf42* were more likely to have tongue hamartomas or multiple lingual frenulae (107). Three cases from our cohort showed a phenotype that is consistent with OFD-VI, including individual 2049.708 who had a tongue hamartoma, an

upper lip notch and a hypothalamic hamartoma, individual 1304.474 who had mesoaxial polydactyly, and HSJ-JBTS-4 who had a bifid epiglottis and mesoaxial polydactyly.

The majority of the cases in our cohort (13/17) with mutations in *C5orf42* carried at least one truncating mutation. The 4 individuals with compound missense mutations (1281.468, 1673.590, HSJ-JBTS-3 and HSJ-JBTS-4) had a mild neurologic phenotype, with only mild developmental delay, borderline intelligence, and minimal gait ataxia. Five cases with homozygous truncating mutations in *C5orf42* have been previously reported in the literature, one fetus with the MKS phenotype, and 4 cases with the JBTS phenotype (including one with occipital encephalocele and retinopathy(104, 106). Although it is possible that cases with homozygous truncating mutations overall show a more severe phenotype, more patients carrying such mutations need to be characterized before concluding that this is the case.

Though mutations in *CC2D2A* may be associated with retinal and renal findings(108), no one from our cohort had any extraneural manifestations. Because there are 2 missense founder mutations in *CC2D2A* in the FC population, the majority of our patients (10/11) had missense mutations. Overall, patients seemed to have a mild phenotype with mild-moderate

Gene	*C5ORF42*	*CC2D2A*	*TMEM231*	*NPHP1*	*OFD1*	*CEP290*	*B9D1*	*C2CD3*	*TCTN1*	*TMEM67*	*CEP104*
No. of patients	17	11	3	3	1	2	1	2	1	1	1
MTS	16/17	10/11	3/3	3/3	1/1	2	1/1	2/2	1/1	1/1	1/1
OMA	15/16	11/11	3/3	3/3	1/1	2/2	1/1	1/2	NA	1/1	1/1
Respiratory abnormalities	11/16	1/11	3/3	1/3	1/1	NA	0/1	1/2	NA	1/1	1/1
Developmental Delay	14/14	10/11	3/3	2/3	1/1	NA	1/1	2/2	NA	1/1	1/1
Renal	0/17	0/11	2/3	1/3	1/1	2/2	0/1	0/2	0/1	0/1	0/1
Liver	0/17	0/11	0/3	0/3	0/1	0/2	0/1	0/2	0/1	0/1	0/1
Retinal	1/17	0/11	2/3	0/3	0/1	NA	0/1	0/2	NA	0/1	1/1
Limb abnormalities	4/17	0/11	2/3	0/3	0/1	0/2	0/1	0/2	1/1	0/1	0/1

Table 8. Summary of the clinical features of 43 FC patients with JBTS

developmental delay, and intelligence in the normal to mild intellectual disability (ID) range. Nevertheless, there was intrafamilial variability. For example, in family 385, one sibling had oculomotor apraxia without ataxia nor MTS, whereas the second sibling had all the classic features of JBTS. In another family (family 488), one sibling had autism and moderate ID, whereas the second sibling completed regular high school and attended college. Both brothers carried the recurrent FC mutations in *CC2D2A*. It is not known whether modifying alleles in

other cilia genes may contribute to the variable phenotype in this family, a mechanism that has been previously described in ciliopathies(65).

The most severely affected individuals in our cohort were those with mutations in *TMEM231*. The three patients had severe developmental delay. Indeed, they could not stand independently, ambulate, nor say any words. They had severe behavioural issues with automutilation and head banging. The 3 individuals had extraneural manifestations with 2/3 having renal cysts but no renal dysfunction, 2/3 pre-axial polydactyly and 2/3 retinopathy. Mutations in *TMEM231* are also responsible for MKS(109).

Finally, we report on a patient with a homozygous splice-site mutation in *B9D1*. To date, there have only been reports of 3 other individuals harboring mutations in *B9D1*. Hopp *et al* reported one newborn with MKS, who died after a few hours of life with posterior encephalocele, multicystic dysplastic kidneys, clubbed feet and ambiguous genitalia(110). He carried an inherited splice-site mutation (c.505+2T>C) in *B9D1* as well as a de-novo 1.7Mb deletion encompassing *B9D1*. Romani *et al* reported 2 individuals with JBTS with mutations in *B9D1*, both of whom had a mild phenotype without extraneural manifestations: a 9 year old boy carrying a homozygous c.G467A (p.R156Q) with mild intellectual disability, and a 7 year old girl carrying c.A95G (p.Y32C) and c.520_522delGTG (p.V174del) with normal intelligence. Interestingly, our patient also has a mild phenotype with no extraneural manifestations and normal intelligence.

In summary, we have identified the definitive causal mutations in 32 out of 35 FC families with JBTS. We expand the phenotype associated with mutations to include JBTS. In addition, we implicate *CEP104* as strong JBTS candidate gene. Though the genetic landscape of JBTS is greatly heterogeneous, even within the FC population, it is becoming well understood in great part due to WES.

Acknowledgements

Foremost we thank the families who generously contributed their time and materials to this research study. This work was selected for study by the FORGE Canada Steering Committee, consisting of K. Boycott (U. Ottawa), J. Friedman (U. British Columbia), J. Michaud (U.

Montreal), F. Bernier (U. Calgary), M. Brudno (U. Toronto), B. Fernandez (Memorial U.), B. Knoppers (McGill U.), M. Samuels (U. de Montreal), and S. Scherer (U. Toronto). We would like to thank Janet Marcadier (Clinical Coordinator) and Chandree Beaulieu (Project Manager) for their contribution to the infrastructure of the FORGE Canada Consortium. The authors wish to acknowledge the contribution of the high-throughput sequencing platform of the McGill University and Génome Québec Innovation Centre, Montréal, Canada. This work was funded by the Government of Canada through Genome Canada, the Canadian Institutes of Health Research (CIHR), Genome Quebec and the Ontario Genomics Institute (OGI-049). J.L. Michaud is a National Scholar from the Fonds de la Recherche du Québec - Santé (FRQ-S). M. Srour holds a CIHR clinician-scientist training award. D. Labuda receives financial support from RMGA FRSQ. The authors have no conflicts of interest to declare.

WEB RESOURCES

1000 Genomes Project, http://browser.1000genomes.org/index.html

dbSNP, http://www.ncbi.nlm.nih.gov/projects/SNP/

Ensemble Genome Browser: http://www.ensembl.org

ESP Exome Variant Serve (EVS)r: http://evs.gs.washington.edu/EVS/

Mutation Taster: http://www.mutationtaster.org/

NCBI homologene, http://www.ncbi.nlm.nih.gov/homologene

NCBI Nucleotide database, http://www.ncbi.nlm.nih.gov/nuccore

Online Mendelian Inheritance in Man (OMIM), http://www.omim.org

Polyphen-2: http://genetics.bwh.harvard.edu/pph2/

SIFT: http://sift.jcvi.org/

Contributorship statements: MS: study design, data analysis and interpretation, writing and revision, patient recruitment, examination and counseling. FFH and JLM: study design, data analysis and interpretation and writing and revision. JS and JM: data analysis. CN and LP: laboratory follow-up of candidate variants and segregation studies. MS, JLM, EL, DA, EA, RL, BM, JCD, FR, CFB, JFS, KB, BB, RMB: patient recruitment, examination and

counseling. DL, GAR: contribution of control samples. CM: coordination of samples and patient consents.

Chapter 5:
General Discussion

We have used a combination of Sanger sequencing and whole exome sequencing to study the genetic basis of Joubert syndrome in 43 affected individuals from 35 unrelated French-Canadian families. Our work has resulted in the identification of 2 novel JBTS genes (*C5orf42* and *TMEM231*) and 1 strong candidate JBTS gene (*CEP104*)(77, 82). It has also enabled the deciphering of the genetic landscape of JBTS in French-Canadians. Prior to the start of this research endeavor, the underlying genetic etiology was unknown in all 35 families. Now, a definite molecular diagnosis has been identified in 32 families, and a probable molecular diagnosis in the remaining 3.

Mutations in *C5orf42* are the most common cause of JBTS in French-Canadians and worldwide

Mutations in *C5orf42* explain JBTS in 14 of our 35 FC families. There is a presence of a complex founder effect with 3 recurrent mutations (c.4006C>T [p.Arg1336Trp], c.7400+1G>A and, c.4690G>A [p.Ala1564Thr]) of which c.4006C>T [p.Arg1336Trp] is the most common being present in 9 of 14 families. Each of these mutations was found to be on a common haplotype indicating the presence of 3 separate founder mutations. As previously discussed in manuscript 1, the large size of the *C5orf42* and the complicated population migration patterns partly explain this phenomenon. In addition, the c.4006C>T corresponds to a CpG site, thus it has a higher susceptibility to spontaneous mutation.

Since our original publication in 2012 (77), further insight into the function and localization of C5orf42 is available thanks to a JBTS17 mouse model harbouring a homozygous missense mutation in the mouse homologue of *C5orf42*, *2410089E03Rik* (c.757T>C, pS235P)(111). This mouse mutant, named Heart Under Glass (Hug), was recovered from a forward genetic screen with ENU mutagenesis using fetal ultrasound imaging to identify congenital heart defects. The Hug mouse exhibits a number of defects characteristic of ciliopathies, including polydactyly, craniofacial anomalies, cystic kidneys and central nervous system abnormalities. In addition, this mutant mouse has congenital heart defects comprising of outflow tract abnormalities associated with pulmonary atresia. Detailed analysis of the brain shows abnormal cerebellar development with reduction in the number

and size of the cerebellar lobules. This parallels the cerebellar defects observed in JBTS in humans. In addition, Shh signalling is disrupted in Hug mutant fibroblasts, but stereocilia patterning is not perturbed, suggesting that cochlear planar cell polarity regulation is unaffected. Given that PCP defects underlie the cystic kidneys associated in ciliopathies, this observation may explain in part the lack of renal involvement in *C5orf42* patients. C5orf42 localizes to the ciliary transition zone in normal fibroblasts. Fibroblasts derived from Hug mutant mice and from a patient *C5orf42* mutations (patient 1320-480)(77) exhibited ciliogenesis defects, and showed loss of not only C5orf42, but also NPHP1 and CEP290 from the cilia transition zone.

Mutations in *C5orf42* are not only responsible for JBTS in the French-Canadian population. Mutations in *C5orf42* have now been identified in JBTS patients outside of Quebec, and are in fact one of the most common cause of JBTS worldwide. Very shortly after the publication of our manuscript, Alazami *et al.* reported homozygous truncating mutations in *C5orf42* in 3 out 12 Saudi Arabian families with JBTS. More recently, *C5orf42* was screened in a cohort of 313 patients with JBTS (107). Causal mutations were identified in 28 (8.9%), making *C5orf42* one of the most frequently mutated genes in this cohort. In another study, causal mutations in C5orf42 were identified in 12% of a cohort of 51 Northern European JBTS patients (106). Furthermore, mutations in *C5orf42* have been identified in patients with Orofacial digital syndrome 6 (OFDVI), a related ciliopathy. The diagnostic criteria of OFDVI are defined as presence of the molar tooth sign and one or more of the following: (1) tongue hamartoma and/or additional frenula and/or upper lip notch; (2) mesoaxial polydactyly of one or more hands or feet and (3) hypothalamic hamartoma (90). Lopez et al reported that *C5orf42* mutations accounted for 82% of their OFDVI patients, although a second group found that *C5orf42* mutations only explained 11.7% (2 of 17) of their OFDVI patient cohort (107). Comparison of the phenotypes of the two groups revealed that *C5orf42* was mainly associated with preaxial and/or mesoaxial polydactyly and hypothalamic hamartomas. OFDVI patients without mutations in *C5orf42* were more likely to have tongue hamartomas or multiple lingual frenulae.

Mutations in *C5orf42* have never been associated with renal or liver abnormalities. Retinal abnormalities have been reported, though rarely (in 2 patients only, one from manuscript 3 and one from a separate publication (104)). Thus, C5orf42-related JBTS is either associated with a pure neurologic phenotype or an OFDVI phenotype, usually sparing the kidneys, liver and retina. Neurodevelopmental outcomes are variable and difficult to predict, as reviewed in manuscript 3.

Finally, mutations in *C5orf42* have been reported in one Saudi Arabian fetus with Meckel syndrome, a JBTS-related ciliopathy considered on the more severe end of the spectrum of JBTS, that is characterized by dysplastic kidneys, polydactyly, occipital encephalocele and early lethality(109). It is important to note however, that the fetus did not have the classic findings of Meckel syndrome, as it had neither polycystic kidneys nor polydactyly. This fetus had a cleft lip and palate, and an occipital encephalocele, suggesting that a diagnosis of OFDVI may have been more accurate.

Mutations in *TMEM231* cause JBTS

Our work has resulted in the identification of *TMEM231* as a novel JBTS gene. It is a rare cause of JBTS, as only one other JBTS patient has been reported to date (107). However, following our publication, mutations in *TMEM231* were identified in patients with Meckel syndrome and OFD type 3 (112, 113). In fact, mutations in *TMEM231* were found to be a relatively common cause of Meckel syndrome, as homozygous or compound heterozygous mutations were identified in 9 out of 95 Meckel syndrome families. Both missense and truncating *TMEM231* mutations have been described. Interestingly, our JBTS patients were the most severely affected patients from our cohort, having polydactyly, retinal involvement, renal cysts and the most severe neurodevelopmental impairment. Our 3 patients were nonverbal and nonambulatory.

TMEM231 is a transmembrane protein that localizes to the ciliary transition zone. It is a member of the B9/tectonic complex, one of four transition zone complexes.. Mutations in all 15 members of the B9/tectonic complex have been found to underlie human disease and are responsible for overlapping JBTS / Meckel syndrome and orofacial digital phenotypes.

Tandem affinity purification and mass spectroscopy experiments have determined that TMEM231 interacts with multiple other components of the MKS complex(79, 113). TMEM231 knock-out or mutant mice (lacking exons 2 and 3) have a ciliary phenotype with polydactyly, central nervous system abnormalities and Shh signaling defects, cystic kidneys and hepatic ductal plate malformations(79, 113). Tmem231 mutant mouse embryonic fibroblasts (MEFs) fail to localize ciliary proteins such as Adcy3, Arl13b and other transition zone proteins such as B9D1, TMEM67 and MKS1. Robertson *et al* show that the *TMEM231* mutations identified in MKS and OFD3 patients are hypomorphic. The localization of Arl13b and B9D1 in *Tmem231*-/- MEFs is fully rescued by transient transfection with wild-type Tmem231, but is only partially rescued with the mutant forms of Tmem231. siRNA knockdown of TMEM231 disrupts both the integrity of the ciliary barrier and the localization of B9 complex components to the transition zone, resulting in reduced cilia formation and ciliary localization of signaling receptors[19]. Furthermore, loss of Tmem231 in C. elegans sensory neurons results in the inappropriate leak of nonciliary proteins into the cilia. This suggests that the MKS complex serves either as an entry barrier, excluding entry of nonciliary proteins into the cilia, or as an exit barrier, retaining certain membrane-associated proteins within the cilia while allowing the exit of nonciliary proteins.

JBTS- a ciliary transition zone-opathy

Dysfunction of the transition zone in TMEM231 mutants provides additional support to the mounting evidence suggesting that dysfunction of the transition zone is central to the pathophysiology underlying JBTS. *In vitro* or *in vivo* knock-down of the other individual components of the transition zone B9 complex results in reduced cilia formation, reduction of the expression of receptors in the ciliary membranes, and defective Shh signaling. Multiple lines of evidence demonstrate that the B9 complex prevents the rapid diffusion of unselected proteins across the transition zone, while at the same time promoting the access of selected proteins and receptors to the cilium. For example, the membrane-associated GPI–GFP and GFP-tagged CEACAM1 accumulate at higher levels in cilia with dysfunctional transition zones (79); in *C. elegans*, abrogation of six different transition zone-localized proteins causes

abnormal ciliary entry of the TRAM protein and membrane-associated RP2 homologues. Ciliary proteins, such as AC3 and PKD2, no longer localize to the cilia in cells with transition zone disruption(114).

Recent data have shown that ciliary proteins interact within functional networks that largely relate to specific ciliopathy phenotypes. For example, two motor complexes of proteins (intraflagellary transport complex B and A) mediate the anterograde and retrograde intraflagellary transport systems that bidirectionally move ciliary proteins along the axoneme These use the microtubule motor proteins kinesins and dyneins,. Mutations in the intraflagellary transport proteins are a major cause of skeletal ciliopathies, including Sensenbrenner syndrome, Jeune syndrome, and other short rib polydactyly syndromes. The correct assembly of intraflagellary transport complexes at the ciliary base, and the turnaround from anterograde to retrograde transport at the ciliary tip, are mediated by another protein complex, the BBSome, that consists of several proteins that are mutated in Bardet-Biedl syndrome.

Variability of JBTS phenotype

There is large phenotypic variability associated with mutations in JBTS genes. As mentioned previously, mutations in the same JBTS gene can be associated with differing severity of neurodevelopmental deficits, and extra-neural involvement. Substantial variability can also occur within the same family. Furthermore, mutations in the same gene can result in different, though related diagnoses, such as JBTS, Meckel syndrome, nephronophthesis or isolated retinopathy.

A possible explanation for this wide variability is the oligogenic model of transmission, whereby inherited recessive mutations in one gene are not sufficient to fully explain the clinical phenotype: concurrent presence of additional mutations, rare allelic variants or even common polymorphisms in other ciliary genes contribute to the mutational load, which modulates the phenotype of the patient(115). This mechanism has been demonstrated in Bardet-Biedl syndrome (BBS), another ciliopathy, where affected individuals

with non-fully penetrant mutations also carried heterozygous mutations on other BBS loci. This mechanism has also been documented in JBTS patients: individuals with mutations in *NPHP1* have muticystic renal dysfunction either in isolation (in the form of nephronophthiasis), or combined with neurologic abnormalities (such as MTS) to give a JBTS phenotype. JBTS individuals harboring homozygous *NPHP1* deletions had an enriched incidence of pathogenic lesions in *trans* in *CEP290* or *AHI1*, other known JBTS genes, likely explaining the presence extra-renal manifestations [31].

The landscape of JBTS in French-Canadians is largely unraveled

Prior to the start of this study, the genetic etiology of JBTS was largely unknown in the French-Canadian population. Now, however, it is well characterized. There is the presence of significant genetic and allelic heterogeneity, with the involvement of at least 10 separate genes. Of these, *C5orf42* and *CC2D2A* explain the largest proportion of affected families, and are responsible for 14 of 35 (40%) and 9 of 35 (26%) families respectively. We have uncovered the presence of a complex founder effect.

The reason for the presence of multiple founder mutations is several-fold. Although JBTS it is unified by a relatively specific phenotype reflecting ciliary dysfunction, it is nonetheless a markedly genetically heterogeneous disorder. Since founder effects are capable of increasing disease prevalence associated with any mutation, a genetically heterogenous disorder is more prone to have multiple founder effects. Furthermore, both *CC2D2A* and *C5orf42* are very large genes thus are more likely to accumulate mutations, explaining the presence of multiple founder mutations. The migration and population history of Quebec provided favorable conditions for the development of such complex founder effect given the initial small number French pioneers in the 17th century who gave rise to the French-Canadian population, the relative isolation of the population, and later waves of pioneering fronts in the mid-19th century along the eastern area of the Lower Saint-Lawrence region, creating a series of genetic bottle necks and a regionalization of the gene pool(36, 100).

The deciphering of the genetic etiology of JBTS in the French-Canadian population has made an important impact on the affected children and their families. Carrier parents can now be offered pre-implantation genetic testing and early screening of pregnancies. Carrier status of the siblings, spouses and the extended family can be tested in order to facilitate genetic counseling. For the children affected with JBTS, knowledge of the molecular diagnosis can help tailor management, though caution is used, given the imprecise genotype-phenotype correlations. These generalizations are very helpful to the clinician and informative to the affected families. For example, individuals with mutations in *NPHP1* will need to be followed extremely closely for renal dysfunction with renal imaging and function testing; patients with mutations in *C5orf42* will likely have a pure neurologic phenotype and thus very close monitoring of renal and liver function will not be necessary; patients with *TMEM231* mutations are likely to be have more severe neurodevelopmental disabilities with extraneural complications including renal, skeletal and retinal involvement requiring close monitoring; however, though mutations in *CC2D2A* can be associated with a broad clinical phenotype with extra-neurologic complications, French-Canadian patients with the recurrent FC *CC2D2A* mutations are more likely to have a mild neurologic phenotype with no extra-neurologic manifestations.

Role of WES in JBTS gene discovery

Next generation sequencing technologies such as WES have revolutionized the study of genetically and clinically heterogeneous diseases such as JBTS. Classic genetic strategies such as linkage analysis and homozygosity mapping rely heavily on consanguineous families or multiple large families with multiple affected individuals. Given the extreme allelic and genetic heterogeneity that we uncovered in the French-Canadian JBTS population, this doctoral project would not have been possible without Next Generation sequencing technologies. Indeed, our initial approach of using homozygosity mapping failed. WES has been instrumental in the deciphering of the genetics and pathophysiology of JBTS in the past decade. The first JBTS gene, *AHI1*, was identified in 2004. In 2010, when this project started, only 8 causal genes were known. This number has exploded since, with at least 24 known genes. It is important to note that the exploration of JBTS genes is dramatically facilitated by

the known unifying underlying pathogenesis of ciliary dysfunction, particularly with analysis of candidate genes from WES.

The use of Next Generation sequencing technologies is also very important in the clinical setting. Despite some general phenotype-genotype correlations, it is very difficult to predict the causal gene in a given patient. Next Generation sequencing gene panels are affordable and time efficient. Even for French-Canadian patients, in which 65% of mutations are in two genes, next generation sequencing is still more efficient than Sanger sequencing of targeted genes. Thus, in the diagnostic exploration of a patient with the clinical diagnosis of JBTS, a clinician would order forst a chromosomal microarray (to look for large deletions involving JBTS genes such as *NPHP1*) followed by a Next Generation JBTS gene panel.

In summary, starting from a cohort of 35 French-Canadian families with JBTS in which none had identified causative mutations, we identified the definitive causal mutations in 32, and the possible causal mutation in the remaining 3. Our work has resulted in the identification of two novel JBTS genes- *C5orf42* and *TMEM231*, and implicated *CEP104* as strong JBTS candidate gene. Though the genetic landscape of JBTS is greatly heterogeneous, even within the French-Canadian population, it has now become largely mapped.

REFERENCES

1. Joubert M, Eisenring JJ, Robb JP et al. Familial agenesis of the cerebellar vermis. A syndrome of episodic hyperpnea, abnormal eye movements, ataxia, and retardation. Neurology 1969: 19: 813-825.
2. Maria BL, Hoang KB, Tusa RJ et al. "Joubert syndrome" revisited: key ocular motor signs with magnetic resonance imaging correlation. Journal of child neurology 1997: 12: 423-430.
3. Valente EM, Dallapiccola B, Bertini E. Joubert syndrome and related disorders. Handbook of clinical neurology 2013: 113: 1879-1888.
4. Maria BL, Boltshauser E, Palmer SC et al. Clinical features and revised diagnostic criteria in Joubert syndrome. Journal of child neurology 1999: 14: 583-590; discussion 590-581.
5. Fennell EB, Gitten JC, Dede DE et al. Cognition, behavior, and development in Joubert syndrome. Journal of child neurology 1999: 14: 592-596.
6. Hodgkins PR, Harris CM, Shawkat FS et al. Joubert syndrome: long-term follow-up. Developmental medicine and child neurology 2004: 46: 694-699.
7. Poretti A, Huisman TA, Scheer I et al. Joubert syndrome and related disorders: spectrum of neuroimaging findings in 75 patients. AJNR American journal of neuroradiology 2011: 32: 1459-1463.
8. Friede RL, Boltshauser E. Uncommon syndromes of cerebellar vermis aplasia. I: Joubert syndrome. Developmental medicine and child neurology 1978: 20: 758-763.
9. Yachnis AT, Rorke LB. Neuropathology of Joubert syndrome. Journal of child neurology 1999: 14: 655-659; discussion 669-672.
10. Poretti A, Boltshauser E, Loenneker T et al. Diffusion tensor imaging in Joubert syndrome. AJNR American journal of neuroradiology 2007: 28: 1929-1933.
11. Gleeson JG, Keeler LC, Parisi MA et al. Molar tooth sign of the midbrain-hindbrain junction: occurrence in multiple distinct syndromes. American journal of medical genetics Part A 2004: 125A: 125-134; discussion 117.
12. Saraiva JM, Baraitser M. Joubert syndrome: a review. American journal of medical genetics 1992: 43: 726-731.
13. Hildebrandt F, Zhou W. Nephronophthisis-associated ciliopathies. Journal of the American Society of Nephrology : JASN 2007: 18: 1855-1871.
14. Ferland RJ, Eyaid W, Collura RV et al. Abnormal cerebellar development and axonal decussation due to mutations in AHI1 in Joubert syndrome. Nature genetics 2004: 36: 1008-1013.
15. Castori M, Valente EM, Donati MA et al. NPHP1 gene deletion is a rare cause of Joubert syndrome related disorders. Journal of medical genetics 2005: 42: e9.

16. Quinlan RJ, Tobin JL, Beales PL. Modeling ciliopathies: Primary cilia in development and disease. Current topics in developmental biology 2008: 84: 249-310.
17. Guemez-Gamboa A, Coufal NG, Gleeson JG. Primary cilia in the developing and mature brain. Neuron 2014: 82: 511-521.
18. Czarnecki PG, Shah JV. The ciliary transition zone: from morphology and molecules to medicine. Trends in cell biology 2012: 22: 201-210.
19. Valente EM, Rosti RO, Gibbs E et al. Primary cilia in neurodevelopmental disorders. Nature reviews Neurology 2014: 10: 27-36.
20. Sasai N, Briscoe J. Primary cilia and graded Sonic Hedgehog signaling. Wiley interdisciplinary reviews Developmental biology 2012: 1: 753-772.
21. Bai CB, Stephen D, Joyner AL. All mouse ventral spinal cord patterning by hedgehog is Gli dependent and involves an activator function of Gli3. Developmental cell 2004: 6: 103-115.
22. Spassky N, Han YG, Aguilar A et al. Primary cilia are required for cerebellar development and Shh-dependent expansion of progenitor pool. Developmental biology 2008: 317: 246-259.
23. Vaillant C, Monard D. SHH pathway and cerebellar development. Cerebellum 2009: 8: 291-301.
24. Kenney AM, Cole MD, Rowitch DH. Nmyc upregulation by sonic hedgehog signaling promotes proliferation in developing cerebellar granule neuron precursors. Development 2003: 130: 15-28.
25. Stamataki D, Ulloa F, Tsoni SV et al. A gradient of Gli activity mediates graded Sonic Hedgehog signaling in the neural tube. Genes & development 2005: 19: 626-641.
26. Dessaud E, Yang LL, Hill K et al. Interpretation of the sonic hedgehog morphogen gradient by a temporal adaptation mechanism. Nature 2007: 450: 717-720.
27. Dessaud E, Ribes V, Balaskas N et al. Dynamic assignment and maintenance of positional identity in the ventral neural tube by the morphogen sonic hedgehog. PLoS biology 2010: 8: e1000382.
28. McGlinn E, Tabin CJ. Mechanistic insight into how Shh patterns the vertebrate limb. Current opinion in genetics & development 2006: 16: 426-432.
29. Anderson E, Peluso S, Lettice LA et al. Human limb abnormalities caused by disruption of hedgehog signaling. Trends in genetics : TIG 2012: 28: 364-373.
30. Louvi A, Grove EA. Cilia in the CNS: the quiet organelle claims center stage. Neuron 2011: 69: 1046-1060.
31. Tissir F, Goffinet AM. Planar cell polarity signaling in neural development. Current opinion in neurobiology 2010: 20: 572-577.
32. Aberle H, Bauer A, Stappert J et al. beta-catenin is a target for the ubiquitin-proteasome pathway. The EMBO journal 1997: 16: 3797-3804.

33. Corbit KC, Shyer AE, Dowdle WE et al. Kif3a constrains beta-catenin-dependent Wnt signalling through dual ciliary and non-ciliary mechanisms. Nature cell biology 2008: 10: 70-76.
34. Gerdes JM, Liu Y, Zaghloul NA et al. Disruption of the basal body compromises proteasomal function and perturbs intracellular Wnt response. Nature genetics 2007: 39: 1350-1360.
35. Cardenas-Rodriguez M, Badano JL. Ciliary biology: understanding the cellular and genetic basis of human ciliopathies. American journal of medical genetics Part C, Seminars in medical genetics 2009: 151C: 263-280.
36. Laberge AM, Michaud J, Richter A et al. Population history and its impact on medical genetics in Quebec. Clinical genetics 2005: 68: 287-301.
37. Scriver CR, Gregory D, Bernstein M et al. Feasibility of chemical screening of urine for neuroblastoma case finding in infancy in Quebec. CMAJ : Canadian Medical Association journal = journal de l'Association medicale canadienne 1987: 136: 952-956.
38. Brancati F, Dallapiccola B, Valente EM. Joubert Syndrome and related disorders. Orphanet journal of rare diseases 2010: 5: 20.
39. Fortin JC, and Lechasseur, A. Le Bas-Saint-Laurent. Québec: Presses de l'Université Laval, 1999.
40. Hébert PM. Les Acadiens du Québec. Montréal: Éditions de l'écho, 1994.
41. Bielas SL, Silhavy JL, Brancati F et al. Mutations in INPP5E, encoding inositol polyphosphate-5-phosphatase E, link phosphatidyl inositol signaling to the ciliopathies. Nature genetics 2009: 41: 1032-1036.
42. Edvardson S, Shaag A, Zenvirt S et al. Joubert syndrome 2 (JBTS2) in Ashkenazi Jews is associated with a TMEM216 mutation. American journal of human genetics 2010: 86: 93-97.
43. Valente EM, Logan CV, Mougou-Zerelli S et al. Mutations in TMEM216 perturb ciliogenesis and cause Joubert, Meckel and related syndromes. Nature genetics 2010: 42: 619-625.
44. Dixon-Salazar T, Silhavy JL, Marsh SE et al. Mutations in the AHI1 gene, encoding jouberin, cause Joubert syndrome with cortical polymicrogyria. American journal of human genetics 2004: 75: 979-987.
45. Parisi MA, Bennett CL, Eckert ML et al. The NPHP1 gene deletion associated with juvenile nephronophthisis is present in a subset of individuals with Joubert syndrome. American journal of human genetics 2004: 75: 82-91.
46. Sayer JA, Otto EA, O'Toole JF et al. The centrosomal protein nephrocystin-6 is mutated in Joubert syndrome and activates transcription factor ATF4. Nature genetics 2006: 38: 674-681.
47. Baala L, Romano S, Khaddour R et al. The Meckel-Gruber syndrome gene, MKS3, is mutated in Joubert syndrome. American journal of human genetics 2007: 80: 186-194.

48. Arts HH, Doherty D, van Beersum SE et al. Mutations in the gene encoding the basal body protein RPGRIP1L, a nephrocystin-4 interactor, cause Joubert syndrome. Nature genetics 2007: 39: 882-888.
49. Delous M, Baala L, Salomon R et al. The ciliary gene RPGRIP1L is mutated in cerebello-oculo-renal syndrome (Joubert syndrome type B) and Meckel syndrome. Nature genetics 2007: 39: 875-881.
50. Cantagrel V, Silhavy JL, Bielas SL et al. Mutations in the cilia gene ARL13B lead to the classical form of Joubert syndrome. American journal of human genetics 2008: 83: 170-179.
51. Noor A, Windpassinger C, Patel M et al. CC2D2A, encoding a coiled-coil and C2 domain protein, causes autosomal-recessive mental retardation with retinitis pigmentosa. American journal of human genetics 2008: 82: 1011-1018.
52. Gorden NT, Arts HH, Parisi MA et al. CC2D2A is mutated in Joubert syndrome and interacts with the ciliopathy-associated basal body protein CEP290. American journal of human genetics 2008: 83: 559-571.
53. Dafinger C, Liebau MC, Elsayed SM et al. Mutations in KIF7 link Joubert syndrome with Sonic Hedgehog signaling and microtubule dynamics. The Journal of clinical investigation 2011: 121: 2662-2667.
54. Garcia-Gonzalo FR, Corbit KC, Sirerol-Piquer MS et al. A transition zone complex regulates mammalian ciliogenesis and ciliary membrane composition. Nature genetics 2011: 43: 776-784.
55. Sang L, Miller JJ, Corbit KC et al. Mapping the NPHP-JBTS-MKS protein network reveals ciliopathy disease genes and pathways. Cell 2011: 145: 513-528.
56. Huang L, Szymanska K, Jensen VL et al. TMEM237 is mutated in individuals with a Joubert syndrome related disorder and expands the role of the TMEM family at the ciliary transition zone. American journal of human genetics 2011: 89: 713-730.
57. Lee JE, Silhavy JL, Zaki MS et al. CEP41 is mutated in Joubert syndrome and is required for tubulin glutamylation at the cilium. Nature genetics 2012: 44: 193-199.
58. Valente EM, Silhavy JL, Brancati F et al. Mutations in CEP290, which encodes a centrosomal protein, cause pleiotropic forms of Joubert syndrome. Nature genetics 2006: 38: 623-625.
59. Joubert M, Eisenring JJ, Robb JP et al. Familial agenesis of the cerebellar vermis: a syndrome of episodic hyperpnea, abnormal eye movements, ataxia, and retardation. 1969. Journal of child neurology 1999: 14: 554-564.
60. Andermann F, Andermann E, Ptito A et al. History of Joubert syndrome and a 30-year follow-up of the original proband. Journal of child neurology 1999: 14: 565-569.
61. Purcell S, Neale B, Todd-Brown K et al. PLINK: a tool set for whole-genome association and population-based linkage analyses. American journal of human genetics 2007: 81: 559-575.

62. Majewski J, Schwartzentruber JA, Caqueret A et al. Mutations in NOTCH2 in families with Hajdu-Cheney syndrome. Human mutation 2011: 32: 1114-1117.
63. McKenna A, Hanna M, Banks E et al. The Genome Analysis Toolkit: a MapReduce framework for analyzing next-generation DNA sequencing data. Genome research 2010: 20: 1297-1303.
64. Wang K, Li M, Hakonarson H. ANNOVAR: functional annotation of genetic variants from high-throughput sequencing data. Nucleic acids research 2010: 38: e164.
65. Davis EE, Zhang Q, Liu Q et al. TTC21B contributes both causal and modifying alleles across the ciliopathy spectrum. Nature genetics 2011: 43: 189-196.
66. Kumar P, Henikoff S, Ng PC. Predicting the effects of coding non-synonymous variants on protein function using the SIFT algorithm. Nature protocols 2009: 4: 1073-1081.
67. Adzhubei IA, Schmidt S, Peshkin L et al. A method and server for predicting damaging missense mutations. Nature methods 2010: 7: 248-249.
68. Mougou-Zerelli S, Thomas S, Szenker E et al. CC2D2A mutations in Meckel and Joubert syndromes indicate a genotype-phenotype correlation. Human mutation 2009: 30: 1574-1582.
69. Bandyopadhyay S, Chiang CY, Srivastava J et al. A human MAP kinase interactome. Nature methods 2010: 7: 801-805.
70. Ganesan AK, Kho Y, Kim SC et al. Broad spectrum identification of SUMO substrates in melanoma cells. Proteomics 2007: 7: 2216-2221.
71. Huang W, Zhou Z, Asrar S et al. p21-Activated kinases 1 and 3 control brain size through coordinating neuronal complexity and synaptic properties. Molecular and cellular biology 2011: 31: 388-403.
72. Wilkinson KA, Nakamura Y, Henley JM. Targets and consequences of protein SUMOylation in neurons. Brain research reviews 2010: 64: 195-212.
73. Yotova V, Labuda D, Zietkiewicz E et al. Anatomy of a founder effect: myotonic dystrophy in Northeastern Quebec. Human genetics 2005: 117: 177-187.
74. Roddier K, Thomas T, Marleau G et al. Two mutations in the HSN2 gene explain the high prevalence of HSAN2 in French Canadians. Neurology 2005: 64: 1762-1767.
75. Sattar S, Gleeson JG. The ciliopathies in neuronal development: a clinical approach to investigation of Joubert syndrome and Joubert syndrome-related disorders. Developmental medicine and child neurology 2011: 53: 793-798.
76. Lee JH, Silhavy JL, Lee JE et al. Evolutionarily assembled cis-regulatory module at a human ciliopathy locus. Science 2012: 335: 966-969.
77. Srour M, Schwartzentruber J, Hamdan FF et al. Mutations in C5ORF42 cause Joubert syndrome in the French Canadian population. American journal of human genetics 2012: 90: 693-700.

78. Valente EM, Brancati F, Silhavy JL et al. AHI1 gene mutations cause specific forms of Joubert syndrome-related disorders. Annals of neurology 2006: 59: 527-534.
79. Chih B, Liu P, Chinn Y et al. A ciliopathy complex at the transition zone protects the cilia as a privileged membrane domain. Nature cell biology 2012: 14: 61-72.
80. Romani M, Micalizzi A, Valente EM. Joubert syndrome: congenital cerebellar ataxia with the molar tooth. Lancet neurology 2013: 12: 894-905.
81. Szymanska K, Johnson CA. The transition zone: an essential functional compartment of cilia. Cilia 2012: 1: 10.
82. Srour M, Hamdan FF, Schwartzentruber JA et al. Mutations in TMEM231 cause Joubert syndrome in French Canadians. Journal of medical genetics 2012: 49: 636-641.
83. Otto EA, Ramaswami G, Janssen S et al. Mutation analysis of 18 nephronophthisis associated ciliopathy disease genes using a DNA pooling and next generation sequencing strategy. Journal of medical genetics 2011: 48: 105-116.
84. Tuz K, Bachmann-Gagescu R, O'Day DR et al. Mutations in CSPP1 Cause Primary Cilia Abnormalities and Joubert Syndrome with or without Jeune Asphyxiating Thoracic Dystrophy. American journal of human genetics 2014: 94: 62-72.
85. Shaheen R, Shamseldin HE, Loucks CM et al. Mutations in CSPP1, Encoding a Core Centrosomal Protein, Cause a Range of Ciliopathy Phenotypes in Humans. American journal of human genetics 2014: 94: 73-79.
86. Akizu N, Silhavy JL, Rosti RO et al. Mutations in CSPP1 Lead to Classical Joubert Syndrome. American journal of human genetics 2014: 94: 80-86.
87. Thauvin-Robinet C, Lee JS, Lopez E et al. The oral-facial-digital syndrome gene C2CD3 encodes a positive regulator of centriole elongation. Nature genetics 2014: 46: 905-911.
88. Romani M, Micalizzi A, Kraoua I et al. Mutations in B9D1 and MKS1 cause mild Joubert syndrome: expanding the genetic overlap with the lethal ciliopathy Meckel syndrome. Orphanet journal of rare diseases 2014: 9: 72.
89. Coppieters F, Lefever S, Leroy BP et al. CEP290, a gene with many faces: mutation overview and presentation of CEP290base. Human mutation 2010: 31: 1097-1108.
90. Poretti A, Vitiello G, Hennekam RC et al. Delineation and diagnostic criteria of Oral-Facial-Digital Syndrome type VI. Orphanet journal of rare diseases 2012: 7: 4.
91. Lopez E, Thauvin-Robinet C, Reversade B et al. C5orf42 is the major gene responsible for OFD syndrome type VI. Human genetics 2013.
92. Thomas S, Legendre M, Saunier S et al. TCTN3 mutations cause Mohr-Majewski syndrome. American journal of human genetics 2012: 91: 372-378.
93. Adly N, Alhashem A, Ammari A et al. Ciliary genes TBC1D32/C6orf170 and SCLT1 are mutated in patients with OFD type IX. Human mutation 2014: 35: 36-40.

94. Shamseldin HE, Rajab A, Alhashem A et al. Mutations in DDX59 implicate RNA helicase in the pathogenesis of orofaciodigital syndrome. American journal of human genetics 2013: 93: 555-560.
95. Jakobsen L, Vanselow K, Skogs M et al. Novel asymmetrically localizing components of human centrosomes identified by complementary proteomics methods. The EMBO journal 2011: 30: 1520-1535.
96. Jiang K, Toedt G, Montenegro Gouveia S et al. A Proteome-wide screen for mammalian SxIP motif-containing microtubule plus-end tracking proteins. Current biology : CB 2012: 22: 1800-1807.
97. Satish Tammana TV, Tammana D, Diener DR et al. Centrosomal protein CEP104 (Chlamydomonas FAP256) moves to the ciliary tip during ciliary assembly. Journal of cell science 2013: 126: 5018-5029.
98. Thiffault I, Dicaire MJ, Tetreault M et al. Diversity of ARSACS mutations in French-Canadians. The Canadian journal of neurological sciences Le journal canadien des sciences neurologiques 2013: 40: 61-66.
99. Dupre N, Gros-Louis F, Chrestian N et al. Clinical and genetic study of autosomal recessive cerebellar ataxia type 1. Annals of neurology 2007: 62: 93-98.
100. Moreau C, Vezina H, Yotova V et al. Genetic heterogeneity in regional populations of Quebec--parental lineages in the Gaspe Peninsula. American journal of physical anthropology 2009: 139: 512-522.
101. Spektor A, Tsang WY, Khoo D et al. Cep97 and CP110 suppress a cilia assembly program. Cell 2007: 130: 678-690.
102. Tsang WY, Dynlacht BD. CP110 and its network of partners coordinately regulate cilia assembly. Cilia 2013: 2: 9.
103. Tsang WY, Bossard C, Khanna H et al. CP110 suppresses primary cilia formation through its interaction with CEP290, a protein deficient in human ciliary disease. Developmental cell 2008: 15: 187-197.
104. Alazami AM, Alshammari MJ, Salih MA et al. Molecular characterization of Joubert syndrome in Saudi Arabia. Human mutation 2012: 33: 1423-1428.
105. Ohba C, Osaka H, Iai M et al. Diagnostic utility of whole exome sequencing in patients showing cerebellar and/or vermis atrophy in childhood. Neurogenetics 2013: 14: 225-232.
106. Kroes HY, Monroe GR, van der Zwaag B et al. Joubert syndrome: genotyping a Northern European patient cohort. European journal of human genetics : EJHG 2015.
107. Romani M, Mancini F, Micalizzi A et al. Oral-facial-digital syndrome type VI: is C5orf42 really the major gene? Human genetics 2015: 134: 123-126.
108. Bachmann-Gagescu R, Ishak GE, Dempsey JC et al. Genotype-phenotype correlation in CC2D2A-related Joubert syndrome reveals an association with ventriculomegaly and seizures. Journal of medical genetics 2012: 49: 126-137.

109. Shaheen R, Ansari S, Mardawi EA et al. Mutations in TMEM231 cause Meckel-Gruber syndrome. Journal of medical genetics 2013: 50: 160-162.
110. Hopp K, Heyer CM, Hommerding CJ et al. B9D1 is revealed as a novel Meckel syndrome (MKS) gene by targeted exon-enriched next-generation sequencing and deletion analysis. Human molecular genetics 2011: 20: 2524-2534.
111. Damerla RR, Cui C, Gabriel G et al. Novel Jbts17 mutant mouse model of Joubert syndrome with cilia transition zone defects and cerebellar and other ciliopathy related anomalies. Human molecular genetics 2015.
112. Shaheen R, Faqeih E, Alshammari MJ et al. Genomic analysis of Meckel-Gruber syndrome in Arabs reveals marked genetic heterogeneity and novel candidate genes. European journal of human genetics : EJHG 2013: 21: 762-768.
113. Roberson EC, Dowdle WE, Ozanturk A et al. TMEM231, mutated in orofaciodigital and Meckel syndromes, organizes the ciliary transition zone. The Journal of cell biology 2015: 209: 129-142.
114. Reiter JF, Blacque OE, Leroux MR. The base of the cilium: roles for transition fibres and the transition zone in ciliary formation, maintenance and compartmentalization. EMBO reports 2012: 13: 608-618.
115. Davis EE, Katsanis N. The ciliopathies: a transitional model into systems biology of human genetic disease. Current opinion in genetics & development 2012: 22: 290-303.

Annex 1:

Recessive and dominant mutations in retinoic acid receptor beta cause microphthalmia and diaphragmatic hernia

Am J Hum Genet. 2013 Oct 3;93(4):765-72.

Recessive and dominant mutations in the retinoic acid receptor beta in cases with microphthalmia and diaphragmatic hernia

Myriam Srour[1]*, David Chitayat[2,3]*, Véronique Caron[1]*, Nicolas Chassaing[4,5]*, Pierre Bitoun[6], Lysanne Patry[1], Marie-Pierre Cordier[7], José-Mario Capo-Chichi[1], Christine Francannet[8], Patrick Calvas[4,5], Nicola Ragge[9,10], Sylvia Dobrzeniecka[11], Fadi F. Hamdan[1], Guy A Rouleau[11], André Tremblay[1], Jacques L. Michaud[1#]

[1]CHU Sainte-Justine Research Center, Montreal, Quebec, H3T1C5, Canada; [2]The Prenatal Diagnosis and Medical Genetics Program, Mount Sinai Hospital, Toronto, Ontario, M5G 1X5, Canada; [3]Division of Clinical and Metabolic Genetics, Hospital for Sick Children, Toronto, Ontario, M5G 1X8, Canada, [4]Service de Génétique Médicale, Hôpital Purpan, CHU Toulouse, 31059, Toulouse, France; [5]Université Paul-Sabatier, Toulouse III, EA-4555, 31000, Toulouse, France; [6]Génétique Médicale, Hôpital Jean Verdier AP-HP, C.H.U. Paris Nord, 93140 Bondy, France; [7]Service de Génétique, Hospices Civils de Lyon, F-69677 Bron, France; [8]Service de Génétique Médicale, Hôtel Dieu, 63058 Clermont Ferrand, France; [9]School of Life Sciences, Oxford Brookes University, Oxford, OX3 0BP, United Kingdom; [10]Clinical Genetics Unit, Birmingham Women's Hospital, Birmingham, B15 2TG, United Kingdom ; [11]Montreal Neurological Institute, McGill University, Montreal, Quebec, H3A 2B4, Canada.

* Equal contribution

ABSTRACT

Anophthalmia and/or microphthalmia, Pulmonary hypoplasia, Diaphragmatic hernia and Cardiac defects are the main features of PDAC syndrome. Recessive mutations in *STRA6*, a membrane-receptor for the retinol-binding protein, have been identified in some cases with PDAC syndrome, though many cases remained unexplained. Using whole-exome sequencing, we found that 2 siblings with PDAC syndrome, but not their unaffected sibling, were compound heterozygous for nonsense (c.355C>T, p.Arg119*) and framefhift (c.1201_1202insCT, p.Ile403Serfs*15) mutations in the retinoic acid receptor beta gene (*RARB*). Transfection studies showed that the p.Arg119* and p.Ile403Serfs*15 RARB mutants had no transcriptional activity in response to ligands confirming that the mutations induced a loss of function. We then sequenced *RARB* in 15 subjects with microphthalmia and/or anophthamia and at least one other feature of PDAC syndrome. Surprisingly, we identified 3 unrelated subjects with microphthalmia and diaphragmatic hernia who showed *de novo* missense mutations affecting the same codon; two of the subjects had the mutation c.1159C >T (Arg387Cys) whereas the other one carried the mutation c.1159C >A (p.Arg387Ser). We found that the p.Arg387Ser and p.Arg387Cys RARB mutants induced a 2 to 3-fold increase in transcriptional activity compared to wild-type receptor in response to retinoic acid ligands, suggesting a gain-of-function mechanism. Our study thus suggests that both recessive and dominant mutations in *RARB* cause microphthalmia and/or anophthalmia and diaphragmatic hernia, providing further evidence of the crucial role of the retinoic acid pathway during eye development and organogenesis.

Anophthalmia and microphthalmia (A/M) refer to the absence or reduced size of the axial diameter of the globe in the ocular orbit, respectively. In over 50% of cases, A/M is associated with other congenital abnormalities[1,2]. The combination of, Pulmonary hypoplasia or agenesis, Diaphragmatic hernia or eventration, A/M and Cardiac defects are the features of the acronym PDAC syndrome, which is also known as Matthew-Wood or Spear syndrome [MCOPS9, MIM 601186][3]. In some individuals, PDAC syndrome is caused by autosomal recessive mutations in *STRA6* (MIM 610745), a membrane receptor for the retinol-binding protein[4, 5]. Many cases of PDAC syndrome, however, remain unexplained.

In this study, we performed whole-exome sequencing in a non-consanguineous family with PDAC syndrome to uncover the genetic cause (Figure 1A). The couple has 2 healthy daughters and four progenies of whom 2 had all the features of PDAC, and 2 others with at least 2 features of PDAC (family A, individuals II-1, 4, 5 and 6, see table 1 for clinical details). This family was previously described (family A in Chitayat et al, 2007[3]; Case 1A is individual II-4, case 2A is II-5 and case 3A is II-6). *STRA6* was previously sequenced in one affected individual of this family and no mutation was identified.

This study was approved by our institutional ethics committee and informed consent was obtained from each participant or legal guardian. Blood genomic DNA from the affected individuals II-4 and II-5 and the non-affected sister (II-2) from family A was captured with the Agilent SureSelect Human All Exon Capture V4 Kit (Mississauga, ON), and sequenced (paired-end, 2x100bp, 3 exomes/lane format) using the Illumina HiSeq2000 at the McGill University Genome Quebec Innovation Center (Montreal,

Canada). Sequence processing, alignment (using a Burroughs-Wheeler algorithm, BWA), and variant calling were done according to the Broad Institute Genome Analysis Tool Kit (GATK v4) best practices, and variant annotation was done using Annovar[6]. The exome target base average coverage was 111-114X, with 95% of the target bases being covered by at least 20 reads. Only the variants whose positions were covered at ≥ 8x and supported by ≥ 3 variant reads that constitute at least 20% of the total reads for each called position were retained. To identify potentially pathogenic variants we filtered out: 1) synonymous variants or intronic variants other than those affecting the consensus splice sites; 2) variants seen in more than 2% of our in-house exomes dataset (n = 1000) from unrelated projects; and 3) variants with a minor allele frequency greater than 0.5% in either the 1000 genomes or NHLBI exome sequencing project (ESP) datasets (Exome Variant Server, EVS). There were no rare coding or splicing variants that were shared between the affected individuals in *STRA6* or in *ALDH1A3* (MIM 600463), another gene involved in A/M and retinoic acid signaling [7].

Since transmission of the phenotype in this family was consistent with an autosomal recessive inheritance, we searched the whole-exome datasets for genes that harboured homozygous or multiple rare variants in both affected probands but not in their unaffected sibling. There were no such genes with rare homozygous variants. We identified only 3 genes containing multiple rare variants in both affected individuals, not shared by the unaffected sister: *PRPF39* (MIM 614907), *RARB* (MIM 180220) and *GAPVD1* (MIM 611714). Sanger sequencing in the parents and the siblings revealed that the variants in *PRPF39* were inherited in *cis*, thus excluding this gene as a candidate. The affected probands, but not the unaffected sister, were compound heterozygous and the

parents were singly heterozygous for the variants in *RARB* and *GAPVD1* (Figure 1A). *RARB* (NM_000965.3), which encodes Retinoic acid receptor beta, harboured two protein-truncating mutations: a nonsense c.355C>T (p.Arg119*) and a frameshift c.1201_1202insCT (p.Ile403Serfs*15). These variants are absent from all public SNP databases (1000 Genomes, EVS, dbSNP138) and from our in-house exome data sets (n>1000). *RARB* has 2 major isoforms noted as reference sequences (Refseq) in the UCSC Genome Browser, as well as 3 additional isoforms noted in the Ensembl Genome Browser. The major Refseq isoform (NM_000965.3) has 8 exons and encodes a 448 amino acid protein. Both identified mutations affect all known *RARB* isoforms (Figure 2A). *GAPVD1* (NM_015635*)*, which encodes GTPase activating protein and VPS9 domain 1, harboured two rare missense variants, c.2809C>T (p.Arg937Trp) and c.3266G>T (p.Gly1089Val) in the probands. The p.Arg937Trp substitution is predicted damaging in both SIFT and Polyphen-2 (score=0.0 and 1.0 respectively), however the p.Gly1089Val substitution is predicted benign in both SIFT and Polyphen-2 (score=0.2, and 0.145 respectively). *GAPVD1* is involved in endocytosis[8], phagosome maturation[9] and regulation of the epidermal growth factor receptor[10] but is not known to have a role in eye development or embryogenesis. Because of the importance of the retinoic acid pathway for eye and diaphragm development (discussed below), mutations in *RARB* were deemed more likely to be pathogenic than those in *GAPVD1*.

Retinoic acid receptors bind to DNA motifs known as Retinoic Acid Response Elements (RAREs) to modulate transcription of target genes by interacting with transcriptional co-repressors and co-activators. Upon binding to retinoic acid (RA), the

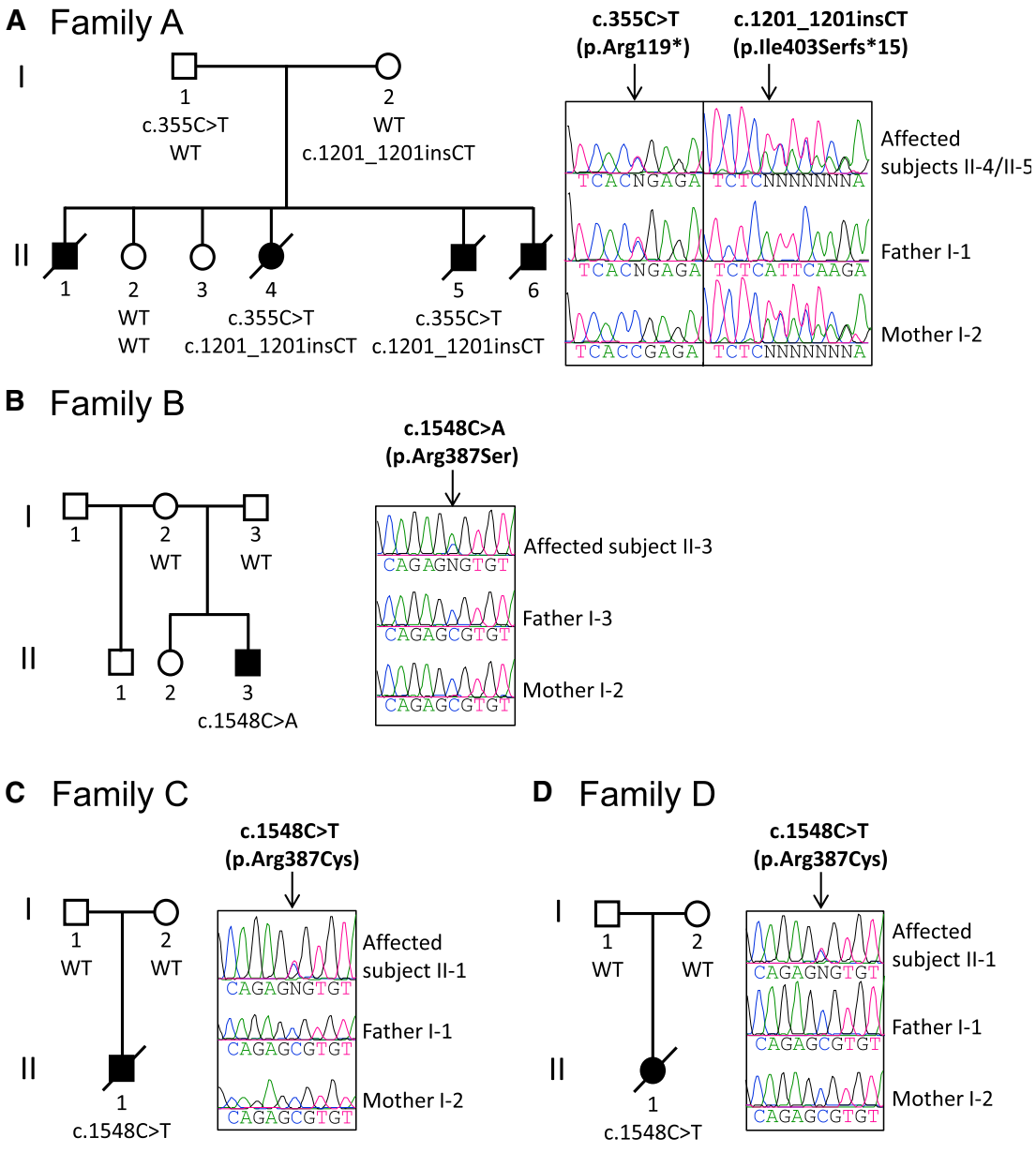

Figure 1. **Mutations in *RARB* in individuals with PDAC syndrome**. Sanger sequencing confirmed segregation of the recessive mutations in *RARB* in family A (A), and revealed that the mutations were *de novo* in family B, C and D (B-D).

co-repressor docking site becomes hindered by helix-12 positioning, resulting in the recruitment of co-activators and an increase in transcription of target genes [11]. The c.355C>T (p.Arg119*) nonsense mutation is predicted to result in an inactive truncated receptor, lacking the second zinc finger of the DNA-binding domain as well as the entire ligand-binding domain (Fig. 2B). Moreover, this mutation has the potential of activating the non-sense mediated mRNA decay pathway, resulting in the degradation of the corresponding transcript. The c.1201_1202insCT (p.Ile403Serfs*15) mutation results in the substitution of a hydrophobic isoleucine by serine, a polar residue, as well as the replacement of the last 52 amino acids by an aberrant extension of 15 amino acids (Fig. 2B). As part of helix 12, residue Ile403 is thus predicted to play a key role in the recruitment of transcriptional cofactors and response to ligand. As such, *in vitro* studies have shown that Ile403 substitution with serine in RARB conferred an increased binding to co-repressor SMRT in absence of ligand, resulting in reduced transcriptional activity[12]. Both mutations found in family A are thus predicted to disrupt *RARB* function.

We tested the impact of these truncating mutations on RARB activity using a cellular one-hybrid luciferase reporter transcriptional assay as described[13]. Expression plasmids encoding transcription factor Gal4 DNA-binding domain fusions to wild-type RARB or truncated variants p.Arg119* and p.Ile403Serfs*15 were generated and used to transfect human embryonic kidney (HEK) 293 cells in the presence of a luciferase reporter gene construct under the control of a Gal4-binding DNA upstream-activating sequence (UAStkLuc). This assay allows direct determination of transcriptional activity and response to ligand of variants compared to wild-type receptor, avoiding any background effect of endogenously-expressed RARB in cells. Transfected HEK293 cells

were treated with the natural ligands all-*trans* retinoic acid (atRA) and its stereoisomer 9-*cis* retinoic acid (9-cis RA), which both act as pan-RAR agonists. As expected, the transcriptional response of the p.Arg119* mutant to the two RA ligands was completely abolished compared to wild-type RARB, correlating with its lack of ligand-binding domain (Fig. 3). Similarly, the transcriptional response to retinoids was impaired in the p.Ile403Serfs*15 mutant compared to wild-type RARB. The disruption, in the p.Ile403Serfs*15 mutant, of helix-12 and its replacement by an aberrant extension likely interferes with its ability

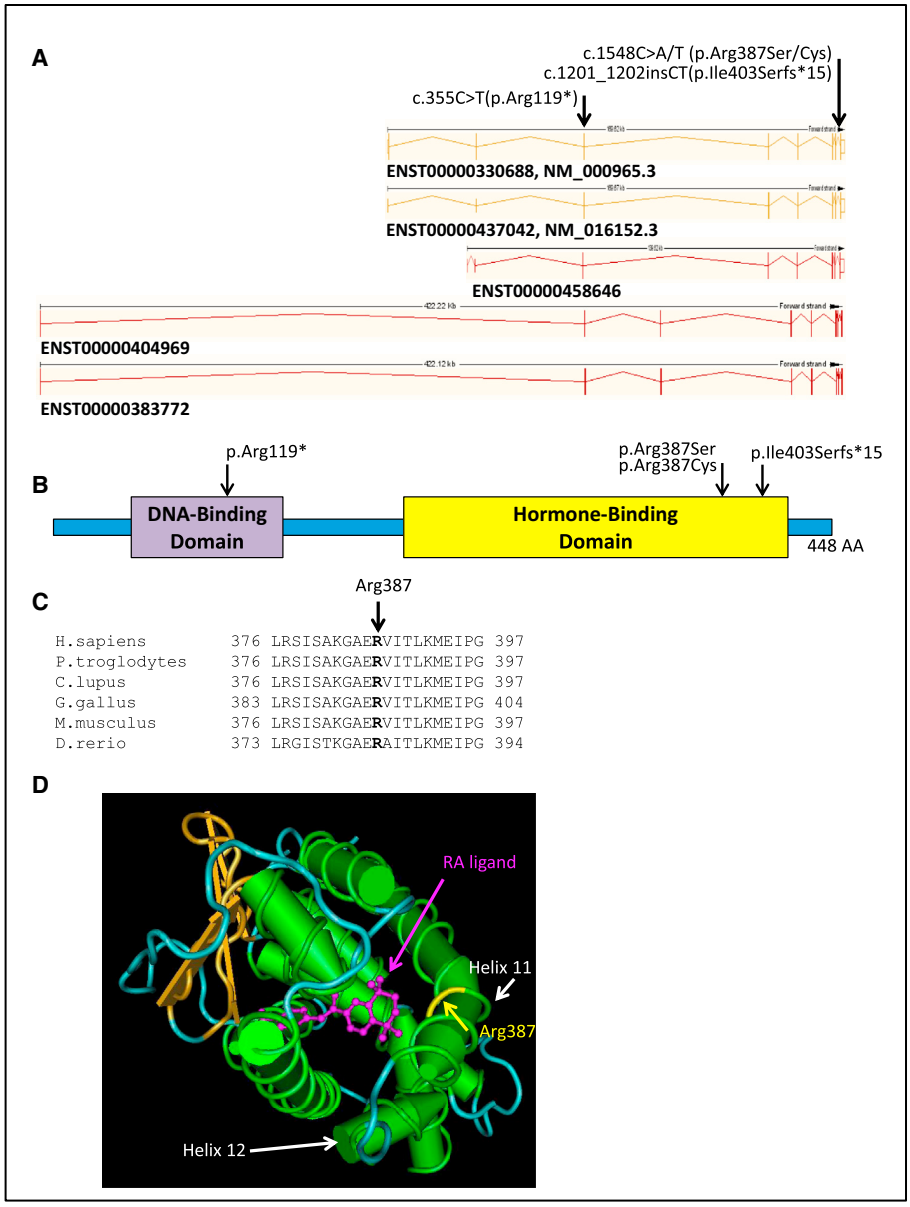

Figure 2. **Localization and impact of the mutations in** ***RARB*****.** (A) Shown are the positions of the mutations with respect to the different *RARB* ENSEMBLE-annotated transcripts that are predicted to produce proteins. Numbering on top is based on the cDNA positions of ENST00000330688 (identical to NCBI Refseq # NM_000965.3). (B) Schematic of the RARB protein, showing the DNA-binding and hormone-binding domains. Arrowheads above the protein show the positions of the mutations. (C) Homologene-generated (NCBI) amino acid alignment of human RARB with its predicted orthologues showing the conservation of the p.Arg387 residue. (D) 3-dimensional structure of RARB (PDB ID: 4DM8) in the presence of the retinoic acid (RA) ligand (purple) showing the proximity of the Arg387 residue in helix 11 to the RA ligand.

to occlude the corepressor docking site. All together, these results strongly suggest that these truncating mutations confer a loss of RARB function and explain the occurrence of PDAC syndrome in family A.

We next sequenced all the coding exons and intron/exon boundaries of *RARB* (NM_000965.3) as well as the alternate exon 1 (ENST00000404969) in 15 additional individuals with bilateral or unilateral M/A and at least one additional feature of PDAC (diaphragmatic hernia, cardiac defect or lung hypoplasia) who were previously screened for mutations in *STRA6* [14]. In three unrelated subjects, who were all simplex cases, we identified single heterozygous *RARB* missense mutations affecting the same nucleotide. Of these, two subjects (II-1 from family C and II-1 from family D) harboured the c.1159C >T (p.Arg387Cys) missense, and one individual (II-3 from family B) harboured the c.1159C >A (p.Arg387Ser) missense (Fig. 1B-C). These mutations were absent from the genomic DNA of the parents, indicating that they occurred *de novo*. Using 6 informative unlinked microsatellite markers (D3S1754, D4S3351, D8S1179, D15S659, D14S587, and D19S215), we confirmed the paternity and maternity in these families, as previously described[15]. Both c.1159C >T (p.Arg387Cys) and c.1159C >A (p.Arg387Ser) are absent from public SNP databases (EVS, 1000 Genomes, and dbSNP138) and from our entire collection of in-house exomes (>1000). They are both predicted damaging by SIFT and Polyphen-2 (scores= 0.0 and 1.0 for both, respectively) and affect a highly conserved amino acid in helix 11 of the ligand binding domain (Figure 2C). Subject II-1 from family C is a fetus for whom pregnancy was terminated because of unilateral microphthalmia and left diaphragmatic hernia on prenatal ultrasound (Table 1). Autopsy also showed hypoplasia of a pulmonary lobe of the left side. Subject II-1 from family D

is a newborn who passed away within a few hours after birth because of a left diaphragmatic hernia. This subject also showed bilateral microphthalmia and pulmonary hypoplasia. Subject II-3 from family B is currently a 14-year-old male with bilateral microphthalmia, corrected diaphragmatic hernia, and abnormal cognitive development with spasticity (for clinical details, see case # 6 in Chitayat et al., 2007[3]). We also sequenced *RARB* in 11 cases with isolated bilateral A/M but we did not find any mutation in this gene.

The fact that the *de novo* mutations involved the same residue (Arg387) suggests that they confer a specific property to the protein. These mutations could induce a dominant-negative effect or act through a gain-of-function mechanism. In order to distinguish between these possibilities, we sought to study the impact of these mutations using our one-hybrid functional assay. The p.Arg387Ser and p.Arg387Cys RARB mutants exhibited a significant increase in their transcriptional response to all-*trans* retinoic acid (atRA), reaching respectively 23- and 28-fold induction compared to 9-fold for wild-type RARB (Fig. 3). Similar activation levels were also obtained using 9-cis RA ligand. These results suggest that the two mutations at Arg387 provide an increased transcriptional potential to respond to retinoid ligands through a gain-of-function mechanism. A more detailed mechanistic analysis remains to be done to explain such increase in activity.

We have identified compound heterozygous truncating mutations as well as *de novo* mutations affecting the same nucleotide in the *RARB* gene of individuals with PDAC syndrome. The occurrence of such mutations in individuals with a similar and rare phenotype strongly suggests that they cause PDAC syndrome. Indeed, several

observations indicate that the retinoic acid (RA) pathway plays a major role in the development of the eyes, diaphragm and lungs. RA is a metabolite of retinol, a derivative of vitamin A. The importance of the RA pathway in embryogenesis has been recognized for decades, as rats deficient in vitamin A give birth to progeny with multiple congenital malformations, including ocular abnormalities and diaphragmatic hernia[16]. Circulating retinol is bound to retinol binding protein 4 (RBP4). The transmembrane protein STRA6 (Stimulated by Retinoic acid) facilitates the intracellular uptake of the retinol-RBP complex [4]. Mutations in *STRA6* have been identified in at least 24 individuals with M/A[5, 14, 17-19]. Most of these subjects showed other features of the PDAC syndrome but some of them had isolated M/A. Once transported into the cell, retinol is successively oxidized to retinaldehyde and retinoic acid. Mutations in *ALDH1A3*, which encodes a retinaldehyde dehydrogenase that is responsible for the oxidation of retinaldehyde into RA, have been found to be responsible for M/A with variable neurodevelopmental and cardiac features[7].

In target cells, RA acts as a ligand for nuclear RA receptors. Several observations in mice suggest that these receptors play a major role in eye, diaphragm and lung development. Mice lacking all *Rarb* isoforms display microphthalmia[20,21]. RA is generated in the epithelial ocular compartment and diffuses in the neural crest-cell derived periocular mesenchyme to activate RARB and RARG. In turn, these receptors regulate the remodeling of the periocular mesenchyme, the growth of the ventral retina as well as the expression of *Foxc1* and *Pitx2*, which play central roles in anterior eye segment development[22]. Studies of RA receptor double null-mutant mice, lacking both *Rara* and *Rarb* subtypes, have also demonstrated the presence of diaphragmatic hernias in a subset of offsprings[23]. Moreover, administration of nitrofen to pregnant rodents is

thought to cause diaphragmatic hernias, in part through down-regulation of RA receptor signaling (reviewed in Greer et al[24]). Recent studies indicate that *Rarb* functions along a pathway that directs development of the central tendon of the diaphragm[25]. Finally, *Rarb*$^{-/-}$ knock-out mice have smaller and more numerous alveoli in their lungs[26]. *Rarb* has been shown to have a critical role in lung morphogenesis by inducing *Fgf10* expression in bud fields[27]. Overall, these studies support our conclusion that loss of RARB function causes PDAC syndrome in family A. Our transfection experiments suggest that the *de novo* mutations affecting Arg387 result in enhanced activity of RARB in response to retinoic acid ligands, suggesting a gain-of-function mechanism. Whether these two substitutions induce a conformational change that enhances protein stability, favors co-activator recruitment and/or increases RA binding affinity remains to be determined. Consistent with this latter possibility, crystallographic studies have

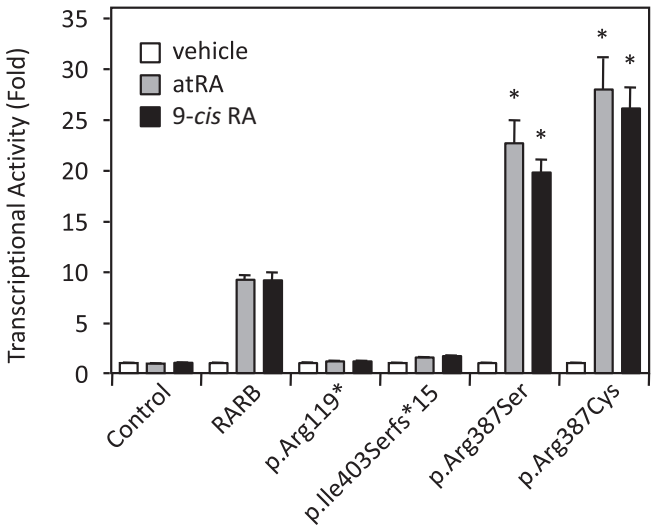

Figure 3. **Transcriptional response of human RARB mutants to retinoic acid ligands.** HEK293 cells were seeded in 24-well plates and transfected with 100 ng per well of expression plasmid encoding either Gal4 fusion of wild-type human RARB, p.Arg119*, p.Ile403Serfs*15, p.Arg387Ser, or p.Arg387Cys RARB mutants in the presence of 500 ng of UAStkLuc reporter gene construct. All mutated constructs were generated by site-directed mutagenesis, including the p.Ile403Serfs*15 carrying the additional out-of-frame amino acid extension. Cells were treated with 1μM all-*trans* retinoic acid (atRA), 1μM 9-*cis* retinoic acid (9-cis RA), or with vehicle (DMSO; 1/1000, v/v) for 16hrs. Luciferase values were normalized to β-Galactosidase activity and expressed as fold response compared to empty Gal4-transfected control cells. Data are derived from three independent experiments performed in triplicates. *, P<0.005 *vs* wild-type RARB response to respective RA ligand.

established that Arg387 residue is facing inward of the ligand-binding pocket, in close proximity of the retinoid ligand (Fig. 2D). Our model of gain-of-function mutations thus suggests that an increase in RARB response to retinoids might represent a primary cause of PDAC syndrome. Indeed, excess of vitamin A or RA during development in mice cause various malformations, including microphthalmia and diaphragmatic hernia[28-32]. Moreover, expression of a constitutively active RAR transgene in the developing eye resulted in animals that exhibited microphthalmia[33]. Similarly, Zebrafish embryos exposed to 9-cis-RA develop multiple developmental abnormalities including microphthalmia[34]. RA is also teratogenic in humans[35]. Interestingly, microphthalmia and diaphragmatic hernia have been reported in some babies from women exposed to RA during pregnancy [35, 36].

All together, our findings and the previous work described above therefore suggest that both decreased and increased RARB activity can result in PDAC syndrome. A recent study showed that RA exposure during embryonic development in mice was followed by decreased levels of *Raldh* transcripts encoding retinoic acid-synthesizing enzymes and increased levels of *Cyp26a1* and *Cyp26b1*, mRNAs encoding enzymes that catabolize retinoic acid[32]. Overall, these changes resulted in a decrease of RA levels. Restoration of RA levels by maternal supplementation with low doses of RA following the teratogenic insult rescued several developmental defects. Paradoxically, increased RARB signaling could thus result in a secondary state of RA deficiency, which could impact on this pathway at specific stages of development. Alternatively, it is possible that some developmental processes require a tight regulation of RARB targets, too little or too much signaling having the same consequence on these pathways.

In summary, we found that both recessive and dominant mutations affect RARB function in the context of PDAC syndrome, opening a new window on the structural and mechanistic basis of retinoic acid receptor activity with relation to human disease.

ACKNOWLEDGEMENTS

J.L. Michaud is a National Scientist of the Fonds de Recherche du Québec - Santé. M. Srour holds a clinician-scientist award from the Canadian Institute for Health Research. We wish to thank the members of the bioinformatic analysis team of Réseau de Médecine Génétique Appliquée du Québec (Alexandre Dionne-Laporte, Dan Spiegelman, Edouard Henrion, and Ousmane Diallo) for the analysis of the exome sequencing data. This research has been funded by a grant from the Canadian Institutes of Health Research (MOP 106499) to J.L. Michaud, and by grants from the Clinical Research Hospital Program from the French Ministry of Health (PHRC 09 109 01) and Retina France to N. Chassaing.

Web resources

GATK best practices: http://www.broadinstitute.org/gatk/guide/topic?name=best-practices
1000 Genomes Project, http://browser.1000genomes.org/index.html
dbSNP, http://www.ncbi.nlm.nih.gov/projects/SNP/
UCSC Genome Browser: http://genome.ucsc.edu/
Ensemble Genome Browser: http://www.ensembl.org
ESP Exome Variant Server (EVS): http://evs.gs.washington.edu/EVS/
NCBI homologene, http://www.ncbi.nlm.nih.gov/homologene
Online Mendelian Inheritance in Man (OMIM), http://www.omim.org
Polyphen-2: http://genetics.bwh.harvard.edu/pph2/
SIFT: http://sift.jcvi.org/

Protein Data Bank: http://www.rcsb.org/pdb

REFERENCES

1. Shaw GM, Carmichael SL, Yang W, Harris JA, Finnell RH, Lammer EJ. Epidemiologic characteristics of anophthalmia and bilateral microphthalmia among 2.5 million births in California, 1989-1997. American journal of medical genetics Part A 2005;137:36-40.
2. Kallen B, Robert E, Harris J. The descriptive epidemiology of anophthalmia and microphthalmia. International journal of epidemiology 1996;25:1009-1016.
3. Chitayat D, Sroka H, Keating S, et al. The PDAC syndrome (pulmonary hypoplasia/agenesis, diaphragmatic hernia/eventration, anophthalmia/microphthalmia, and cardiac defect) (Spear syndrome, Matthew-Wood syndrome): report of eight cases including a living child and further evidence for autosomal recessive inheritance. American journal of medical genetics Part A 2007;143A:1268-1281.
4. Kawaguchi R, Yu J, Honda J, et al. A membrane receptor for retinol binding protein mediates cellular uptake of vitamin A. Science 2007;315:820-825.
5. Pasutto F, Sticht H, Hammersen G, et al. Mutations in STRA6 cause a broad spectrum of malformations including anophthalmia, congenital heart defects, diaphragmatic hernia, alveolar capillary dysplasia, lung hypoplasia, and mental retardation. American journal of human genetics 2007;80:550-560.
6. Wang K, Li M, Hakonarson H. ANNOVAR: functional annotation of genetic variants from high-throughput sequencing data. Nucleic acids research 2010;38:e164.
7. Fares-Taie L, Gerber S, Chassaing N, et al. ALDH1A3 Mutations Cause Recessive Anophthalmia and Microphthalmia. American journal of human genetics 2013;92:265-270.
8. Hunker CM, Galvis A, Kruk I, Giambini H, Veisaga ML, Barbieri MA. Rab5-activating protein 6, a novel endosomal protein with a role in endocytosis. Biochemical and biophysical research communications 2006;340:967-975.
9. Kitano M, Nakaya M, Nakamura T, Nagata S, Matsuda M. Imaging of Rab5 activity identifies essential regulators for phagosome maturation. Nature 2008;453:241-245.
10. Su X, Kong C, Stahl PD. GAPex-5 mediates ubiquitination, trafficking, and degradation of epidermal growth factor receptor. The Journal of biological chemistry 2007;282:21278-21284.
11. Glass CK, Rosenfeld MG. The coregulator exchange in transcriptional functions of nuclear receptors. Genes & development 2000;14:121-141.
12. Farboud B, Privalsky ML. Retinoic acid receptor-alpha is stabilized in a repressive state by its C-terminal, isotype-specific F domain. Mol Endocrinol 2004;18:2839-2853.

13. Demers A, Caron V, Rodrigue-Way A, Wahli W, Ong H, Tremblay A. A concerted kinase interplay identifies PPARgamma as a molecular target of ghrelin signaling in macrophages. PloS one 2009;4:e7728.
14. Chassaing N, Ragge N, Kariminejad A, et al. Mutation analysis of the STRA6 gene in isolated and non-isolated anophthalmia/microphthalmia. Clinical genetics 2013;83:244-250.
15. Berryer MH, Hamdan FF, Klitten LL, et al. Mutations in SYNGAP1 cause intellectual disability, autism, and a specific form of epilepsy by inducing haploinsufficiency. Human mutation 2013;34:385-394.
16. Wilson JG, Roth CB, Warkany J. An analysis of the syndrome of malformations induced by maternal vitamin A deficiency. Effects of restoration of vitamin A at various times during gestation. The American journal of anatomy 1953;92:189-217.
17. Chassaing N, Golzio C, Odent S, et al. Phenotypic spectrum of STRA6 mutations: from Matthew-Wood syndrome to non-lethal anophthalmia. Human mutation 2009;30:E673-681.
18. Casey J, Kawaguchi R, Morrissey M, et al. First implication of STRA6 mutations in isolated anophthalmia, microphthalmia, and coloboma: a new dimension to the STRA6 phenotype. Human mutation 2011;32:1417-1426.
19. White T, Lu T, Metlapally R, et al. Identification of STRA6 and SKI sequence variants in patients with anophthalmia/microphthalmia. Molecular vision 2008;14:2458-2465.
20. Ghyselinck NB, Dupe V, Dierich A, et al. Role of the retinoic acid receptor beta (RARbeta) during mouse development. The International journal of developmental biology 1997;41:425-447.
21. Zhou G, Strom RC, Giguere V, Williams RW. Modulation of retinal cell populations and eye size in retinoic acid receptor knockout mice. Molecular vision 2001;7:253-260.
22. Matt N, Dupe V, Garnier JM, et al. Retinoic acid-dependent eye morphogenesis is orchestrated by neural crest cells. Development 2005;132:4789-4800.
23. Mendelsohn C, Lohnes D, Decimo D, et al. Function of the retinoic acid receptors (RARs) during development (II). Multiple abnormalities at various stages of organogenesis in RAR double mutants. Development 1994;120:2749-2771.
24. Greer VP, Mason P, Kirby AJ, Smith HJ, Nicholls PJ, Simons C. Some 1,2-diphenylethane derivatives as inhibitors of retinoic acid--metabolising enzymes. Journal of enzyme inhibition and medicinal chemistry 2003;18:431-443.
25. Coles GL, Ackerman KG. Kif7 is required for the patterning and differentiation of the diaphragm in a model of syndromic congenital diaphragmatic hernia. Proceedings of the National Academy of Sciences of the United States of America 2013;110:E1898-1905.

26. Massaro GD, Massaro D, Chan WY, et al. Retinoic acid receptor-beta: an endogenous inhibitor of the perinatal formation of pulmonary alveoli. Physiological genomics 2000;4:51-57.
27. Desai TJ, Chen F, Lu J, et al. Distinct roles for retinoic acid receptors alpha and beta in early lung morphogenesis. Developmental biology 2006;291:12-24.
28. Padmanabhan R, Singh G, Singh S. Malformations of the eye resulting from maternal hypervitaminosis A during gestation in the rat. Acta anatomica 1981;110:291-298.
29. Sulik KK, Dehart DB, Rogers JM, Chernoff N. Teratogenicity of low doses of all-trans retinoic acid in presomite mouse embryos. Teratology 1995;51:398-403.
30. Ozeki H, Shirai S. Developmental eye abnormalities in mouse fetuses induced by retinoic acid. Japanese journal of ophthalmology 1998;42:162-167.
31. Ozeki H, Shirai S, Ikeda K, Ogura Y. Critical period for retinoic acid-induced developmental abnormalities of the vitreous in mouse fetuses. Experimental eye research 1999;68:223-228.
32. Lee LM, Leung CY, Tang WW, et al. A paradoxical teratogenic mechanism for retinoic acid. Proceedings of the National Academy of Sciences of the United States of America 2012;109:13668-13673.
33. Balkan W, Klintworth GK, Bock CB, Linney E. Transgenic mice expressing a constitutively active retinoic acid receptor in the lens exhibit ocular defects. Developmental biology 1992;151:622-625.
34. Shi H, Zhu P, Sun Z, Yang B, Zheng L. Divergent teratogenicity of agonists of retinoid X receptors in embryos of zebrafish (Danio rerio). Ecotoxicology 2012;21:1465-1475.
35. Benke PJ. The isotretinoin teratogen syndrome. JAMA : the journal of the American Medical Association 1984;251:3267-3269.
36. Loureiro KD, Kao KK, Jones KL, et al. Minor malformations characteristic of the retinoic acid embryopathy and other birth outcomes in children of women exposed to topical tretinoin during early pregnancy. American journal of medical genetics Part A 2005;136:117-121.

Table 1: Clinical characteristics of subjects with mutations in *RARB*

Family	**A**				**B**	**C**	**D**
Individual	**II-1**	**II-4**	**II-5**	**II-6**	**II-3**	**II-1**	**II-1**
Ethnicity	French Canadian/English				French	Africa (Angola [father] and Congo [mother])	French
Consanguinity	-				-	-	-
Mutation	NA	c.355C>T (p.Arg119*), c.1201_1202insCT(p.Ile403Serfs*15)	c.355C>T (p. Arg119*), c.1201_1202insCT(p.Ile403Serfs*15)	NA	c.1159>A (p.Arg387Ser)[c]	c.1159C>T (p.Arg387Cys)[c]	c.1159C>T (p.Arg387Cys)[c]
Gender	M	F	M	M	M	M	F
Age (age at death)	(Few hours, 34 wks gestation)[a]	(Few hours, 38 wks gestation)	(21 wks fetus)[b]	(few hours, term)	16 years	(34 wks fetus)[b]	(Few hours, 39 wks gestation)[b]
Bilateral Microphthalmia/ Anophthalmia	+	+	+	+	+	Unilateral (left) microphthalmia Right eye normal	Bilateral microphthalmia
Pulmonary hypoplasia	NA	+	+	NA	-	Left lung with one hypoplastic lobe; Right lung normal	Bilateral (predominant on the left side)
Diaphragmatic hernia	NA	+	+	+	+	+ (Left)	+ (Left)
Cardiac abnormality	NA	+	-	NA	-	-	-
Intellectual disability	NA	NA	NA	NA	+	NA	NA
Other	-	Cleft palate, dysmorphisms, small spleen, bicornate and small uterus	Dysmorphisms, unfixed malrotated bowel	Dysmorphisms	-	Malrotated bowel right cryptorchydy mild IUGR (W, L and OFC at the 5[e] percentile	Bicornate uterus

[a]Died shortly after birth at 34 weeks due to presumed tangled cord, though a diagnosis of PDAC is strongly suspected [b]Terminated pregnancy [c]*De novo* mutation. NA=Not available